CRITICAL REVIEWS IN ANALYTICAL CHEMISTRY
https://doi.org/10.1080/10408347.2020.1828029

Taylor & Francis
Taylor & Francis Group

Sensor and Bioimaging Studies Based on Carbon Quantum Dots: The Green Chemistry Approach

Mustafa Oguzhan Caglayan, Ferda Mindivan, and Samet Şahin

Faculty of Engineering, Department of Bioengineering, Bilecik Şeyh Edebali University, Bilecik, Turkey

ABSTRACT

Since carbon quantum dots have high photoluminescent efficiency, it has been a desired material in sensor and bioimaging applications. In recent years, the green chemistry approach has been preferred and the production of quantum dots has been reported in many studies using different precursors from natural, abundant, or waste sources. Hydrothermal, chemical oxidation, microwave supported, ultrasonic, solvothermal, pyrolysis, laser etching, solid-state, plasma, and electrochemical methods have been reported in the literature. In this review article, green chemistry strategies for carbon quantum dot synthesis is summarized and compared with conventional methods using methodologic and statistical data. Furthermore, a detailed discussion on sensor and bioimaging applications of carbon quantum dots produced with green synthesis approaches are presented with a special focus on the last decade.

KEYWORDS

Green chemistry; carbon quantum dots; bioimaging; sensor

GRAPHICAL ABSTRACT

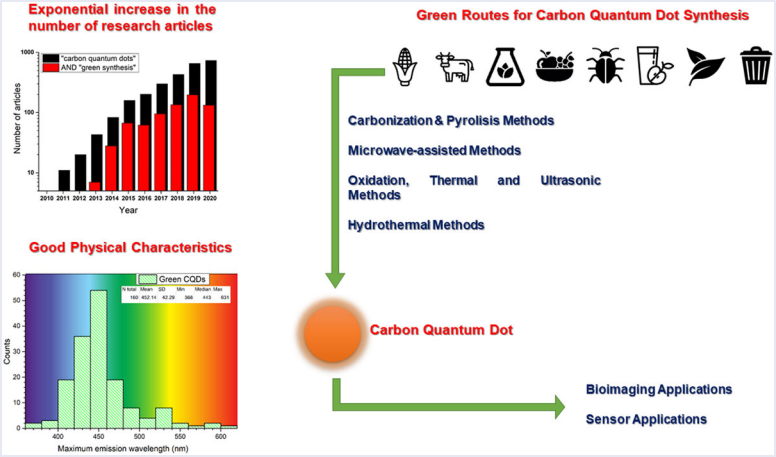

Introduction

Nanocrystals of carbon materials with dimensions smaller than 10 nm are known as carbon quantum dots (CQDs).[1] The optical properties of CQDs can be fine-tuned by producing them with different sizes and morphologies or by surface modifications, and are therefore preferred in many applications.[2] CQDs typically have an absorption characteristic that extends from the ultraviolet region to the visible range. The triplet state-excited aromatic carbonyls on the surface of CQDs can cause photoluminescence (PL), moreover, the emission wavelength and intensity can be changed by excitation, modification, or electron/energy transfer.[3,4] Another desired optical feature of CQDs in fluorescent applications is its ability to perform up-conversion photoluminescence (UCPL) and stimulation of CQDs in the near-infrared (NIR) region can result in an emitted light at 540 nm.[5] Besides, CQDs provide chemiluminescence (CL) and electro-chemiluminescence (ECL).[6] CL and ECL properties can be adjusted by changing the surface properties of CQDs.[7,8] Besides, CQDs can show the behavior of photoinduced electron transfer and charge separation.[9] A recently published review article on the unique optical properties of CQDs can be found in the literature.[10]

CQDs have been synthesized by different techniques after they were discovered accidentally in 2014.[11] These techniques include laser ablation,[12] arc discharge,[13] electrochemical methods,[14] chemical oxidation,[1] hydrothermal/solvothermal treatment,[15,16] microwave irradiation,[17]

CONTACT Mustafa Oguzhan Caglayan oguzhan.caglayan@bilecik.edu.tr Faculty of Engineering, Department of Bioengineering, Bilecik Şeyh Edebali University, Bilecik, 11230 Turkey.

Table 1. Features of CQDs produced using various conventional methods.

Method	Precursor	CQDs size (nm)	Emission (nm)	QY%	References
Electrochemical	Alcohols	3.2	495	15.9	[36]
Electrochemical	Carbon nanotube	2.8	410	6.4	[17]
Electrochemical	Graphite	4	437	11.2	[37]
Electrochemical	Sodium citrate, urea	2.3	433	11.9	[38]
Hydrothermal	Ascorbic acid	2	430	6.8	[27]
Hydrothermal	Citric acid, ethylene diamine	4	443	80	[24]
Hydrothermal	Dopamine	3.8	400	6.4	[16]
Hydrothermal	Polyethyleneimine	3.5	460	53.4	[39]
Hydrothermal	Sodium citrate	1.6	435	68.2	[40]
Hydrothermal	Streptomycin	2.9	410	7.6	[41]
Laser ablation	Graphite	1.7	410	6.2	[42]
Laser ablation	Toluene	4.2	475	18	[43]
Microwave	Citric acid	2.6	420	20.6	[44]
Microwave	Citric acid	3.5	480	19.9	[45]
Microwave	Citric acid, urea	4	450	15	[46]
Microwave	Citric acid, urea	4	518	36	[47]
Oxidation	Carbohydrates	5	512	13	[48]
Oxidation	Carbon soot	4	520	3	[49]
Pyrolysis	Citric acid	7	420	16.3	[50]
Pyrolysis	Glucose	2.3	545	7.5	[51]
Pyrolysis	Sodium alginate	10	450	2	[52]
Thermal	Citric acid	4.2	456	88.6	[53]
Thermal	Citric acid	6	464	2.3	[54]
Thermal	Citric acid, *N*-(β-Aminoethyl)- γ-aminopropyl methyl dimethoxy silane	0.9	455	47	[55]
Thermal	Hydroquinone	7	368	16	[56]
Ultrasonic	Ascorbic acid, ammonia	3.4	446	10.9	[57]
Ultrasonic	Glucose	5	540	7	[58]
Ultrasonic	Polyamide	3	510	28.3	[18]

ultrasonic treatment,[18] and thermal decomposition techniques.[19] The advantages of CQDs such as the ability to disperse well in the aqueous environment, biocompatibility, chemical stability, and structure suitable for modification allowed CQDs to be used in different areas. Therefore, CQDs are employed in biological imaging,[20] sensors,[21] biomedical applications,[22] and material science.[23] CQDs can be produced using different precursor materials such as citric acid,[24–26] ascorbic acid,[27] ammonium citrate,[28] ethylene glycol,[29] benzene,[30] phenylenediamine,[31] phytic acid,[32] ethylenediaminetetraacetic acid (EDTA),[33,34] and thiourea.[35] In Table 1, conventional CQDs production methods, and maximum emission wavelength, quantum yield (QY, %) and reported CQDs dimensions of CQDs produced by these methods were compared.

In the literature, 2,330 research articles and 149 review articles were found in the Scopus database, which was carried out in June 2020, with the keyword "carbon quantum dots", including the title, summary, and subject contents. Figure 1 shows the number of articles published in the last decade by years. There is an exponential increase in the number of research articles with both carbon quantum dots and green synthesis content. In this review article, sensor and bioimaging applications of CQDs produced by green chemistry methods are classified and analyzed according to the synthesis methods of CQDs and summarized in Tables 2–5. In this review, the following criterion has been applied to all tabulated literature data:

- If more than one different CQDs was synthesized, the data of the CQDs providing the highest QY are given.
- If the material of different sizes is produced, the average reported size is taken.
- The wavelength of the maximum emission peak was reported. Emission color represented here are calculated RGB value of the corresponding wavelength with ±20 nm accuracy, and just for demonstration purposes.

Green chemistry strategies for carbon quantum dot synthesis

Due to the increasing demand for more sustainable processes in the chemical industry, the "Green Chemistry" field was introduced by the Environmental Protection Agency reporting a set of principles more than two decades ago. It was aimed to reduce or prevent the use of toxic and hazardous substances and to minimize or prevent waste.[59] Green chemistry provides opportunities for sustainable production as it has advantages such as minimizing environmental impact, reducing environmental burden, and improving process economy as a process that supports efforts to increase efficiency, reduce waste and improve quality.[60]

Green synthesis of nanoparticles used in comprehensive applications such as catalysis, sensor, electronics, photonics, and medicine has been a remarkable subject especially in recent years.[59] Particularly in the last decade, there has been a great deal of interest in the synthesis of CQDs and their application in various fields, due to their superior properties such as high photobleaching resistance, good biocompatibility, easy synthesis and functioning, and luminescence emission that can be changed with excitation wavelength along with the CQDs size.[61] Synthetic methods used to produce CQDs are categorized into two classes: "bottom-up" and "top-down." These production methods use chemical, electrochemical or physical processes.[62] Top-down approaches include the processes of breaking up large

Table 2. Green CQDs produced using the carbonization and pyrolysis methods, and their use in sensor and bioimaging applications.

Method	Precursor	λ_{em} max.	Size (nm)	QY (%)	Analyte	LOD	Range	Cell line	Reference
Carbonization	Alkali lignin	466	8	8	Fe^{3+}	0.44 μM	0–1000 μM		[73]
Carbonization	*Azadirachta indica*	518	6-12	NA				HeLa	[81]
Carbonization	Ice-biryani	432	3.5	41				A549	[80]
Carbonization	Lentil grain flour	510	≤50 nm	10				NA	[78]
Carbonization	Lychee peel	NA	3.1	NA	Ascorbic acid	0.14 μM	1–105 μM		[77]
Carbonization	Lychee seed	440	1.12	10.6	MB	50 μM	0.2–10 μM	HepG2	[71]
Carbonization	Mango	450	7	3.9				A549	[251]
Carbonization	Peanut shell	440	1.4	9.9				HepG2	[72]
Carbonization	Vitamin B1	475	3.5	76				CHO	[79]
Carbonization	Waste carbon paper	450	4.8	5.1	TNT	7.4 ppb	4.4 nM–26.4 μM		[74]
Carbonization	Water hyacinth	370	5.2	17	Pretilachlor	2.9 μM	5.7–61.5 μM		[75]
Carbonization	Watermelon peels	490	2	7.1				HeLa	[70]
Pyrolysis	Chia seeds	NA	4	NA	Hydrazine	39.7 μM	125–1125 μM		[85]
Pyrolysis	CDPC	450	2.8	22.3	Vitamin B12	81 nM	0.5–300 μM		[82]
Pyrolysis	EDTA	410	3.8	11	Hg^{2+}	4.2 nM	0–3 μM		[34]
Pyrolysis	Finger millet ragi	425	6	NA	Cu^{2+}	10 nM	0–100 μM		[86]
Pyrolysis	Konjac flour	434	3.4	13/22	Fe^{3+}, L- lysine	NA	NA	HeLa	[83]
Pyrolysis	Mango	525	6	18.2	Fe^{2+}	0.62 ppm	NA		[76]
Pyrolysis	Oxalic acid	426	3.3	28.7	Fe^{3+} and Ag^{+}	4.8 and 2.4 nM	1.0–130 and 0.50–200 μM		[249]
Pyrolysis	Plant leaf	461	3.7	16.4	Fe^{3+}	1 ppm	0–300 ppm		[250]
Pyrolysis	Waste polyolefins	540	2.5	4.8	Cu^{2+}	6.33 nM	1–8.0 μM.	MDA-MB 468	[84]

Agricultural Animal Biomass Fruit Insect Juice Plant Conventional Waste

Table 3. Green CQDs produced using the microwave-assisted method and their use in sensor and bioimaging applications.

Precursor	λ_{em} max.	Size (nm)	QY (%)	Analyte	LOD	Range	Cell line	Reference
Aspartic acid and urea	450	2.8	17	Myricetin	18.4 nM	1–80 μM		[87]
Citric acid, urea, sodium fluoride	600	10	1.2				C6 glioma cells	[102]
Cotton linter waste	420	10.1	NA				H2452 and HUVEC	[101]
Eggshell membrane	450	5	14	Glutathione	0.48 μM	0.5–80 μM		[88]
Flour	442	1-4	5.4	Hg^{2+}	0.5 nM	0.5–10 nM		[96]
Gallic acid	455	3	25				HeLa	[90]
Garlic	440	5	5				Macrophages	[97]
Glucose	NA	≤10 nm	NA	Ascorbic acid	10 μM	0.01–3 mM		[100]
Onion peel	450	3	NA				MG63/HFFs cells	[98]
Quince fruit	450	4.9	8.6	As^{3+}	0.02 μg/mL	0.1–2 μg/mL	HT-29	[99]
Silk fibroin	420	6.1	15				KB cells Female nude Balb/c mice	[89]
Xylan and BPEI	463	8.6	8	Tannic acid	36.8 nM	0.1–5 μM		[103]

Agricultural Animal Biomass Fruit Insect Juice Plant Conventional Waste

carbon structures to smaller dimensions using methods such as arc discharge, laser ablation, and electrochemical. On the other hand, bottom-up approaches are based on the formation of CQDs from molecular precursors with supporting synthetic techniques such as thermal routes, pyrolytic process, hydrothermal and aqueous techniques, reverse micelle technique, microwave-assisted strategy, and substance oxidation.[61,62] These methods are summarized in Figure 2, and the relative proportions of the studies discussed in this review article are also represented here.

The bottom-up approach has advantages in terms of sustainability and compliance with green chemistry principles. Among these methods, chemical or thermal oxidation of molecular precursors is an important way to synthesize CQDs in large quantities.[61] The hydrothermal method is mostly used because it is simple, repeatable, and cost-effective and can be applied to most carbon sources.[63] The luminescence efficiency of CQDs can be increased during synthesis and the use of natural resources in the synthesis of CQDs results in adjustable emission and high PL efficiency due to self-passivation and heteroatom doping (such as N, S, and P).[64] Furthermore, the addition of other elements is relatively easy and inexpensive when using natural resources. Also, the QY values of different precursors can result in a wide range of PL yields depending on the process (from 2% to 70%).[65] In this section, we focused on CQDs production methods with different green-chemistry approaches and presented them by classifying them.

Carbonization and pyrolysis methods

Carbonization and pyrolysis methods have been used for carbon production from waste biomass for many years. The fact that these methods are cheap and provide large amounts of carbon for industrial production has attracted great interest. Besides, other methods are complex (multi-step), require additional post-synthesis processes, and need expensive equipment, making carbonization and pyrolysis methods preferred.[70–72]

Using the simplicity of carbonization and using different precursors, heteroatom-doped CQDs were obtained. Jiang et al. reported a simple and green method to prepare nitrogen-doped CQDs (N-CQDs) using alkali lignin carbon sources and deep eutectic solvent as solution and nitrogen source.[73] Another N-CQDs with approximately the same PL efficiency was obtained using waste carbon paper as a carbon source.[74] The water hyacinth derivative phosphorus-doped CQDs (P-CQDs) obtained using phosphoric acid as an activator, emitted at 370 nm (17% QY) and were ~5 nm in size.[75] CQD with approximately the same PL yield was obtained by pyrolysis of mango leaves and showed excellent fluorescent properties with blue emission spectra (around 525 nm) upon excitation at 435 nm.[76] A carbonization method using the litchi peel as a carbon source has also been reported.[77] CQDs obtained using the watermelon rind contained 1.13% N and 26.6% O by mass and provided 7% QY.[70] Some green-synthesized CQDs produced by carbonization methods had approximately similar dimensions (~2 nm), quantum efficiencies (~10%), and maximum

Table 4. Green CQDs produced using the oxidation, thermal, ultrasonic, and other methods and their use in sensor and bioimaging applications.

Method	Precursor	λ_{em} max.	Size (nm)	QY (%)	Analyte	LOD	Range	Cell line	Reference
Oxidation	Bread	535	6	4.5				Human blood cells	[112]
Oxidation	Carbon black	440	15	4				MCF-7	[113]
Oxidation	Carbon soot	520	12.5	3				HepG2	[49]
Oxidation	Coconut shell	NA	1	NA	Hg^{2+}	2.5 nM	0.5–300 nM		[111]
Oxidation	Cow manure	405	4.8	65				MCF-7	[107]
Oxidation	Hair fiber	383	6	11.1				HeLa	[108]
Oxidation	Luffa sponge	473	6	2.1	Cr^{6+}	NA (~0.1 μg/L)	0–0.4 μg/L		[110]
Oxidation	Palm shell waste	410	7	NA	Nitrophenol	0.079 μM	0.2–0.40 μM		[109]
Oxidation	Plant soot	430	2-4.3	4.3				Chinese Hamster Ovary (CHO)	[104]
Oxidation	*Trapa bispinosa* peel	450	7	1.2				MDCK	[105]
Oxidation	Waste frying oil	405	1-4	3.66	pH sensing	NA	3–9	HeLa	[106]
Thermal	Banana juice	460	3	9				NA	[116]
Thermal	Coffee grounds	440	5	3.8				LLC-PK1	[65]
Thermal	Fullerenes	400	2	4.8	Fe^{3+}	20 nM	0.02–0.6 μM		[117]
Thermal	Hair	415	2-8	10.75	Hg^{2+}	10 nM	0–1 mM		[114]
Thermal	Hair	430	2.3	17				NA	[115]
Thermal	Lac dye	570	1.8	40	Ethanol	1% alcohol	1.0–50.0% v/v		[120]
Thermal	Lactose and NaOH	420	< 5	NA	Folic acid	1.2 nM	80 nM–60 μM		[119]
Thermal	Nescafe	465	4.4	5.5				SMMC-7721	[66]
Thermal	Overcooked BBQ	520	NA	40				NA	[64]
Thermal	Soya bean grounds	440	13	3				NIH3T3	[118]
Ultrasonic	Waste edible oil	472	2.5	7.5	Fe^{3+}	0.18 nM	0 – 100 μM		[122]

(*continued*)

Table 4. Continued.

Method	Precursor	λ_{em} max.	Size (nm)	QY (%)	Analyte	LOD	Range	Cell line	Reference
Ultrasonic	Dopamine in dimethylformamide	434	4	3.6	Fe^{3+}	38 nM	$0-50\ \mu M$	HepG2	[123]
Laser Ablation	Platanus biomass	447	8	32.4				HeLa	[124]
Plasma	Chicken egg	430	2.8	6-8				NA	[125]

Agricultural Animal Biomass Fruit Insect Juice Plant Conventional Waste

Table 5. CQDs produced by green chemistry and hydrothermal method and used in sensor and bioimaging applications. Sensor applications of some CQDs produced with different strategies for comparison purposes but produced with conventional methods without using a green chemistry approach are also given.

Precursor	λ_{em} max.	Size (nm)	QY (%)	Analyte	LOD	Range	Cell line	Reference
Aegle marmelos leaves	450	6	22	Fe^{3+}	0.12 μM	0–300 μM		[126]
Apple juice	465	4.5	4.3				Bacteria, and fungi	[180]
Apple juice	428	2.8	6.4	Hg^{2+}	2.3 nM	5–100 nM		[181]
Azadirachta indica	467	3.2	27.2	Peroxide	0.035 mM	0.1–0.5 mM		[127]
Bagasse	450	1.8	12.3				A549	[160]
Banana juice	410	1.3	32	Cu^{2+}	0.3 μg/mL	1–800 μg/mL		[176]
Bee pollen	425	1.6	12.8				LoVo	[203]
Beetroot extract	450	5	6				Caenorhabditis elegans, and BALB/c mice	[163]
Bitter orange juice	440	1.5	19.9				SKBR3 and NIH/3T3 mouse embryonic fibroblast	[178]
Biomass tar	420	2.6	26.1	Fe^{3+}	60 nM	0.06–1400 μM		[212]
Bombyx mori silk	450	5	13.9				A549	[202]
Broccoli	450	4	NA	Ag^{+}	0.5 µM	0–600 µM		[164]
Cabbage	432	4	16.5				HaCaT	[152]
Carica papaya juice	488	3	7				Bacteria	[183]
Cellulose/ionic liquid	444	5	28.9	Fe^{3+}	0.40 μM	2.5–500 μM		[213]
Cherry tomatoes	430	7	9.7	Trifluralin	0.5 nM	0.050–200 μM		[165]
Chicken blood	440	2.4	NA	Cysteine	0.4 μM	0.5–20 μM		[209]
Chitosan	418	6	6.6	Fe^{3+}	1.57 μM	0–0.18 mM		[217]
Chitosan	410	2	NA	Fe^{3+}	0.15 μM	0–200 μM		[218]
Cigarette filter	465	8	14	Sudan I	0.95 μM	2.40–104.0 μM		[216]
Cinnamon, red chili, turmeric, and black pepper	465, 477, 460 and 489	3.4, 3.1, 4.3, and 3.5	35.7, 26.8, 38.3 and 43.6				LN-229 and HK-2	[128]

(*continued*)

Table 5. Continued.

Precursor	λ_{em} max.	Size (nm)	QY (%)	Analyte	LOD	Range	Cell line	Reference
Citric acid	410	2.8	52	Fe^{3+}	1.3 μM	2–50 μM		[219]
Citric acid	450	2	50				MCF-7	[220]
Citric acid	594	4.4	29	Fe^{3+}	9.7 nM	50 nM–4 μM		[221]
Citric acid and ammonia	440	2	35.4	Hg^{2+}	1.48 nM	0–10 μM		[223]
Citric acid and boric acid	405	2.3	30.8	Amoxicillin	0.83 μM	1.43–429 μM		[224]
Citric acid and ethylene diamine	445	3.9	NA	Acrylamide	0.81 μM	5–500 μM		[252]
Citric acid and urea	443	3	35.6				HeLa	[222]
Citrus lemon	452	3	31	Hg^{2+}	5.3 nM	0.001–1 μM	MCF-7	[147]
Coccinia indica	440	5	14.2	Hg^{2+}	3.3 nM	0–0.025 mM		[156]
Cocoon silk	430	70	38	Hg^{2+} and Fe^{3+}	NA	50–250 μM	HeLa and 293T cells	[197]
Collagen	510	1.3	15				RL-14 human fetal ventricular cardiomyocytes	[214]
Corncob	414	9.3	NA	Fe^{3+}	0.75 μM	0–321 μM		[166]
Cornstalk	450	2.9	NA	*Candida albicans*	1124 cfu/mL	2.60×10^5-1.99×10^8 cfu/mL		[167]
Crown daisy leaves	380	7.5	NA	Cu^{2+}	1 nM	10 nM–120 nM		[135]
Cyanobacteria biomass	439	2.5	9.2				PC12	[207]
Dried shrimp	475	6	54				MCF-7	[196]
Eggshell membrane	420	8	9.6	Hg^{2+}	2.6 μM	10–100 μM		[208]
Eleocharis dulcis juice	493	3	11.2	Fe^{3+}	0.56 μM	50–350 μM		[182]
Enteromorpha prolifera	450	2.8	8	Fe^{3+}	0.5 μM	0–1.7 mM	HeLa	[168]
Foxtail millet	413	2	21.2	Fe^{3+}	0.046 μM.	5–150 μM		[149]
Fructose and L-cysteine	405	5	NA	Clenbuterol	23 pg/mL	0.07–1.7 ng/mL		[215]
Fungus fibers	440	6.5	28.1	Tetracycline	15.6 nM	0.5–47.6 μM	HepG2	[148]

Garlic	442	11		17.5				MCF-7	[151]
Ginger	420	4.3		13.4				HepG2, MCF-10A, HeLa, A549, MDA-MB-231	[159]
Glucose and monopotassium phosphate	435	2.8		2.4				HepG2	[254]
Graphene oxide and ammonia	436	3.5		24.6				HeLa	[225]
Grape juice	429	2.7		13.5				HeLa	[179]
Grape peel	419	1.5–3.0		3.1	Fe^{3+}	NA	0–1000 μM	HeLa	[193]
Grapefruit peel	510	4.2	NA		p53 protein	2.7 pg/mL	0.01–50 ng mL^{-1}		[194]
Grass	443	3–5		2.5-6.2	Cu^{2+}	1 nM	0.5–2.5 μM		[136]
Hair	480	29–80		24.8	Hg^{2+}	3.7 nM	10–100 nM.		[198]
Honey	420	2		19.8	Fe^{3+}	1.7 nM	5 nM–100 μM	Hep-G2 and HeLa	[200]
Hydroquinone and BBr_3	368	16		14.8	Glucose	8 μM	8–80 μM		[56]
Jackfruit	485	2.5		14.6	Hg^{2+}, and Cr^{6+}	8 nM, and10 nM	5–70 nM		[153]
Jinhua bergamot	440	10		50.78	Hg^{2+} and Fe^{3+}	5.5 nM (Hg^{2+}) and 0.075 μM (Fe^{3+})	0.01–100 μM for Hg^{2+} and 0.025–100 μM for Fe^{3+}		[145]
Jujube	530	3.1	NA		Fe^{3+}	NA	0–200 μM		[137]
Lemon juice	631	4.6		28				HeLa	[174]
Lemon juice	540	4.5		79	V^{5+}	3.2 ppm	0–100 ppm		[173]
Lemon juice	482	3.1		16.7				Onion epidermal cell	[175]
Lemon peel	441	1–3		14	Cr^{6+}	~ 73 nM	2.5–50 μM		[195]
Mandelic acid	429	2.5		41.4	Picric acid	0.041 μM	0.5–30 μM		[211]
Maojian green tea	385	13		12.8	Hg^{2+}	6.32 nM	200 nM–60 μM		[132]
Milk	454	3		12				U87	[204]
Milk	460	4		7.6				SMMC-7721	[206]

(*continued*)

Table 5. Continued.

Precursor	λ_{em} max.	Size (nm)	QY (%)	Analyte	LOD	Range	Cell line	Reference
Mustard seeds	423	4.6	4.6	Peroxide	0.015 mM	0.02–0.20 mM		[253]
Ocimum tenuiflorum	405	2	11.5	Malachite green	18 nM	0–120 nM		[138]
Oil palm waste	440	6	24.6				Vero cells	[188]
Onion waste	464	7-25	28	Fe^{3+}	0.31 μM	0–20 μM	HEK-293 and HeLa	[187]
Orange peel, ginkgo biloba leaves, paulownia leaves, and magnolia flower	445, 435, 435, 435	2.6	4.3, 7.7, 4.7 and 8.1	Fe^{3+}	0.073 μM	0.2–100 μM		[139]
Orange waste peel	431	4.5	36				NA	[186]
Orange juice	455	2.5	26				L929 and MG-63	[177]
Orange pericarp	524	2.9	2.9				NA	[191]
Orange waste peel	432	2.9	11.4				NA	[192]
Papaya	450	2–6/8–18	18.39-18.98	Fe^{3+}	0.29 and 0.48 μM	10–800 μM and 1–8 μM	HeLa	[150]
Pear, avocado, and kiwi	538, 529, and 538	4.1, 4.4, and 4.4	20, 35, and 23				HK-2 and Caco-2	[146]
Phyllanthus acidus	411	5	12.5				*Caenorhabditis elegans*	[157]
Pig liver	416	5	NA	Permanganate	0.06 μM	0.1–50 μM		[205]
Pigskin	460	3.5–7.0	24.1	Co^{2+}	0.68 μM	1–300 μM	HeLa	[199]
Pinellia ternata	444	5.2	21.3	Cr^{6+}	15 nM	0–200 μM		[129]
Pipe tobacco	450	5	3.2	Cu^{2+}	0.01 μM	0–40 μM		[255]
Polycyclic aromatic hydrocarbon	498	5.5	11.7				MCF-7	[226]
Pomelo peels	444	2–4	6.9	Hg^{2+}	0.23 nM	0.5–500 nM		[190]
Potato	474	3.2	6.1				*E. coli* and *S. cerevisiae* cells	[162]
Prickly pear cactus	446	5.6	12.7	As^{3+} and ClO^{-}	2.3 nM and 0.016 μM	2–12 nM and 10–90 μM		[158]
Prosopis juliflora	437	5.8	5	Hg^{2+}	6.3 nM	5–500 ng/mL		[141]

Purple perilla		450	2.8		9	Ag^{+}	1.4 nM	0–3000 nM	HeLa [134]
Rice residue and glycine		440	2.7		23.5	Fe^{3+}	0.7462 μM	3.32–32.26 μM	[189]
Sandalwood		458	3.5		12				MG-63 [161]
Scallion leave		418	3.5		3.2	Hemin	0.1 μM	0.5–10.0 μM	[142]
Scindapsus leaves		458	4	NA					NA [143]
Soy milk		475	26.5		2.6				NA [169]
Spider silk		447	178		17.6				U87 cell [201]
Strawberry juice		427	5.2		6.3	Hg^{2+}	3 nM	10 nM–50 μM	[185]
Sugar cane juice		474	2.7		5.8				*E. coli* and *S. cerevisiae* cells [162]
Sweet corn		470	2.4		14.6	Sulfide ions	8 nM	5–100 nM	Human RBCs, Vero, and A549 [154]
Sweet potato		442	2.5-5.5		8.64	Fe^{3+}	0.32 μM	1–100 μM	HeLa and HepG2 [171]
Sweet potato		442	1-3		2.8	Hg^{2+}	1 nM	0.01–0.12 μM	[172]
Tamarindus indica leaves		433	3.4		46.6	Hg^{2+}	6 nM	0–0.1 μM	[130]
Tartaric acid and bran		539	4.9		46	Cu^{2+}	0.05 μM	0–0.5 mM	[210]
Tetrahydrofuran		460	6.5		11.5	Ag^{+}	0.08 μM	0.2–50 μM	[227]
Conventional Chinese medicine		430	35		11.5	Hg^{2+}	8.2 nM	50 nM–100 μM	[131]
Walnut oil		420	12		14.5				PC3, MCF-7 and HT-29 [155]
Waste green tea		436	5		12				HeLa, HepG2, and B16F10 [133]
Watermelon juice		439	5		10.6	Fe^{3+} Cysteine	0.16 μM 0.27 μM	0–300 μM 0–250 μM	HepG2 [184]
Willow bark		444	1–4		6				NA [170]
Willow leaves		NA	2–4	NA					NA [144]

Agricultural Animal Biomass Fruit Insect Juice Plant Conventional Waste

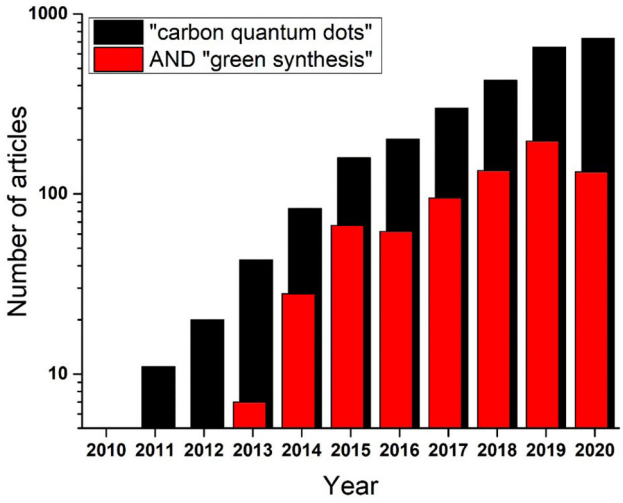

Figure 1. Number of related articles obtained by Scopus database search dated June 2020.

emission wavelength (~450 nm). Lychee seed and peanut shells were used as precursors in the synthesis of these CQDs.[71,72] Compared to these CQDs, slightly larger particles (≤50 nm) were synthesized as CQDs using a lentil grain flour precursor.[78] The highest QY value of 76% obtained using the carbonization method was from vitamin B1 precursor.[79] Processing food-waste with carbonization methods to obtain CQDs also reported recently to provide a high efficiency of 41% at 432 nm maximum emission.[80] Stabilizing these CQDs using the nitric acid treatment and glutathione contributed to this high QY. In another study where ayurvedic leaves (*Azadirachta indica*, *Ocimum tenuiflorum*, and *Tridax procumbens*) were used as precursors, the produced CQDs had a maximum emission at 518 nm.[81]

The highest QY (22.3%) N, P-CQDs obtained by pyrolysis were produced by co-pyrolysis of cytidine diphosphate choline (CDPC) and ethylenediamine showing strong emission at 450 nm as illustrated in Figure 3.[82] Another green-CQDs with 22% QY was produced by pyrolysis using Konjac flour precursor and had a maximum emission at 434 nm.[83] It has been proven that using the pyrolysis method together with suitable precursors, green-CQDs with high luminescence efficiency can be produced. CQDs that provide lower QY were also produced with the pyrolysis method. Kumari synthesized CQDs using waste polyolefin as a carbon source and pyrolysis in the initial phase and then ultrasonic-assisted process. The PL efficiency of the 2.5 nm dots emitting at 540 nm was ~5%.[84] Besides, there is also CQDs synthesis using pyrolysis and chia seeds&finger millet ragi (*Eleusine coracana*) as a carbon source.[85,86]

Microwave-assisted methods

Microwave-assisted methods are generally desired in the production of green-CQDs because they can be applied easily and quickly with repeatable temperature adjustments. With this method, various green-CQDs with PL efficiency ≥15% are produced using different carbon sources. N-CQDs were synthesized from aspartic acid and urea precursor using the microwave-assisted method and had a strong emission at 450 nm and an average size of 2.8 nm.[87] In the study conducted by Wang et al., the first study in microwave-assisted green-CQDs production, CQDs with 14% QY at 450 nm were produced from eggshell membrane precursor.[88] CQDs with approximately the same PL performance was produced using silk fibroin as the carbon source.[89] Within this method, the highest PL efficiency was reported by Lu using gallic acid as a carbon source (QY 25%@ 455 nm λ_{em}).[90]

Various precursors such as, eutrophic algae flowers,[91] rose petals,[92] crab shell with chitin content and Gd^{3+}, Eu^{3+} and Mn^{2+} additive,[93] winged animal feather containing 16.3% N, 1.90% S and 33.3% O by mass,[94] silkworm chrysalis containing 5.72% N by mass (QY 46%),[95] flour (QY 11%),[96] garlic (QY 5%),[97] onion peel,[98] quince fruit (QY 8.6%),[99] glucose[100] and cotton linter waste containing ~5% N and S by mass,[101] were used in the microwave supported green-CQDs synthesis. The quantum yields of CQDs produced with these precursors are generally higher than the CQDs with N and F additives (QY 1.2%) synthesized using the conventional precursor citric acid, urea, and sodium fluoride.[102]

Recently, Yang et al. synthesized polyamine-functionalized CQDs from xylan and branched polyethyleneimine from renewable sources using a microwave-assisted method. These ~9 nm CQDs with an emission maximum at 463 nm had 8% efficiency and showed excitation-independent emission behavior.[103] CQDs were also produced using gallic acid precursor provided 25% QY at 455 nm emission peak and was shown to be utilized as a bioimaging material and retain the antitumor activity gallic acid.[90]

Oxidation, thermal, and ultrasonic methods

Oxidation, thermal and ultrasonic methods are among the methods that are easy to apply and suitable for the production of fluorescent particles with very high PL efficiency.[62] Many different precursors have been reported in green-CQDs synthesis by the oxidation method. In the earlier reports, CQDs production from plant soot, *Trapa bispinosa* peel, and waste frying oil precursors with QY between 1 and 4% and a particle size between 1 and 7 nm were reported.[104–106] In addition to these precursors, cow manure[107] with a very high QY (65%) and hair fiber[108] precursors (QY 11% and λ_{em} 383 nm) were successfully used in the production of CQDs with oxidation.

Soni et al. used palm shell powder and triflic acid to produce N and S co-doped CQDs. Their CQDs (~7 nm) had a graphitic-like structure with narrow size distribution and exhibited a bright green fluorescence (@410 nm).[109] Luffa sponge derivative CQDs had emissions at 473 nm with 2.1% QY.[110] Also, oxidative methods have been reported in which coconut shells and bread are used as precursors and CQDs with ~4% QY are produced.[111,112] In two methods (QY < 4%) using oxidation and conventional precursors,

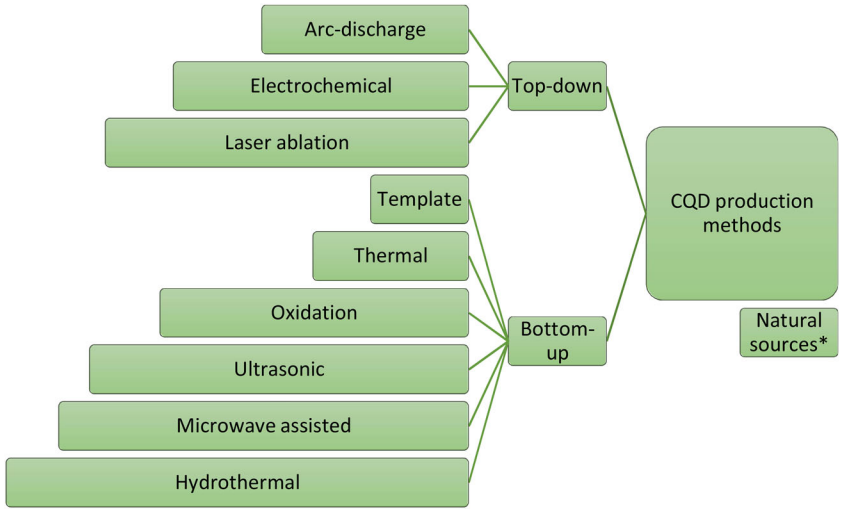

Figure 2. Various methods for the CQDs synthesis (Inspired by Singh et al.[62]). *The presence of CQDs in natural resources has been demonstrated in several studies. Instant coffee powder (Nescafe®, QY 5.5%),[66] commercial beer (QY 7.4%),[67] honey[68] and tea[69] are known examples.

13 nm and 15 nm size CQDs with an emission maximum at 520 and 440 nm were obtained.[49,113]

Different precursors have been used in obtaining green-CQDs with thermal methods. Hair, as in the oxidative method, was used as a precursor in this method, and a very high 11% to 17% QY was obtained.[114,115] Since creatine contains high levels of C, N, and O, the CQDs produced is N doped. Another material, coffee grounds, was used as a precursor and CQDs with 3.8% QY (λem@440 nm) were produced.[65] In one of the first thermal method CQDs studies, banana juice derived CQDs provided 9% QY.[116] The average 2 nm size CQDs produced in a study using fullerenes as a conventional precursor had 4.8% QY, and these CQDs had nearly similar performance to green-synthesized CQDs.[117]

Compared to other CQDs produced by the thermal method, CQDs with low QY was reported in two separate studies using soybean grounds, and lactose and NaOH as precursors.[118,119] Liu et al. synthesized a highly photoluminescent (40% QY@570 nm) CQDs with a mean diameter of 1.76 nm for the first time using lac dye as a precursor by one-pot ethanol thermal method.[120] An interesting precursor used in the thermal method is urine with a high nitrogen content.[121]

The use of waste kitchen chimney oil (7.5% QY@472 nm) and dopamine (3.6% QY@434 nm) precursors have been reported in green-CQDs production by ultrasonic methods.[122,123] CQDs produced with dopamine have also been reported to exhibit possess superior water dispersibility and stability, bright and stable fluorescence against variations of pH and ionic strength, low cytotoxicity, and high photostability.[123]

The laser ablation method, which is rarely encountered, was used in CQDs production using Platanus biomass precursor and with an average size of 8 nm CQDs, an emission maximum of 447 nm, 32% QY was obtained.[124] Another rare method is plasma treatment, and in a previous study, Wang et al. produced CQDs with 8% QY using chicken egg precursor.[125] It has been reported that another advantage of direct solid-state synthesis is CQDs product yield, and the product can be obtained with a yield of up to 95%.[114]

Hydrothermal methods

Hydrothermal methods are frequently preferred in the production of green-CQDs. The proper control of the conditions and product uniformity are some of the main reasons for choosing this method. Natural resources such as plant leaves, juices, fruit peels are precursors that are successfully used in the hydrothermal synthesis of green-CQDs.

CQDs with high QYs were obtained using various leaf-based green-precursors such as Aegle marmelos (22%),[126] *Azadirachta indica* (27%),[127] cinnamon (36%), red chili (27%), turmeric (38%) and black pepper (44%),[128] *Pinellia ternata* (21%),[129] and *Tamarindus indica* (47%).[130] Figure 4 shows the synthesis of CQD using a leaf-based green-precursor, *Tamarindus indica.* Moreover, CQDs with somewhat low PL efficiencies were obtained using the leaves of conventional Chinese medicine (12%),[131] Maojian green tea (13%),[132] waste green tea (12%),[133] and purple perilla (9%)[134] as a precursor. Studies utilizing crown daisy, grass, jujube, *Ocimum tenuiflorum*, orange peel, ginkgo biloba, paulownia and magnolia flower, pipe tobacco, *Prosopis juliflora*, scallion, scindapsus, and willow leaves have also been reported.[135–144]

CQDs synthesis methods have also been reported in which plants, fruits and plant roots are used as precrusors. Jinhua bergamot (51%),[145] pear, avocado and kiwi (20, 35, and 23%),[146] citrus lemon (31%),[147] fungus fibers (28%),[148] foxtail millet (21%),[149] papaya (19%),[150] and garlic (18%)[151] were used as precrusor for high PL efficiency CQDs. Green- CQDs have somewhat lower PL than these, but >10% QY were produced using precrusors such as, cabbage (17%),[152] jackfruit (15%),[153] sweet corn (15%),[154] walnut oil (15%),[155] *Coccinia indica* (14%),[156] *Phyllanthus acidus* (13%),[157] prickly pear cactus (13%),[158] ginger (13%),[159] bagasse (12%),[160] and sandalwood (12%).[161] In this group, CQDs were also hydrothermally synthesized using potato, beetroot extract, broccoli, cherry

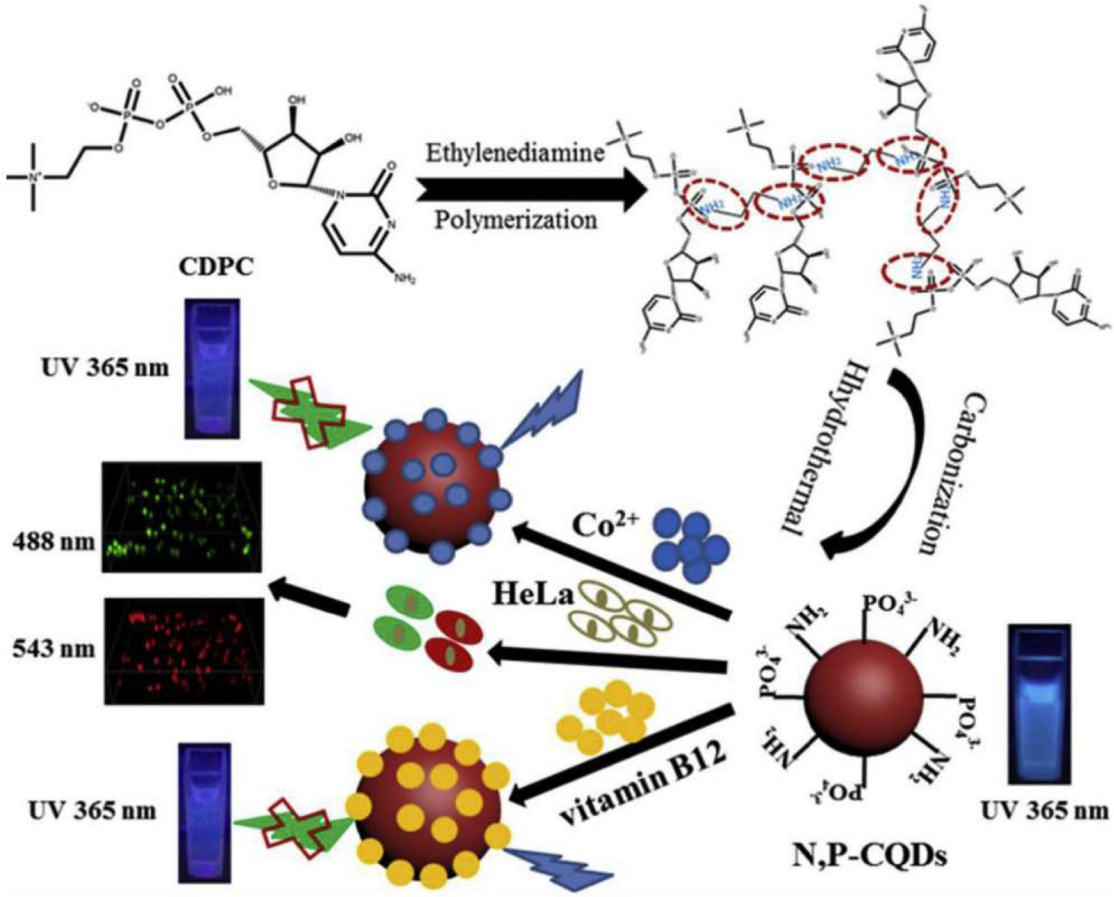

Figure 3. Schematic illustration of the one-step synthesis of bio-inspired CQDs for sensitive and selective detection of vitamin B12 and Co^{2+}. Cellular imaging in living cells was also demonstrated. Reproduced from Ref.[82]

tomatoes, corncob, cornstalk, *Enteromorpha prolifera*, soy milk, willow bark, and sweet potato precursor.[162–172]

Fruit juices are also a good candidate used in the hydrothermal method to produce CQDs with high PL efficiency. Lemon juice (79%, 28%, and 17%),[173–175] banana juice (32%),[176] orange juice (26%),[177] bitter orange juice (20%),[178] and grape juice (14%)[179] precursors were used in the hydrothermal synthesis of green-CQDs. In addition to those specified, CQDs with QY ≤11% were also produced by hydrothermal method using precursors such as apple juice,[180,181] *Eleocharis dulcis* juice,[182] carica papaya juice,[183] watermelon juice,[184] strawberry juice,[185] and sugar cane juice.[162]

Food wastes are another hydrothermal green-CQDs precursor. CQDs with rather high PL efficiency was obtained using the hydrothermal treatment of orange peel waste (36%),[186] onion waste (28%),[187] oil palm waste (25%),[188] and rice residue and glycine (24%)[189] precursors, in the literature. Also, relatively low PL efficiency CQDs were obtained from pomelo peels, orange pericarp, orange waste peel, grape peel, grapefruit peel, and lemon peel precursors.[190–195] Another commonly used type of abundant precursor is an animal and insect-borne carbon precursors. In this context, CQDs with high PL efficiency were synthesized using dried shrimp (54%),[196] cocoon silk (38%),[197] hair (25%),[198] pigskin (24%),[199] honey (20%),[200] spider silk (18%),[201] *Bombyx mori* silk (14%),[202] bee pollen (13%),[203] and milk (12%).[204] CQDs with relatively lower QY values were produced with the hydrothermal treatment of pig liver, milk, *Cyanobacteria* biomass, eggshell membrane, and chicken blood precursors.[205–209]

CQDs that show successful results using biological origin precursors such as tartaric acid and bran (46%),[210] mandelic acid (41%),[211] biomass tar (26%),[212] cellulose/ionic liquid (15%),[213] and collagen (15%)[214] were also produced by hydrothermal route. Besides, fructose and L-cysteine, an interesting abundant resource cigarette filter, and chitosan-based CQDs synthesis have also been reported.[215–218]

When comparing CQDs produced by the hydrothermal method in general, it is seen that the reported QY for CQDs produced with conventional precursors is quite high. For example, 2.8 nm CQDs with a maximum emission of 410 nm obtained with citric acid precursor with 52% QY.[219] CQDs synthesized with other conventional precursors also shown good PL performance such as citric acid only: 50% and 29% QY,[220,221] citric acid and urea precursor (N-CQDs): 36% QY,[222] citric acid and ammonia precursor (N-CQDs): 35% QY,[223] and citric acid and boric acid precursor (B-CQDs) 31% QY.[224] Also, conventional precursors such as graphene oxide and ammonia,[225] hydroquinone and BBr_3,[56] polycyclic aromatic hydrocarbon,[226] and tetrahydrofuran[227] were used in the production of stable CQDs with QY >10%.

In Figure 5, the maximum emission wavelength, particle sizes, and QY values of the CQDs produced with

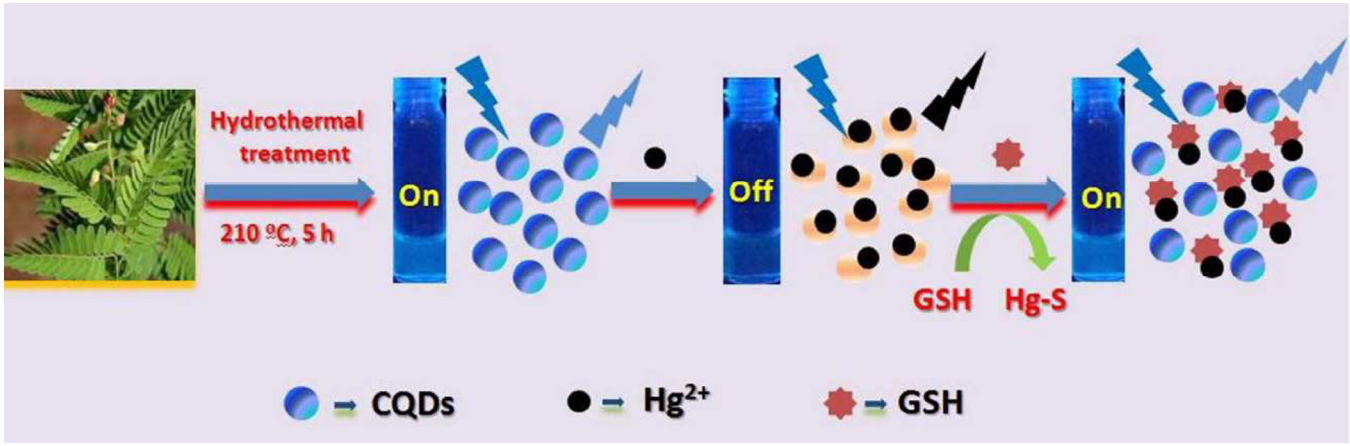

Figure 4. Schematic representation of the synthesis of CQD using a leaf-based green-precursor, *Tamarindus indica* (QY of 47%). A simple and one-step hydrothermal treatment of the leaves was applied and demonstrated in a turn-off and turn-on sensing system. Reproduced from Ref.[130] with permission from The Royal Society of Chemistry.

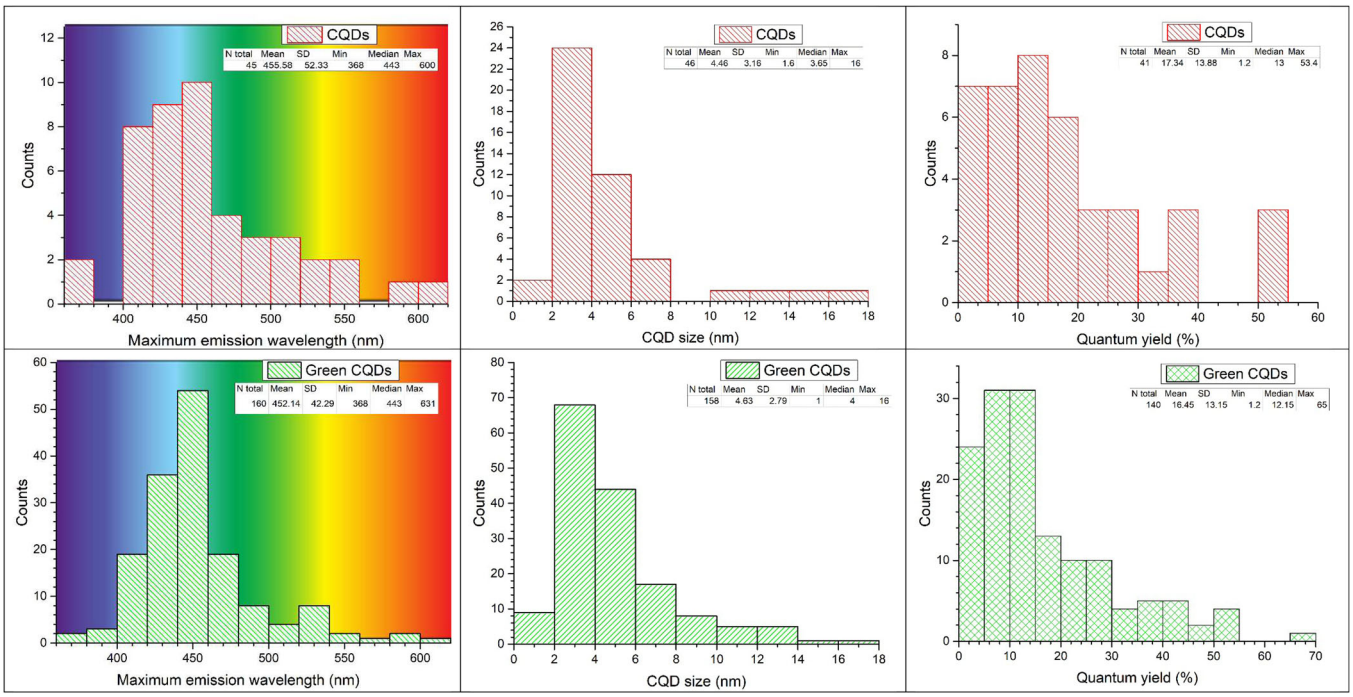

Figure 5. Comparison of the maximum emission wavelength, CQDs size, and CQDs QYs of CQDs produced using various green chemistry and conventional methods. Statistical data are given on the chart.

conventional methods and green-synthesis are compared ($N > 40$ for conventional methods and $N \geq 140$ for green-chemistry). Considering the maximum emission wavelength, it is seen that the CQDs produced by conventional methods have a distribution at 400–460 nm emission maximum. In CQDs produced with green-chemistry, distribution at 450 nm is noticeable for maximum emission. Also, it can be said that CQDs produced with green-chemistry emit at higher wavelengths (red-shift) compared to those produced by conventional methods and are therefore more "greener".

It is seen that the average maximum emission values (both mean and median) are around 450 nm for both groups. It is interesting to note that the CQDs size distribution is similar in both methods. Both mean and median values were approximately the same in both classical and green-chemistry methods, and an average CQDs size of around 4.5 nm was generally achieved. However, considering the QY values of CQDs, it should be noted that while there is a 10% difference in maximum QY, mean and median values are also close to each other. While the distribution of QY 0–20% values is observed with conventional methods, a dense distribution between 0 and 15% is observed with green-chemistry methods. However, it can be concluded that the CQDs produced using both approaches are not so different, after all.

Green CQDs in sensor applications

CQDs are excellent candidates in colorimetric sensor applications as an alternative to conventional fluorescent dyes. The high photoluminescence efficiency of CQDs has been used by many researchers in sensor applications using model analytes. A comparative list of CQDs produced with green chemistry and used in sensor applications is given in Table 2–5. Also, sensor applications of some CQDs produced with different strategies but produced with conventional methods without using green chemistry are given for comparison purposes. The reason why CQDs are preferred in fluorescent-based specific sensor applications is unique advantages such as high photostability and high colloidal solubility in aqueous media, high surface area/volume ratio, surface functionality that can be changed by easy modification methods, the possibility of using multimodal applications, and narrower spectral bands compared to other carbon-based nanomaterials.[228]

In one of the sensor applications of CQDs synthesized using a green chemistry approach, metal ions are generally determined from different aqueous environments. When metal ions interact with CQDs with high selectivity, they cause new electron-hole recombination through energy transfer. In this case, the fluorescent intensity of the CQDs varies, resulting in a measurable signal.[136] In some cation detection strategies, the analyte, which interacts with carboxyl or amine groups on the surface of CQDs, causes the creation of a new non-radiating electron-hole pair and quenching of CQDs fluorescence.[96,190] Similar mechanisms are also valid for the detection of other multivalent cations using the fluorescence method with CQDs.[195,229] Generally, during sensor applications of green-synthesized CQDs, changes in fluorescence properties occur through different mechanisms such as resonance energy transfer, internal filter effect, photo-induced electron, and charge transfer.[199] The sensitivity of some green synthesized CQDs to pH has also been reported, and this sensitivity is associated with the protonation of the carboxyl group on the CQDs surface.[92,106]

Doped CQDs (N-CQDs, sulfur-doped: S-CQDs boron-doped: B-CQDs, etc.) gave even more successful results in the determination of multivalent cations. In addition to the self-passivization of materials used in green chemistry, additional N-CQDs,[136,185,199,230–232] S-CQDs,[106] and branched polyethyleneimine (BPEI) capped CQDs[233] were reported.

For multivalent cation detection, CQDs produced from various precrusors including tea,[69] urine,[121] hair,[114] bergamot,[145] *Ocimum sanctum*,[234] honey,[200] wool,[235] coriander leaf,[236] papaya,[150] rose heart radish,[237] *Prunus avium*,[238] banana,[239] onion waste,[187] bamboo leaves,[233] pig skin,[199] peach gum,[232] and lemon peel[195] has been reported in the literature. In addition, CQDs for the detection of some toxic anions have been produced using precrusors including sweet pepper,[240] fish scales,[241] carrot,[242] and banana.[239] Moreover, CQDs-based intra/inter-cellular biosensors have been used to visually monitor the glucose,[243] cellular copper,[244] phosphate,[245] iron,[24] potassium,[246] pH,[247] and nucleic acid.[248]

Carbonization and pyrolysis methods

Carbonization is another widely used method in CQDs production using a green precursor. Green CQDs produced with this method has been used in sensor applications of different analytes and some applications encountered in the literature have been listed in Table 2. Shu et al. recently used the CQDs they synthesized using the litchi peel as an ascorbic acid sensor. The CQDs that show peroxidase-like activity were used to detect absorbance change, first by the oxidation of tetramethylbenzidine and then by reduction with ascorbic acid in the presence of peroxide. Their results showed that ascorbic acid can be detected in commercial beverages with a low detection limit (LOD) of 0.14 μM and in the range of 1.0–105 μM.[77] Another group of researchers reported colorimetric sensors for methylene blue (MB with 50 µM LOD) using litchi seeds.[71]

Immense efforts have been made on the production of CQDs with carbonization methods as nitrogen-doped. In one study, N-CQDs were obtained using waste carbon paper as a CQDs precursor and 3-aminopropyl triethoxysilane as a nitrogen source, and the resulting CQDs were used as trinitrotoluene (TNT) colorimetric sensor. Researchers reported that this N-CQDs based sensing probe selectively shows high sensitivity for TNT in the 4.4 nM–26.4 μM range, and delivers a 7.4 ppb detection limit.[74] In another study using N-CQDs, the detection of Fe^{3+} with alkaline lignin-based CQDs was performed sensitively and selectively for Fe^{3+} with a LOD of 0.44 μM.[73] Phosphoric acid was also used in one study as an activating agent and water hyacinth as a precursor for P-CQDs, an analysis of soil contaminated with pretilachlor (an herbicide) was performed and 2.9 μM LOD was reported.[75]

Pyrolysis is one of the inexpensive, green, and one-pot synthesis methods used in the production of CQDs from green precursors. Sensor applications of green-CQDs produced with pyrolysis encountered in the literature are also compared in Table 2. Singh et al. have recently reported CQDs using mango leaves to develop an efficient sensing platform for metal ions.[76] The synthesized CQDs had the sensing potential to detect Fe^{2+} ions in water and real sample with a limit of detection of 0.62 ppm. In another study, it was reported that Cu^{2+} strongly quenched the fluorescent intensity of CQDs produced by pyrolysis of the finger millet ragi. In this study, CQDs have been applied in sensing of Cu^{2+} in real water samples with LOD of 10 nM and the range from 0 to 100 µM. In a study where Cu^{2+} is detected in real water samples, the synthesized CQDs shown excellent selectivity and sensitivity toward Cu^{2+} ions with a 6.33 nM LOD, and linear detection range of 1–8.0 µM using waste olefin-based green CQDs.[84]

Wang et al. proposed a green, low-cost, and straightforward method for the synthesis of highly fluorescent biomimetic CQDs that have been developed via pyrolysis of CDPC and ethylenediamine. The CQDs they developed was successfully applied to probe vitamin B12 in living cells, which broaden its potential application in vivo system, over 0.5–300 μM detection range with 81 nM LOD.[50] Sha et al. reported a highly sensitive and selective electrochemical

sensor for the detection of hydrazine using CQDs for the first time that was synthesized by pyrolysis of chia seeds.[85] In their study, they were able to detect hydrazine in a wide detection range (125–1125 µM) with a LOD value of 39.7 µM.

There are also CQDs produced with the pyrolysis method using conventional precursors and cation determination studies performed with them. For example, in a study, highly efficient CQDs (QY∼29% at 426 nm maximum emission) obtained using oxalic acid precursor provided 4.8 and 2.4 nM LOD value in the detection of Fe^{3+} and Ag^{+} as shown in Figure 6.[249] In other studies, using the pyrolysis method, CQDs produced from oriental plant leaves and konjac flour was used for the Fe^{3+} detection.[83,250] Mercuric ion detection was also performed in the range of 0–3 µM with 4.2 nM LOD using EDTA precursors.[34]

Microwave-assisted methods

Microwave-assisted heating and carbonization methods have been preferred in various studies in terms of ease of use and fast production. The sensor applications of green-CQDs produced using the microwave-assisted method are summarized in Table 3. In a study where CQDs were prepared via green and straightforward microwave-assisted heating method using aspartic acid and urea as precursors, Liu et al. reported a label-free fluorescent sensor for the determination of myricetin. The developed CQDs sensor was sensitive to myricetin with a wide linear detection range of 1 to 80 µM and a low LOD of 18.4 nM in red wine samples.[87]

A polyamine-functionalized CQDs from xylan and BPEI precursors have been synthesized using a microwave-assisted method by Yang et al.[103] They reported a tannic acid sensor that was used for real lake water and white wine samples with a dynamic range from 0.1 to 5 µM and reported a LOD of 36.8 nM. Ascorbic acid was detected successfully in the dopamine and uric acid interfering molecules environment using CQDs derived from glucose in a green-CQDs based electrochemical sensor approach (10 µM LOD).[100]

In an earlier study, microwave-assisted green synthesized flour derivative CQDs were used for the detection of Hg^{2+} in real samples.[96] The glutathione sensor was developed in one of the first studies of microwave-assisted green-CQDs synthesis from eggshell membrane precursor by Wang et al.[88] In a more recent study, Ramezani et al. developed an As^{3+} sensor operating in the detection range of 0.1–2 µg/mL with a LOD of 0.02 µg/mL using quince fruit derivative CQDs.[99]

Oxidation, thermal, and ultrasonic methods

CQDs produced by oxidation, thermal and ultrasonic methods are generally of high purity and the size control of CQDs can be easily achieved. These methods used in the synthesis of green CQDs are discussed comparatively in Table 4. Oxidation methods generally refer to chemical oxidation and are preferred due to their low cost, high purity of produced CQDs, high efficiency, and easy size control of produced CQDs. In the first sensor study of CQDs developed with the oxidation method, waste frying oil was used as a precursor and the obtained CQDs were tested as pH sensors in the range of 3–9 pH.[106] Soni et al. used N and S co-doped CQDs prepared using palm shell powder and triflic acid on the sensor they developed for nitrophenol and its derivatives. This sensor was used for nitrophenol detection with a LOD of 79 nM in the linear detection range of 0.2–0.40 µM.[109] Recently the fluorescence quenching effect of Cr^{6+} ion on CQDs was investigated by Luo et al.[110] In this study, Cr^{6+} ion detection in the range of 0 to 0.4 µg/L was performed using luffa sponge based activated carbon fiber-based CQDs (∼0.1 µg/L LOD). In an electrochemical Hg sensor study, the detection was performed against various excess of interfering ions with a wide linearity range (0.5–300 nM) and the lowest LOD value (2.5 nM). In this study, Barvin et al. used the CQDs obtained by chemical oxidation from the coconut shell.[111]

Thermal methods, on the other hand, are very similar to hydrothermal methods and it is a process where different solvents are used instead of water. In one of the first reported studies, CQDs obtained using human hair were used to detect Hg^{2+}.[114] In a study using fullerene as conventional precursors, Fe^{3+} detection was performed with a LOD value of 20 nM in the detection range of 0.02–0.6 µM.[117] In a more recent study, CQDs produced using lactose and NaOH were used for the detection of folic acid in the range of 80 nM–60 µM with a LOD value of 1.2 nM.[119] Ultrasonic methods have also been used in the production of different CQDs and sensor applications. In a study illustrated in Figure 7 in which waste kitchen chimney oil was used as a precursor, Das et al. reported a Fe^{3+} sensor with a 0.18 nM LOD value operating in the 0–100 µM detection range. This CQDs based sensor with a very low LOD value was also tested against the inter-cellular Fe^{3+} ion sensing probe.[122] An approach in the ultrasonic synthesis of CQDs has been achieved using dopamine precursors in dimethylformamide to obtain N-CQDs. Lu et al. used the N-CQDs they obtained with this approach to detect Fe^{2+} ions in the range of 0–50 µM with 38 nM LOD value.[123]

Hydrothermal methods

Hydrothermal methods are the most used method in the synthesis of green CQDs. We examined the sensor applications of CQDs produced by hydrothermal synthesis based on the analytes determined. In general, Fe^{3+} determination in intracellular or intercellular medium, and Fe^{3+} and Hg^{2+} determination in aqueous media have been frequently performed.

Green synthesized CQDs used in the detection of Fe^{3+} and Cu^{2+}

The produced green CQDs generally be used in Fe^{3+} sensor applications because of the high fluorescence quenching feature of Fe^{3+}. CQDs produced in a recent study using orange peel, *Ginkgo biloba* leaves, paulownia leaves, and magnolia

Table 6. Advantages of green synthesized CQDs.

Advantages	Reason
Price 	The synthesis of green CQDs is relatively inexpensive compared to CQDs synthesized using conventional methods. Low-cost precursors (waste material or grass) provide large scale synthesis and easy scale-up capability.
Sustainability 	Green CQDs use renewable natural resources that can provide more sustainable solutions.
Environmental safety 	The synthesis of green CQDs offers an environmentally friendly approach by minimizing the use of hazardous chemicals as well as preventing unintentional contamination.
Recycling 	The use of waste materials for CQDs synthesis offers new ways to manage waste using recycling.
High QY 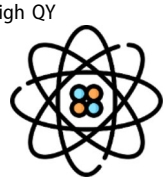	The QY values obtained using green routes to produce CQDs are at comparable levels.

flower as the carbon source was used for the detection of Fe^{3+} ions from pond water in the concentration range of 0.2–100 μM, with 0.073 μM LOD value.[139] In two recent studies, N-CQDs were prepared from chitosan. In one of the studies, Fe^{3+} ion determination from real water samples was performed with a detection limit of 1.6 μM, while in the other study 0.15 μM LOD value was obtained.[217,218] The detection range was approximately the same in these studies (0–200 μM).

Another green CQDs source for the hydrothermal method is various juices. A green hydrothermal strategy has been devised to produce water-soluble N/P co-doped CQDs from edible *Eleocharis dulcis* juice by Bao et al.[182] Using the CQDs developed in this study for the determination of Fe^{3+}, a LOD value of 0.56 µM LOD was reported in the 50 to 350 µM detection range. Using CQDs produced from the watermelon juice precursor, Fe^{3+} was determined with a LOD value of 0.16 μM and a detection range of 0–300 μM.[184] In the same study, the cysteine sensor was also developed (0.27 μM LOD). In their study, Woo et al. obtained the CQDs prepared in the form of both film and dispersion using the hydrothermal method using cellulose/ionic liquid solution. The Fe^{3+} sensor developed using these CQDs with a very high QY provided a LOD value of 0.40 μM in the detection range of 2.5–500 μM.[213] Fe^{3+} was detected from the blood with 0.75 µM LOD value by hydrothermally produced CQDs using enzymatically hydrolyzed corncob.[166] Utilizing N-CQDs synthesized by the presence of functional groups such as carboxylic acids, aldehydes, and aromatics in biomass tar, Fe^{3+} detection took place in a fairly wide range (60 nM–1 mM) and with a relatively low LOD value (60 nM).[212] Chen et al. obtained similar performance using N/S/P co-doped CQDs with the hydrothermal synthesis of the natural foxtail millet. They used the CQDs they produced to detect Fe^{3+} with a LOD value of 46 nM in the detection range of 5 to 150 μM.[149] CQDs that generally provide approximately similar Fe^{3+} detection limits in aqueous environments have been produced by hydrothermal method using green-precursors including *Aegle marmelos* leaves powder,[126] *Enteromorpha prolifera* (a green alga),[168] grape peel,[193] jujube,[137] onion waste,[187] papaya,[150] rice residue and glycine,[189] and sweet potato.[171]

Yang et al reported that honey, as a precursor, has the highest analytical performance in the detection of Fe^{3+} among the green synthesized CQDs. CQDs produced with high emission efficiency (QY$\sim$ 20%), allowed Fe^{3+} detection with 1.7 nM LOD value in the 5 nM–100 µM detection range.[200] Recently, Chaudhary et al. synthesized highly fluorescent N, S co-doped CQDs (NS-CQDs) using banana juice and made a fluorescent sensor for Cu^{2+} detection.

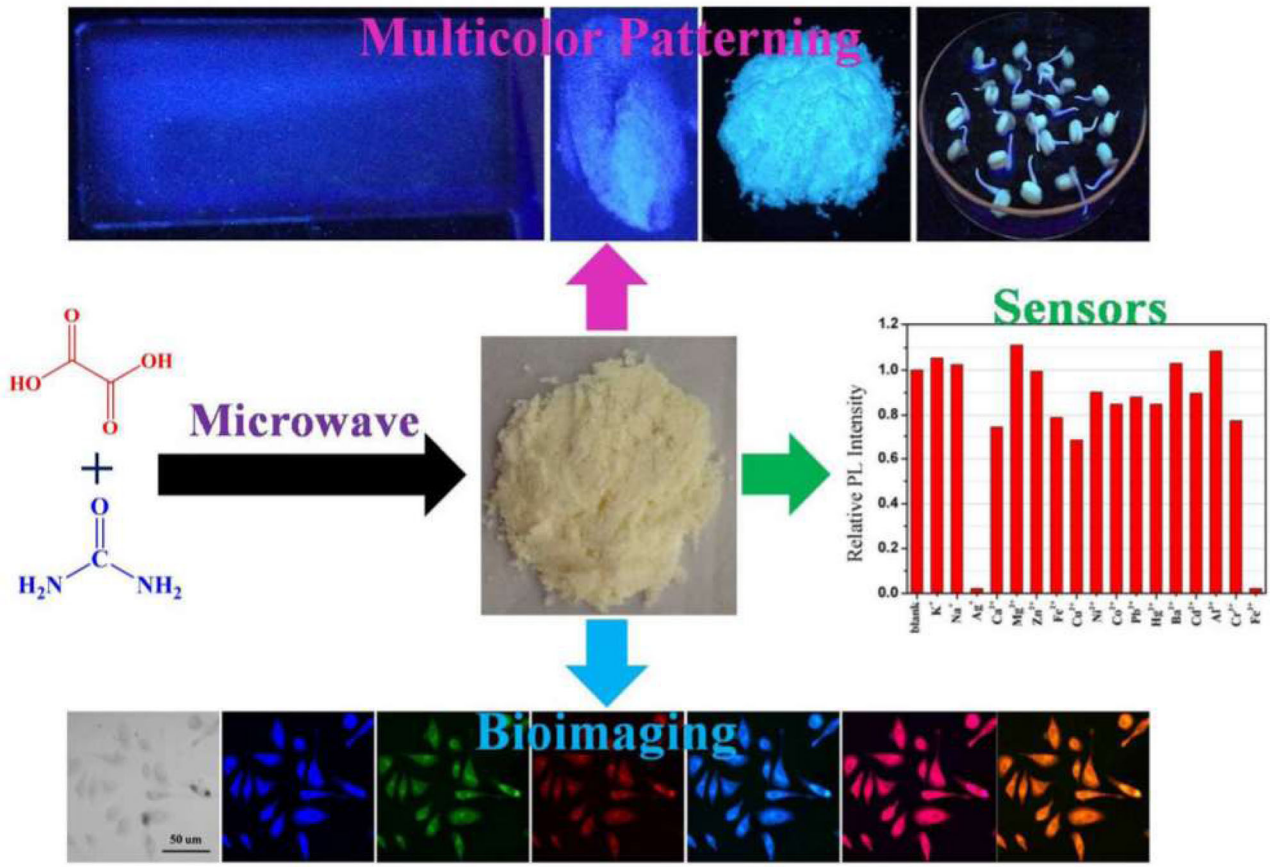

Figure 6. Schematic illustration of a study by Lu et al. demonstrating highly efficient polymer-like CQDs produced using oxalic acid precursor for the detection of Fe^{3+} and Ag^{+}. Produced CQD has low toxicity and distinctive photoluminescence properties. Reproduced from Ref.[249] with permission from The Royal Society of Chemistry.

They detected copper ions in the concentration range of 1–800 μg/mL with the LOD of 0.3 μg/mL with the CQDs they produced.[176] In another study, N-doped CQDs were fabricated using crown daisy leaves, a kitchen waste, as carbon source, and CQDs produced were used for Cu^{2+} detection from river water.[135] The fluorescence efficiencies of the developed sensor were linearly related to the Cu^{2+} concentrations in the range of 10 nM to 120 nM, with a LOD value of 1.0 nM. CQDs produced using tartaric acid and bran had high chemical stability and were used in the determination of Cu^{2+} from real samples with a 50 nM LOD.[210] CQDs produced from grass and pipe tobacco precursors, whose PL efficiency is lower compared to other reported studies (QY$\sim$ 3%), were also used in Cu^{2+} detection.[136,140]

Two CQDs-based Fe^{3+} sensors which have conventionally been obtained from citric acid precursor have been reported, which can operate in the detection range of 2–50 µM and 50 nM–4 µM, reaching 1.3 µM and 9.7 nM LOD values, respectively.[219,221] These two CQDs with very different emission characteristics (e.g., 410 nm and 594 nm) were $\sim$3 nm and $\sim$4.5 nm respectively and had QY $>$ 30%.

Green synthesized CQDs used in the detection of Hg^{2+}, Ag^{+}, and multivalent cations

Tadesse et al. used high PL efficiency N-CQDs (QY$\sim$31%) as a fluorescent probe obtained using citrus lemon as a carbon source in Hg^{2+} detection. 5.3 nM LOD value was reported with a detection range between 1 nM and 1 μM.[147] CQDs with similar Hg^{2+} detection performances were synthesized using the hydrothermal method and Maojian green tea in the presence of ascorbic acid and citric acid. Hg^{2+} was detected from complex samples including wastewater, tea, and rice with a detection limit of 6.3 nM in the detection range of 0.2–60 μM.[132] Approximately the same analytical performance ($\sim$6 nM LOD) was obtained using CQDs produced from *Prosopis juliflora*[141] and *Tamarindus indica*[130] from real samples including water and human serum. An eggshell membrane derivative CQDs, which provides somewhat weaker analytical performance in Hg^{2+} detection, was reported by Ye et al.[208]

The best analytical performance in Ag ion determination applications was obtained using CQDs where purple perilla was used as a carbon source.[134] The wide detection ranges of 0–3 µM obtained in this study and a low LOD value of 1.4 nM were quite good compared to CQDs (75 nM LOD) synthesized using pure tetrahydrofuran as a carbon source.[227] In a study evaluating the performance of broccoli derivative green-CQDs in Ag^{+} detection, a 0.5 µM LOD value was obtained in the detection range of 0 to 600 µM.[164]

CQDs obtained using prickly pear cactus fruit have been passivated with glutathione and a selective fluorescent sensor has been developed for As^{3+}/ClO^{-} ions. In this study, As^{3+}

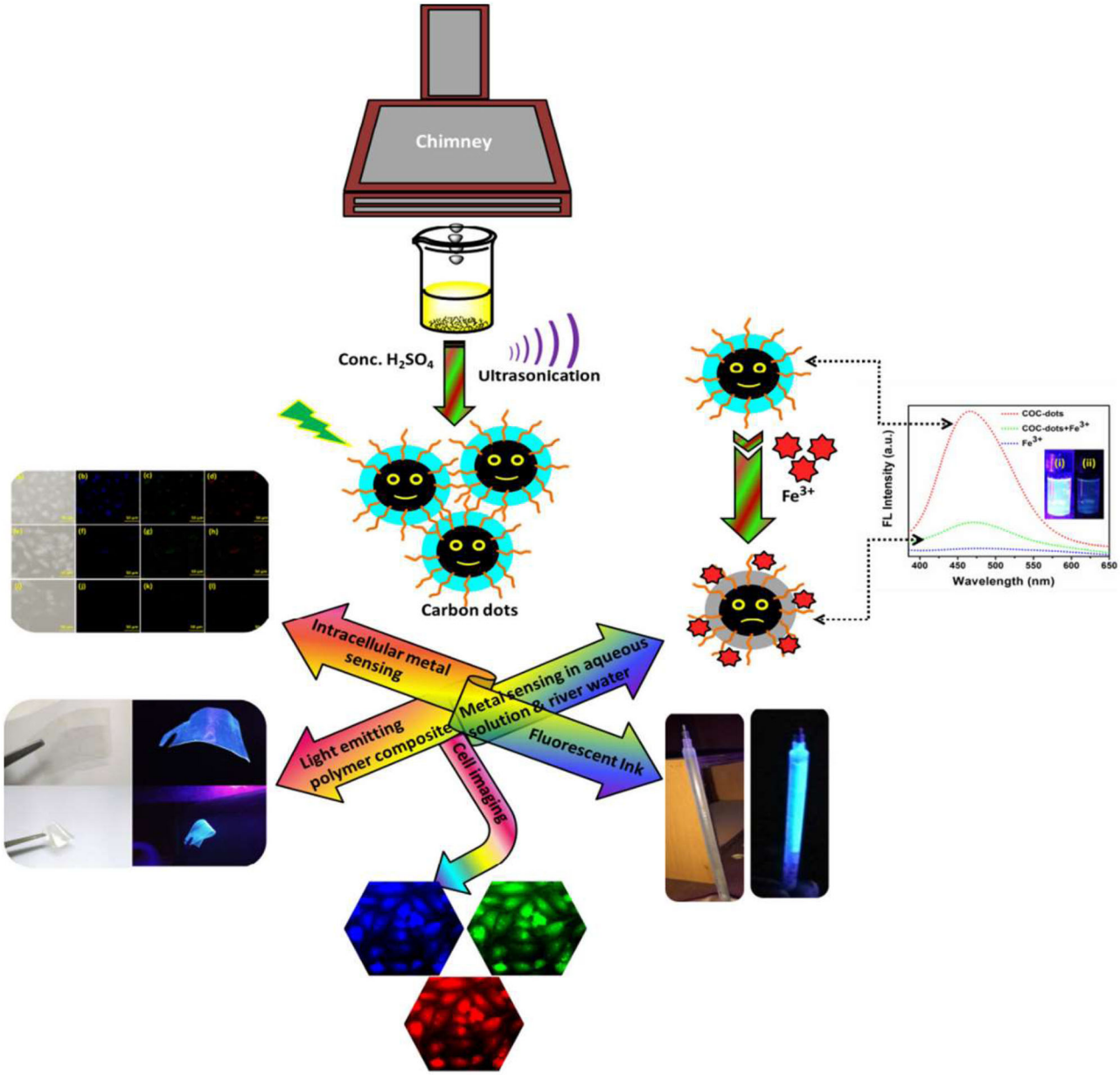

Figure 7. Schematic representation of the preparation of a Fe^{3+} sensor based on CQDs produced using waste kitchen chimney oil as a precursor. A very low LOD value of 0.18 nM was reported for Fe^{3+}. Reproduced from Ref.[122]

and ClO^- ions could be detected in the range of 2–12 nM and 10–90 μM with lower LOD values of 2.3 nM and 0.016 μM, respectively.[158] The CQDs probe has also been reported for the detection of multivalent cations (Cr^{6+} and V^{5+}) using the ethylenediamine and *Pinellia ternata* medicinal plant,[129] and lemon juice as a carbon precursor.[173] LOD values were 15 nM for Cr^{6+} and 3.2 ppm for V^{5+} and both fluorescent probes were tested in real samples such as serum and water.

CQDs (QY 35%) obtained using the hydrothermal route from citric acid and ammonia precursors have been used in the detection of Hg^{2+} with 1.48 nM LOD and a wide detection range of 0–10 μM.[223] In a study in which jackfruit was used as a precursor, Hg^{2+} and Cr^{6+} detection were performed in the range of 5–70 nM with a LOD value of 8 nM and 10 nM, respectively.[153] CQDs (QY ~6%) synthesized using strawberry juice and apple juice were also used in Hg^{2+} detection and a LOD such as 2 nM was obtained in the detection range of 5 nM–50 µM.[181,185] Other CQDs precursors that have applications for the detection of multivalent cations are pigskin,[199] hair,[198] and cocoon silk.[197] Fruit peels such as lemon peel,[195] Jinhua bergamot peel (QY~51%),[145] and pomelo peels[190] have also been used as CQDs precursors and the resulting CQDs has been successfully applied in multivalent cation detection. CQDs (QY 14%) obtained by hydrothermal synthesis from *Coccinia indica* precursor provided a low Hg^{2+} detection limit (3.3 nM) in a very wide detection range (0 to 0.025 mM).[156] In this study, N, S, and O elements added to the structure using organic precursors such as l-cysteine, ethylenediamine, and glycine in production provided this high analytical performance. In the same study, self-passivated CQDs were used to

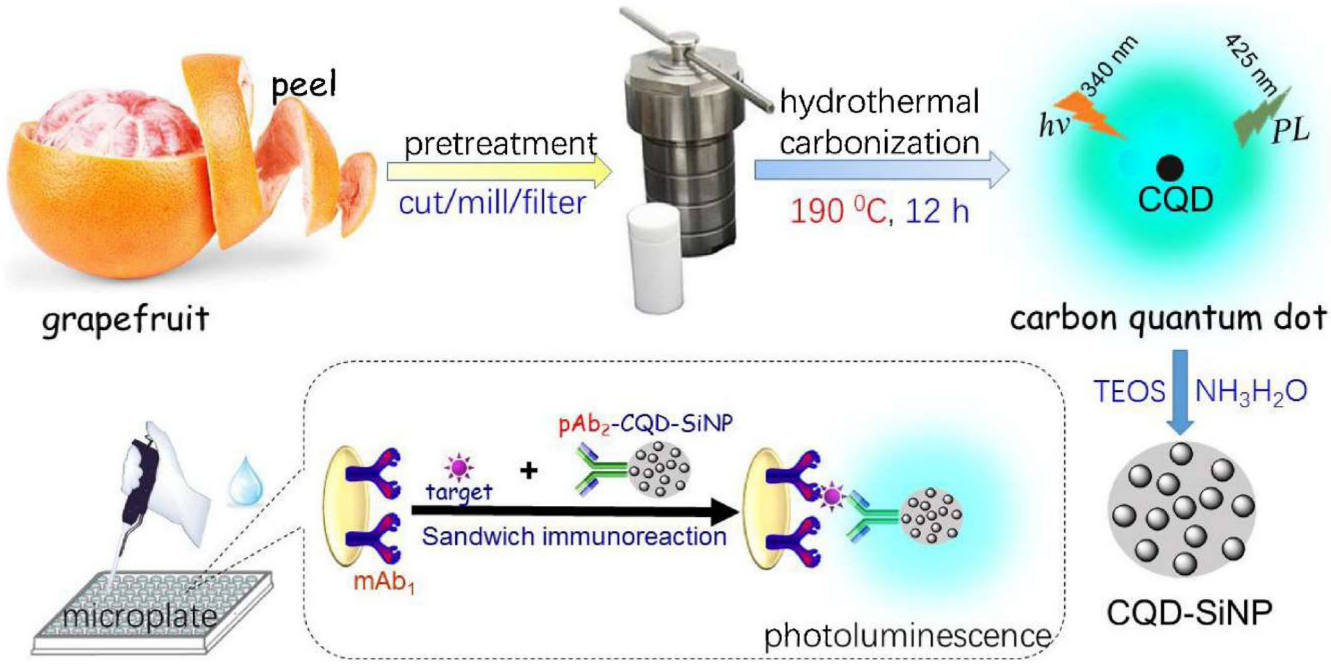

Figure 8. Schematic illustration of a sandwich-type immunosensor based on CQDs produced using grapefruit peel encapsulated with silica nanoparticles. The p53 protein was detected in the range of 0.01–50 ng/mL with a LOD value of 2.7 pg/mL. Reproduced from Ref.[194]

detect Cu^{2+}, Pb^{2+}, and Fe^{3+} ions in a selective manner with lower LOD values of 0.045, 0.27, and 6.2 μM, respectively.[156] In addition, Hg^{2+} sensors using low PL emission efficiency (QY <10%) CQDs (from sweet potato, and conventional Chinese medicine precursor) have also been reported.[131,172]

Green synthesized CQDs used in the detection of pesticide, drug, biological analytes and anions

Some CQDs produced by the hydrothermal method using conventional precursors have been shown to detect different analytes. Zhang et al. developed an Amoxicillin sensor (0.83 µM LOD) using the CQDs with citric acid and boric acid precursors resulting in a 31% QY (maximum emission @ 405 nm) in the detection range of 1.43–429 µM.[224] A citric acid and ethylenediamine derivative CQDs used in the determination of acrylamide and provided a 0.81 µM LOD value.[252] CQDs produced with boron-doped hydroquinone precursor (QY ~15% @368 nm max emission) were used for glucose detection and 8 µM LOD was obtained.[56]

Green-CQDs-based fluorescent probes for use in the detection of adulterants are found in the literature. In a study where malachite green, an adulterant, was detected in food samples, leaf-extracts of *Ocimum tenuiflorum* has been used as a precursor to producing CQDs.[138] They successfully detect this adulterant in food samples with a LOD value of 18 nM and a detection range of 0–120 nM. Anmei et al. reported a study where Sudan I dye was detected in food samples in the range of 2.4–104 μM (950 nM LOD) using cigarette filters as carbon sources for CQDs.[216]

In another study, nitrogen and sulfur dual-doped CQDs were produced using naturally renewable biomaterial fungus fibers as a carbon source and were successfully used with a 15.6 nM LOD value in detecting tetracycline from aquaculture wastewater.[148] In a recent study published by Lai et al., CQDs obtained using fresh cherry tomatoes as a carbon source were used to detect trifluralin with successful analytical performance, such as 0.5 nM LOD in real soil samples in the detection range of 0.050–200 μM.[165]

In two studies where green-CQDs were used as peroxide sensors, mustard seeds[253] and *Azadirachta indica*[127] based CQDs utilizing peroxidase-like mimetic activity were used for peroxide detection in the range of 0–500 µM with 15 µM and 35 µM LOD, respectively. In a study where mustard seeds were used as carbon sources, a sensor was developed for the detection of AA using the reduction of 3,3′,5,5′-tetramethylbenzidine in the presence of AA (3.3 µM LOD).[253] In another sensor working with a similar mechanism, the LOD in AA detection with *Azadirachta indica* based CQDs was 1.8 µM.[127] A CQDs based sensor used for the detection of cysteine utilizing peroxidase-like mimetic activity was produced using chicken blood as a carbon source.[209] This cysteine sensor was used in the human serum sample with a LOD value of 0.4 μM and a detection range of 0.5–20 μM. N, S-CQDs were produced using scallion leaves for detection of hemin from a human serum sample, and detection with 0.1 μM LOD was performed.[142] For the determination of p53 protein in biological fluid samples as shown in Figure 8, a sandwich-type immunosensor was developed encapsulating grapefruit peel-extracted CQDs into silica nanoparticles.[194] With this immunosensor, the p53 protein was detected in the range of 0.01–50 ng/mL with a LOD value of 2.7 pg/mL. A sensor was obtained as a result of modification of N-CQDs obtained using cornstalk as a carbon source for direct detection of pathogenic fungi (*Candida albicans*) with water-soluble amphotericin B. With this sensor, fungi can be detected in real samples such as beef sausage with 1124 CFU/mL LOD.[167] CQDs obtained by the hydrothermal

method from cherry tomatoes were used for trifluralin detection with a very low LOD (0.5 nM),[165] and fructose and L-cysteine derivative CQDs were used in clenbuterol detection (23 pg/mL LOD).[215] A permanganate sensor (0.06 μM LOD) using CQDs produced with pig liver precursor, and a picric acid sensor (41 nM LOD) using CQDs from a mandelic acid precursor with a fairly high QY (41%) has also been reported.[205,211]

Green CQDs in bioimaging applications

Since CQDs are one of the biocompatible fluorescent nanomaterials, they can also be used for fluorescent and multimodal bioimaging of cells and tissues. They have several advantages in bioimaging such as natural fluorescence emission, high resistance to photo-bleaching, high solubility in water, high biocompatibility, and low cytotoxicity. CQDs obtained by both conventional methods and green synthesis have been used successfully in many bioimaging applications. It is known that CQDs can reach the cell nucleus in some cases by passing through the cell membrane and cytoplasm (however, some opposite cases were also reported[91]). Furthermore, the toxicities of CQDs are highly dependent on the production method and precursor type. Table 2–5 also shows some of the CQDs produced using different strategies for bioimaging purposes. Biocompatibility and usability as a bioimaging agent have been demonstrated in the cell-lines provided in these studies. The first *in vitro* and *in vivo* bioimaging study with CQDs was reported in 2009.[256,257] After this study, many CQDs were produced with green-chemistry methods and used successfully in bioimaging. Different cell and tissue types such as bacteria,[258] yeasts,[162] and fish[66] were used in imaging studies as well as cancer cells and mice. Various studies have also been reported on determining analytes in the cell.[171,234,259–262] The fact that CQDs produced in the specified methods are also candidates for multimodal imaging (the combination of magnetic resonance imaging and optical imaging methods) increases the interest in green-CQDs.[93,263] This section summarizes the CQDs produced using different production methods and different precursors and used in bioimaging.

Carbonization and pyrolysis methods

CQDs (5–10 nm to 10–14 nm sizes) produced using mango fruit as a carbon source were used in bioimaging in the A549 cell-line.[251] The CQDs of ~2 nm, which provide approximately 10% QY and have a maximum emission between 440 and 490 nm, were green-synthesized using the carbonization method using watermelon peels,[70] lychee seed,[71] and peanut shell precursors,[72] and bioimaging study was performed in HeLa and HepG2 cell-line, respectively. CQDs with approximately the same PL efficiency and synthesized using lentil grain flour precursor but larger, had a maximum emission at 510 nm, and were claimed to be used in bioimaging by their authors, but a cell-line was not used in this study.[78] Bhunia et al. used CQDs with the highest QY obtained by the carbonization method using vitamin B1 precursor and providing maximum emission at 475 nm in bioimaging in Chinese hamster ovary (CHO).[79] Recently, Anthony et al. used ice-biryani precursor, a food waste. CQDs with maximum emissions of 432 nm (QY 41%), which they obtained with nitric-acid treatment, were stabilized with glutathione and used in bioimaging in A549 cell-line.[80] CQDs with homogeneous size distribution (~6–12 nm) and green fluorescent (518 nm) emissions produced using ayurvedic plant leaves precursors such as *Azadirachta Indica*, *OcimumTenuiflorum*, and *Tridax Procumbens*, used for bioimaging in HeLa cell-line and more than 85% biocompatibility has been reported.[81] CQDs produced by hydrothermal treatment using the residue obtained by pyrolysis of waste polyolefins (QY~5%) were also used in MDA-MB 468 cell-line bioimaging.[84] In a previous study, Teng et al. achieved a high QY of 22% (at 434 nm) using konjac flour as a precursor and used these CQDs in bioimaging in HeLa cell-line.[83]

Microwave-assisted methods

CQDs, which were recently produced with microwave-assisted methods utilizing waste cotton linter precursor, were used in the human mesothelioma cell line, H2452, and human umbilical vein endothelial cells (HUVEC). In this study, cell viability and proliferation assays indicated that the material was cytotoxic against both cell lines and inhibited cell growth in a time- and dose-dependent manner.[101] CQDs (QY 25%) produced by microwave-assisted method from gallic acid, where the precursor is also used as an anti-tumor agent, was used as both a bioimaging agent and antitumor agent in both cell-based assays (HeLa) and mouse xenograft tumors (Figure 9).[90] Ko et al. reported that silk fibroin-based CQDs (QY 15%) showed stable emission, good water dispersity, low toxicity, and good biocompatibility for bioimaging in KB cells and female nude Balb/c mice (Figure 10).[89] Besides, CQDs produced using the microwave-assisted method with <10% QY are obtained using garlic,[97] onion peel,[98] quince fruit[99] precursors were used in bioimaging in macrophages, MG63/HFFs cells, and HT-29 cell-line, respectively. CQDs produced using citric acid, urea, and sodium fluoride conventional precursors had a maximum emission at 600 nm and although they have a low QY of 1.2%, their use in bioimaging was shown using C6 glioma cell-line.[102]

Oxidation, thermal and ultrasonic methods

Various CQDs with maximum emission between 378 and 535 nm with <5% QY produced by oxidation methods have been produced using various green-precursors including bread,[112] *Trapa bispinosa* peel,[105] waste frying oil,[106] and plant soot,[104] and used for bioimaging with human blood cells, MDCK cell-line, HeLa and CHO, respectively. The two different CQDs obtained by conventional methods had a yield of less than 5% QY and a particle size of around 10 nm, and their usability in bioimaging application was demonstrated using HepG2 and MCF-7 cell-line.[49,113] CQDs obtained from hair fiber precursors, whose QYs were slightly better (>10%), were used in the HeLa cell-line.[108] In

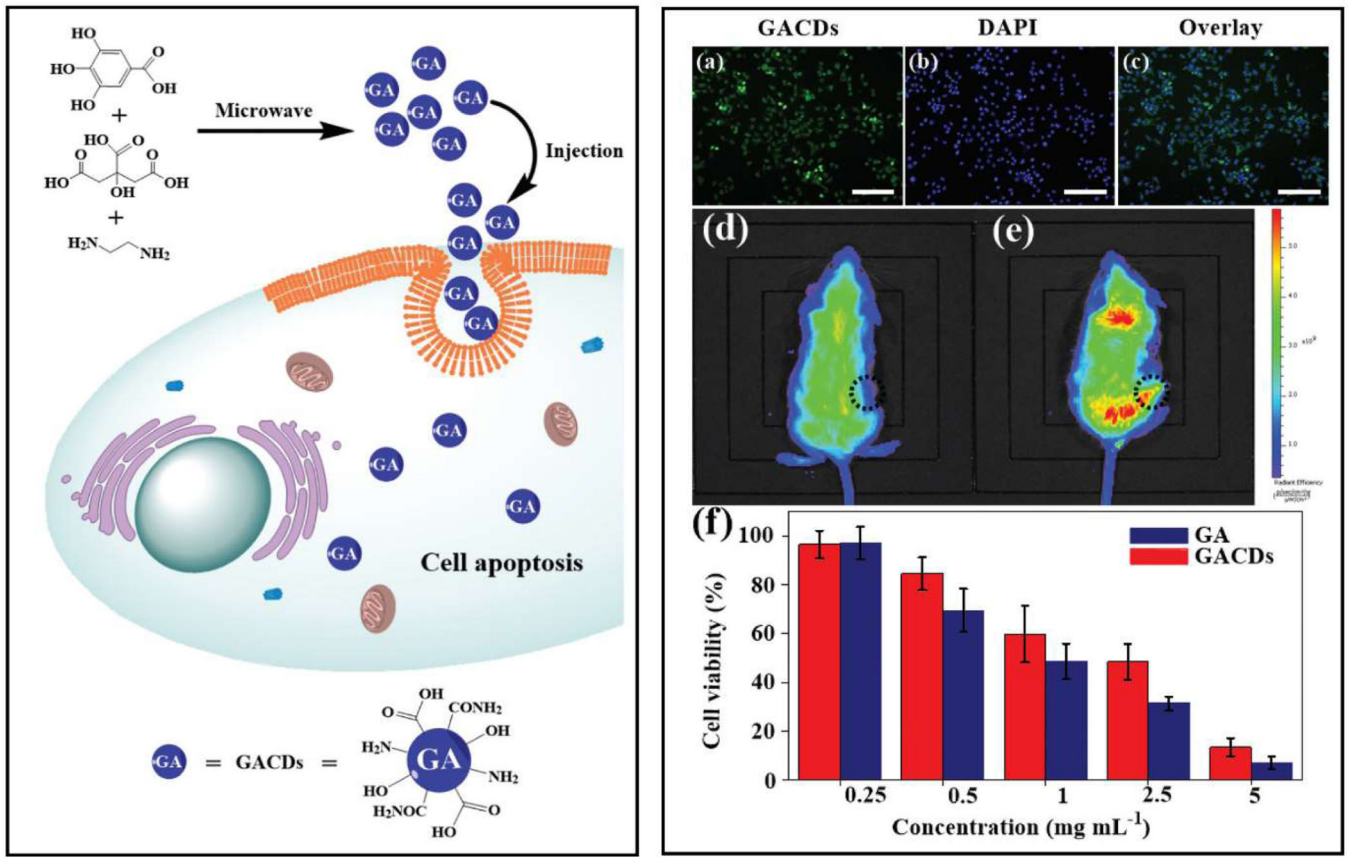

Figure 9. (Left). Schematic illustration of gallic acid-based quantum dots. (Right) Different cell imagings of treated cells (a, b, and c), in-vivo bioimaging of the tumor in mice (d and e), cell viability of HeLa cells after incubating with gallic and gallic-based CQDs. Reproduced from Ref.[90] with permission from The Royal Society of Chemistry.

a more interesting approach, CQDs from cow manure precursors had a very high PL efficiency (65%) and were also used in MCF-7, MDA-MB-231, Caco-2, and DU145 cell-lines.[107]

Thermal methods generally had relatively high PL efficiency compared to carbonization. Some CQDs that are claimed to be used in bioimaging but have not been tested with cell lines were obtained using banana juice, hair, and overcooked BBQ precursors.[64,115,116] CQDs, the presence of which was demonstrated in Nescafe®, was used in the human hepatocellular carcinoma cell-line (SMMC-7721).[66] Hsu et al. used CQDs obtained using coffee grounds in imaging with LLC-PK1 cell-line.[65] Grounded soybean-based CQDs were used in NIH3T3 cell-line.[118] N-CQDs (QY ~ 4%) produced using the ultrasonic method were used in HepG2 cell-line and it was stated that bright and stable fluorescence against variations of pH and ionic strength, low cytotoxicity, and high photostability.[123]

Hydrothermal methods

Adenocarcinomic human alveolar basal epithelial (A549) cells

In studies that confirmed bioimaging performance using the A549 cell-line, green-synthesized CQDs with ~14% QY and maximum emission peak between 420 nm and 470 nm were reported. To produce these CQDs, bagasse,[160] *Bombyx mori* silk,[202] and ginger[159] were used as precursors. Recently CQDs with ~ 15% QY obtained using sweet corn precursors were used in bioimaging applications using Vero and A549 cell-line and produced more than 90% of cell viability in both cell-lines at 250 μg/mL.[154]

Human cervical cancer (HeLa) cells

There are many studies on bioimaging applications of green-synthesized CQDs using the HeLa cell line. CQDs with PL efficiency <10% QY were obtained using grape peel[193] and *Enteromorpha prolifera*[168] precursors. The precursors, which provide CQDs PL yields approximately 2 times higher than these precursors, were papaya[150] and grape juice,[179] and bioimaging was performed using HeLa cell-line. Recently, CQDs obtained using the purple perilla precursor were used in the HeLa cell-line and low cytotoxicity, and good biocompatibility was reported.[134] Besides, two CQDs with high PL yield were obtained using the hydrothermal method using lemon juice[174] and pigskin[199] precursors. High PL efficient QDs (~3 nm in size) produced from graphene oxide and ammonia precursor (QY~25%) and citric acid and urea precursor (QY~36%) were successfully used in HeLa cell-line bioimaging.[222,225]

Human hepatocellular carcinoma (HepG2) cells

In a recent study, Irmania et al. produced manganese-doped CQDs using a waste green tea precursor to include magnetic

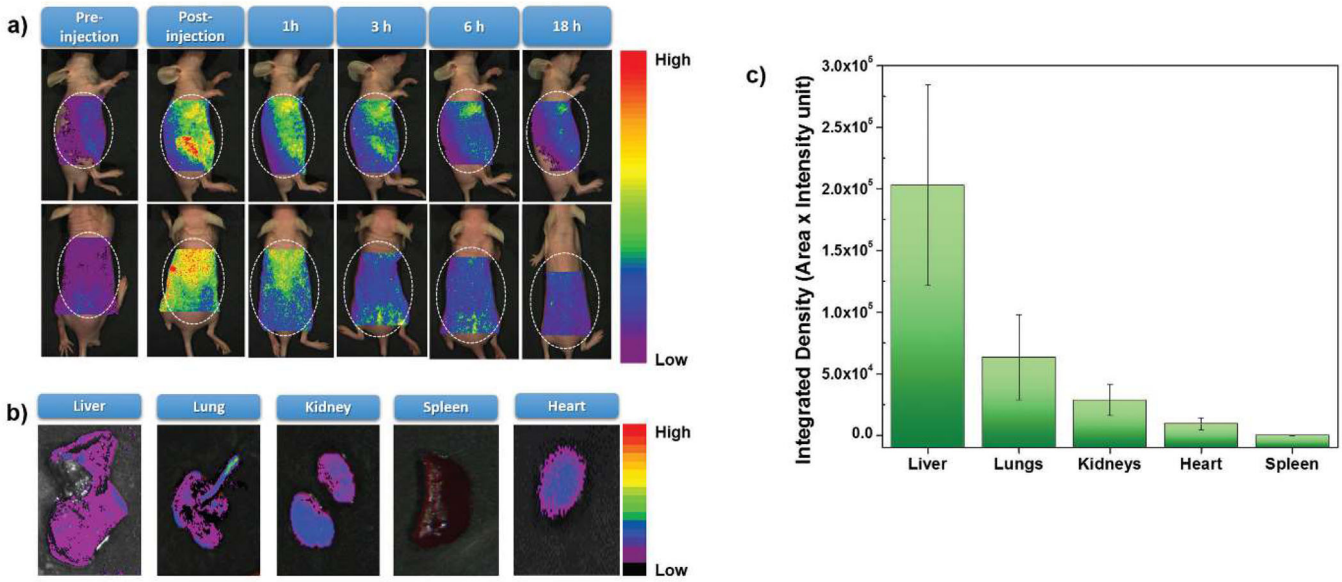

Figure 10. A study by Ko et al. demonstrating (a) side and front views of in-vivo images of silk fibroin-based CQDs injected mice (b) ex-vivo images of isolated organs from silk fibroin-based CQDs injected mice and (c) quantified fluorescence intensity in organs of healthy mice at 18 h post-administration of silk fibroin-based CQDs indicating that there was a negligible amount of accumulation of silk fibroin-based CQDs in the major organs. Reproduced from Ref.[89]

resonance properties, and these CQDs with 12% QY were used to screen HeLa, HepG2, and B16F10 cancer cells.[133] Besides, folic acid and chlorin e6 conjugated Mn-CQDs shown no significant toxicity up to 500 ppm. High QY (28%) nitrogen and sulfur dual-doped CQDs were produced using fungus fibers and used for imaging in the HepG2 cell-line.[148] The CQDs, which have the highest QY (38%) among the green-CQDs used in the HepG2, HeLa, and 293 T cell-lines, was produced by hydrothermal processing of cocoon silk.[197] In studies with different precursors, sweet potato,[171] honey,[200] watermelon juice,[184] and glucose and monopotassium phosphate[254] were used as carbon sources and produced CQDs were used for bioimaging in HepG2 cell line.

Human breast cancer cell lines (MCF-7 and SKBR3)

In a recent study, Tadesse et al. synthesized N-CQDs using citrus lemon precursor (QY 31%) and used it for bioimaging in MCF-7 cell-line.[147] In a study where CQDs with an average diameter of 12 nm were produced using walnut oil precursor, PC3, MCF-7, and HT-29 human carcinoma cell lines were used.[155] In this study, the induction of apoptosis by CQDs was accompanied by an increase in the activation of caspase-3 was reported. Recently, Fatahi et al. used the hydrothermal method in the synthesis of CQDs with ~20% QY derived from the bitter orange juice and utilized it in imaging studies using SKBR3 breast adenocarcinoma cell line and NIH/3T3 mouse embryonic fibroblast. In this study, high biocompatibility was also reported.[178]

CQDs produced using the citric acid precursor have been used for imaging in MCF-7 and HeLa cell lines after functionalization with folic acid. It was stated that these CQDs provide 50% QY at the emission maximum of 450 nm and their biocompatibility is 97%.[220] CQDs obtained using polycyclic aromatic hydrocarbon precursor and providing maximum emission at 498 nm (QY 12%) were also used in MCF-7 imaging.[226] Moreover, there are also MCF-7 imaging studies of CQDs produced from garlic (QY~18%) and dried shrimp (QY 54%) precursor.[151,196]

Human bone osteosarcoma cells (MG63), brain epithelial glioblastoma cells (U87), kidney cell lines (Vero, HEK293, HK2), and Colon carcinoma cell lines (LoVo, Caco-2)

Sahu et al. used orange juice-derived green-CQDs in imaging studies using L929 and human osteosarcoma (MG-63) cell line. The efficiency of the emissions of these CQDs at 455 nm was 26%.[177] Recently, CQDs obtained hydrothermally from sandalwood precursors showed good fluorescence in both cytoplasm and nucleus of MG63 cells.[161] CQDs (QY 24.6%) produced using biomass produced by the palm oil industry as precursors also used for imaging in the Vero cell-line.[188] CQDs (QY 28%) from onion waste were used in HEK-293 and HeLa cells imaging.[187] CQDs with high PL efficiency was produced from cinnamon, red chili, turmeric, and black pepper precursors (QY 27%–44%) used for imaging in LN-229 and HK-2 cell-lines. In this study, it was stated that the uptake in cancer cells is higher than non-cancerous cells and these CQDs can be used to display cancer cells.[128] CQDs (529–538 nm emission) with high PL efficiency and about 4.5 nm in size obtained from pear, avocado and kiwi precursors have been used for imaging of epithelial human kidney cells HK-2 and epithelial human colorectal adenocarcinoma Caco-2 cell-lines.[146] A CQDs with a lower PL efficiency compared to the green-CQDs given in this section were synthesized by the hydrothermal method using bee pollens and used in LoVo human colon carcinoma cell-line imaging.[203]

Bacteria and other cell lines

CQDs produced by the hydrothermal method from *Carica papaya* juice precursor were used for imaging of *Fusarium avenaceum* and *Pseudomonas aeruginosa* cells.[183,263] Mehta et al. used CQDs derived from apple juice for bioimaging of *Mycobacterium tuberculosis*, *Pseudomonas aeruginosa* and *Magnaporthe oryzae*.[165,180] *Escherichia coli* and *S. cerevisiae* cells bioimaging were carried out with CQDs obtained using sugar cane juice and potato precursors.[162] Milk-based CQDs (7.6% QY) were also used for bioimaging of human liver cancer cell lines (SMMC-7721).[206] Dehghani et al. performed the visualization of RL-14 human fetal ventricular cardiomyocytes cells embedded in a luminescent 3D printed scaffold using collagen-based CQDs (QY 15%).[214] Another study using high PL efficient CQDs demonstrated HaCaT cells with cabbage-based CQDs.[152] Recently, a study has been reported on *Cyanobacteria* biomass derivative CQDs that create a clear distinction between cytoplasm and nucleus on the pheochromocytoma PC12 cell-line.[207] In a study using onion epidermal cells for plant cells imaging, lemon juice derivative CQDs (16.7% QY) were used.[175] In the imaging study using *Caenorhabditis elegans* as a model, consistent fluorescence in the gut tissues of the worms without exerting any sign of toxic effects on the nematodes. The CQDs used in this study were obtained using the beetroot extract precursor.[163] In another study, CQDs were obtained using *Phyllanthus acidus* precursor were used for high-contrast *Caenorhabditis elegans* bioimaging and *in-vivo* studies suggested that the N-CQDs showed excellent biocompatibility.[157]

Bioimaging claim only

Some studies declared that green-synthesized CQDs can be used for bioimaging with the hydrothermal method but have not been experimented with cell-line. In one of these studies, 36% QY was obtained at 431 nm using orange waste peel.[186] Recently, 11.4% of QY was obtained using orange waste peel.[192] Some other green-synthesized CQDs with QY yields <6% have also been reported for bioimaging, using soy milk,[169] willow bark, and leaves,[144,170] *Scindapsus* leaves,[143] and orange pericarp[191] as carbon sources.

Other methods

There are a limited number of articles on green-CQDs production using other methods. It has been claimed that CQDs with 8% QY obtained by plasma treatment of chicken egg precursors can be used as a bioimaging agent.[125] In a recent study, Ren et al. obtained high PL efficient CQD up to 32.4% QY by laser ablation method using *Platanus* biomass as a precursor and used these CQDs in HeLa cell-line for bioimaging.[124] For comparison, it should be noted that CQDs produced by the laser ablation method using toluene precursor provides 18% CQDs at 475 nm emission maximum.[43]

Conclusion and future perspective

CQDs synthesis attracted great attention due to its economical and easy synthesis methods, structure enabling surface modification, excellent photoluminescence efficiency, adjustable PL properties, and water solubility. Among all mentioned advantages, especially environmentally friendly and low-cost production is important for industrial-scale production of CQDs. In an earlier demonstration of CQDs synthesis, CQDs with low QY and low solubility were produced using certain carbon materials. Higher PL efficiency can be obtained by both surface passivation and heteroatom addition. Different dopants and citric acid are widely used as precursors in the CQDs synthesis. However, it is easier to add dopants such as N, S, and P to the CQDs during synthesis using green synthesis approaches. Because, "green precursors" are obtained from natural, abundant, or waste sources that already contains such dopants naturally. A wide range of green-precursors, including plants, leaves, juices, biomass, animal-derived biomaterials, and even bacteria, have been proposed by researchers in the literature. Feasibility and scaling studies for uniform and bulk CQDs production using green-precursors should also be studied. The development of the size control, modification strategies, and fine-tuning of PL features of CQDs in the coming years will be helpful for industrial-scale production. Table 6 summarizes the advantages of CQDs obtained with the green-chemistry approach.

It was observed that CQDs produced using green-precursor do not show any significant difference compared to CQDs produced in conventional ways. Furthermore, PL efficiency and biocompatibility of green CQDs were found to be higher than CQDs produced by conventional methods. Therefore, it is expected that CQDs production using green chemistry approaches will attract more attention in the coming years. The wide use of CQDs (such as sensing, bioimaging, and other areas such as photocatalytic reactions drug-delivery systems, electronic and photothermal cancer therapy which are not included in this article) brought many novel approaches to the literature whether these methods are green or not.

There are still undiscovered areas in the production of CQDs using green- precursor and their use in sensor and bioimaging applications. The physicochemical characteristics of the produced CQDs, which depend on the method and precursor, allow any kind of green-precursor to be used as a successful source of CQDs. Therefore, natural resources, including endemic species, different abundant materials, and waste materials are always potential CQDs sources. Also, different material conjugation of CQDs has not been studied deeply enough in sensor applications. This affects the suitability of CQDs for various signal enhancing approaches. Therefore, there is a gap in sensor applications for the detection of a wide variety of analytes with different conjugates such as aptamers, enzymes, or antibodies. Furthermore, a limited number of studies have been carried out on the use of CQDs for a wide range of transducing approaches such as SPR, SERS, ellipsometry, or QCM. On

the other hand, multimodal strategies in bioimaging are also not well investigated using green-approaches.

In this review article, a summary of the studies for CQDs production was presented focusing on sensing and bioimaging applications in the last decade. However, clinical practices such as drug and gene delivery, drug release, and cancer therapy are not in the scope of this review article. Although conventional methods for the production of CQDs are often preferred, literature data on green chemistry approaches indicate that green CQDs show comparable performance in sensing and bioimaging applications. Consequently, it is expected that more researchers will focus on greener solutions to produce CQDs and develop strategies for industrial-scale production.

ORCID

Mustafa Oguzhan Caglayan http://orcid.org/0000-0002-7265-1094
Ferda Mindivan http://orcid.org/0000-0002-6046-2456
Samet Şahin http://orcid.org/0000-0002-0568-4283

References

[1] Wang, Y.; Hu, A. Carbon Quantum Dots: Synthesis, Properties and Applications. *J. Mater. Chem. C.* **2014**, *2*, 6921–6939. DOI: 10.1039/C4TC00988F.

[2] Dong, Y.; Wang, R.; Li, G.; Chen, C.; Chi, Y.; Chen, G. Polyamine-Functionalized Carbon Quantum Dots as Fluorescent Probes for Selective and Sensitive Detection of Copper Ions. *Anal. Chem.* **2012**, *84*, 6220–6224. DOI: 10.1021/ac3012126.

[3] Zhao, Q.-L.; Zhang, Z.-L.; Huang, B.-H.; Peng, J.; Zhang, M.; Pang, D.-W. Facile Preparation of Low Cytotoxicity Fluorescent Carbon Nanocrystals by Electrooxidation of Graphite. *Chem. Commun.* **2008**, *41*, 5116–5118. DOI: 10.1039/b812420e.

[4] Deng, Y.; Zhao, D.; Chen, X.; Wang, F.; Song, H.; Shen, D. Long Lifetime Pure Organic Phosphorescence Based on Water Soluble Carbon Dots. *Chem. Commun.* **2013**, *49*, 5751–5753. DOI: 10.1039/c3cc42600a.

[5] Wen, X.; Yu, P.; Toh, Y.-R.; Ma, X.; Tang, J. On the Upconversion Fluorescence in Carbon Nanodots and Graphene Quantum Dots. *Chem. Commun. (Camb)* **2014**, *50*, 4703–4706. DOI: 10.1039/C4CC01213E.

[6] Wan, J.; Wang, J.-H.; Liu, T.; Xie, Z.; Yu, X.-F.; Li, W. Surface Chemistry but Not Aspect Ratio Mediates the Biological Toxicity of Gold Nanorods in Vitro and in Vivo. *Sci. Rep.* **2015**, *5*, 11398. DOI: 10.1038/srep11398.

[7] Dou, X.; Lin, Z.; Chen, H.; Zheng, Y.; Lu, C.; Lin, J.-M. Production of Superoxide Anion Radicals as Evidence for Carbon Nanodots Acting as Electron Donors by the Chemiluminescence Method. *Chem. Commun. (Camb)* **2013**, *49*, 5871–5873. DOI: 10.1039/c3cc41145a.

[8] Xu, Y.; Wu, M.; Feng, X. Z.; Yin, X. B.; He, X. W.; Zhang, Y. K. Reduced Carbon Dots versus Oxidized Carbon Dots: Photo- and Electrochemiluminescence Investigations for Selected Applications. *Chem. Eur. J.* **2013**, *19*, 6282–6288. DOI: 10.1002/chem.201204372.

[9] Yu, P.; Wen, X.; Toh, Y.-R.; Lee, Y.-C.; Huang, K.-Y.; Huang, S.; Shrestha, S.; Conibeer, G.; Tang, J. Efficient Electron Transfer in Carbon Nanodot–Graphene Oxide Nanocomposites. *J. Mater. Chem. C.* **2014**, *2*, 2894–2901. DOI: 10.1039/c3tc32395a.

[10] Mintz, K. J.; Zhou, Y.; Leblanc, R. M. Recent Development of Carbon Quantum Dots regarding Their Optical Properties, Photoluminescence Mechanism, and Core Structure. *Nanoscale* **2019**, *11*, 4634–4652. DOI: 10.1039/C8NR10059D.

[11] Xu, X.; Ray, R.; Gu, Y.; Ploehn, H. J.; Gearheart, L.; Raker, K.; Scrivens, W. A. Electrophoretic Analysis and Purification of Fluorescent Single-Walled Carbon Nanotube Fragments. *J. Am. Chem. Soc.* **2004**, *126*, 12736–12737. DOI: 10.1021/ja040082h.

[12] Sun, Y.-P.; Zhou, B.; Lin, Y.; Wang, W.; Fernando, K. A. S.; Pathak, P.; Meziani, M. J.; Harruff, B. A.; Wang, X.; Wang, H.; et al. Quantum-Sized Carbon Dots for Bright and Colorful Photoluminescence. *J. Am. Chem. Soc.* **2006**, *128*, 7756–7757. DOI: 10.1021/ja062677d.

[13] Kwon, W.; Rhee, S.-W. Facile Synthesis of Graphitic Carbon Quantum Dots with Size Tunability and Uniformity Using Reverse Micelles. *Chem. Commun. (Camb)* **2012**, *48*, 5256–5258. DOI: 10.1039/c2cc31687k.

[14] Lim, S. Y.; Shen, W.; Gao, Z. Carbon Quantum Dots and Their Applications. *Chem. Soc. Rev.* **2015**, *44*, 362–381. DOI: 10.1039/C4CS00269E.

[15] Zhang, Y.-Q.; Ma, D.-K.; Zhuang, Y.; Zhang, X.; Chen, W.; Hong, L.-L.; Yan, Q.-X.; Yu, K.; Huang, S.-M. One-Pot Synthesis of N-Doped Carbon Dots with Tunable Luminescence Properties. *J. Mater. Chem.* **2012**, *22*, 16714–16718. DOI: 10.1039/c2jm32973e.

[16] Qu, K.; Wang, J.; Ren, J.; Qu, X. Carbon Dots Prepared by Hydrothermal Treatment of Dopamine as an Effective Fluorescent Sensing Platform for the Label-Free Detection of Iron(III) Ions and Dopamine. *Chem. Eur. J.* **2013**, *19*, 7243–7249. DOI: 10.1002/chem.201300042.

[17] Zhou, J.; Booker, C.; Li, R.; Zhou, X.; Sham, T.-K.; Sun, X.; Ding, Z. An Electrochemical Avenue to Blue Luminescent Nanocrystals from Multiwalled Carbon Nanotubes (MWCNTs). *J. Am. Chem. Soc.* **2007**, *129*, 744–745. DOI: 10.1021/ja0669070.

[18] Dang, H.; Huang, L.-K.; Zhang, Y.; Wang, C.-F.; Chen, S. Large-Scale Ultrasonic Fabrication of White Fluorescent Carbon Dots. *Ind. Eng. Chem. Res.* **2016**, *55*, 5335–5341. DOI: 10.1021/acs.iecr.6b00894.

[19] Wang, S.; Chen, Z.-G.; Cole, I.; Li, Q. Structural Evolution of Graphene Quantum Dots during Thermal Decomposition of Citric Acid and the Corresponding Photoluminescence. *Carbon* **2015**, *82*, 304–313. DOI: 10.1016/j.carbon.2014.10.075.

[20] Gao, X.; Cui, Y.; Levenson, R. M.; Chung, L. W. K.; Nie, S. In Vivo Cancer Targeting and Imaging with Semiconductor Quantum Dots. *Nat. Biotechnol.* **2004**, *22*, 969–976. DOI: 10.1038/nbt994.

[21] Peng, H.; Zhang, L.; Kjällman, T. H. M.; Soeller, C.; Travas-Sejdic, J. DNA Hybridization Detection with Blue Luminescent Quantum Dots and Dye-Labeled Single-Stranded DNA. *J. Am. Chem. Soc.* **2007**, *129*, 3048–3049. DOI: 10.1021/ja0685452.

[22] Yin, B. C.; Liu, Y. Q.; Ye, B. C. One-Step, Multiplexed Fluorescence Detection of microRNAs Based on Duplex-Specific Nuclease Signal Amplification. *J. Am. Chem. Soc.* **2012**, *134*, 5064–5067. DOI: 10.1021/ja300721s.

[23] Lee, H.; Song, H.-J.; Shim, M.; Lee, C. Towards the Commercialization of Colloidal Quantum Dot Solar Cells: perspectives on Device Structures and Manufacturing. *Energy Environ. Sci.* **2020**, *13*, 404–431. DOI: 10.1039/C9EE03348C.

[24] Zhu, S.; Meng, Q.; Wang, L.; Zhang, J.; Song, Y.; Jin, H.; Zhang, K.; Sun, H.; Wang, H.; Yang, B. Highly Photoluminescent Carbon Dots for Multicolor Patterning, Sensors, and Bioimaging. *Angew. Chem. Int. Ed. Engl.* **2013**, *52*, 3953–3957. DOI: 10.1002/anie.201300519.

[25] Zhai, X.; Zhang, P.; Liu, C.; Bai, T.; Li, W.; Dai, L.; Liu, W. Highly Luminescent Carbon Nanodots by Microwave-Assisted Pyrolysis. *Chem. Commun. (Camb)* **2012**, *48*, 7955–7957. DOI: 10.1039/c2cc33869f.

[26] Ju, E.; Liu, Z.; Du, Y.; Tao, Y.; Ren, J.; Qu, X. Heterogeneous Assembled Nanocomplexes for Ratiometric Detection of

Highly Reactive Oxygen Species in Vitro and in Vivo. *ACS Nano.* **2014**, *8*, 6014–6023. DOI: 10.1021/nn501135m.

[27] Zhang, B.; Liu, C-y.; Liu, Y. A Novel One-Step Approach to Synthesize Fluorescent Carbon Nanoparticles. *Eur. J. Inorg. Chem.* **2010**, *2010*, 4411–4414. DOI: 10.1002/ejic.201000622.

[28] Yang, Z.; Xu, M.; Liu, Y.; He, F.; Gao, F.; Su, Y.; Wei, H.; Zhang, Y. Nitrogen-Doped, Carbon-Rich, Highly Photoluminescent Carbon Dots from Ammonium Citrate. *Nanoscale* **2014**, *6*, 1890–1895. DOI: 10.1039/C3NR05380F.

[29] Jaiswal, A.; Ghosh, S. S.; Chattopadhyay, A. One Step Synthesis of C-Dots by Microwave Mediated Caramelization of Poly(Ethylene Glycol). *Chem. Commun. (Camb)* **2012**, *48*, 407–409. DOI: 10.1039/C1CC15988G.

[30] Jiang, H.; Chen, F.; Lagally, M. G.; Denes, F. S. New Strategy for Synthesis and Functionalization of Carbon Nanoparticles. *Langmuir* **2010**, *26*, 1991–1995. DOI: 10.1021/la9022163.

[31] Vedamalai, M.; Periasamy, A. P.; Wang, C.-W.; Tseng, Y.-T.; Ho, L.-C.; Shih, C.-C.; Chang, H.-T. Carbon Nanodots Prepared from o-Phenylenediamine for Sensing of Cu^{2+} Ions in Cells. *Nanoscale* **2014**, *6*, 13119–13125. DOI: 10.1039/C4NR03213F.

[32] Zheng, F.; Cheng, Y.; Wang, J.; Lu, J.; Zhang, B.; Zhao, Y.; Gu, Z. Aptamer-Functionalized Barcode Particles for the Capture and Detection of Multiple Types of Circulating Tumor Cells. *Adv. Mater. Weinheim.* **2014**, *26*, 7333–7338. DOI: 10.1002/adma.201403530.

[33] Zhou, L.; Li, Z.; Liu, Z.; Ren, J.; Qu, X. Luminescent Carbon Dot-Gated Nanovehicles for pH-Triggered Intracellular Controlled Release and Imaging. *Langmuir* **2013**, *29*, 6396–6403. DOI: 10.1021/la400479n.

[34] Zhou, L.; Lin, Y.; Huang, Z.; Ren, J.; Qu, X. Carbon Nanodots as Fluorescence Probes for Rapid, Sensitive, and Label-Free Detection of Hg^{2+} and Biothiols in Complex Matrices. *Chem. Commun. (Camb)* **2012**, *48*, 1147–1149. DOI: 10.1039/C2CC16791C.

[35] Wang, L.; Bi, Y.; Gao, J.; Li, Y.; Ding, H.; Ding, L. Carbon Dots Based Turn-on Fluorescent Probes for the Sensitive Determination of Glyphosate in Environmental Water Samples. *RSC Adv.* **2016**, *6*, 85820–85828. DOI: 10.1039/C6RA10115A.

[36] Deng, J.; Lu, Q.; Mi, N.; Li, H.; Liu, M.; Xu, M.; Tan, L.; Xie, Q.; Zhang, Y.; Yao, S. Electrochemical Synthesis of Carbon Nanodots Directly from Alcohols. *Chemistry* **2014**, *20*, 4993–4999. DOI: 10.1002/chem.201304869.

[37] Liu, M.; Xu, Y.; Niu, F.; Gooding, J. J.; Liu, J. Carbon Quantum Dots Directly Generated from Electrochemical Oxidation of Graphite Electrodes in Alkaline Alcohols and the Applications for Specific Ferric Ion Detection and Cell Imaging. *Analyst* **2016**, *141*, 2657–2664. DOI: 10.1039/C5AN02231B.

[38] Hou, Y.; Lu, Q.; Deng, J.; Li, H.; Zhang, Y. One-Pot Electrochemical Synthesis of Functionalized Fluorescent Carbon Dots and Their Selective Sensing for Mercury Ion. *Anal. Chim. Acta.* **2015**, *866*, 69–74. DOI: 10.1016/j.aca.2015.01.039.

[39] Hu, L.; Sun, Y.; Li, S.; Wang, X.; Hu, K.; Wang, L.; Liang, X-j.; Wu, Y. Multifunctional Carbon Dots with High Quantum Yield for Imaging and Gene Delivery. *Carbon* **2014**, *67*, 508–513. DOI: 10.1016/j.carbon.2013.10.023.

[40] Guo, Y.; Wang, Z.; Shao, H.; Jiang, X. Hydrothermal Synthesis of Highly Fluorescent Carbon Nanoparticles from Sodium Citrate and Their Use for the Detection of Mercury Ions. *Carbon* **2013**, *52*, 583–589. DOI: 10.1016/j.carbon.2012.10.028.

[41] Wang, W.; Lu, Y.-C.; Huang, H.; Feng, J.-J.; Chen, J.-R.; Wang, A.-J. Facile Synthesis of Water-Soluble and Biocompatible Fluorescent Nitrogen-Doped Carbon Dots for Cell Imaging. *Analyst* **2014**, *139*, 1692–1696. DOI: 10.1039/C3AN02098C.

[42] Nguyen, V.; Yan, L.; Si, J.; Hou, X. Femtosecond Laser-Induced Size Reduction of Carbon Nanodots in Solution: Effect of Laser Fluence, Spot Size, and Irradiation Time. *J. Appl. Phys.* **2015**, *117*, 084304. DOI: 10.1063/1.4909506.

[43] Yu, H.; Li, X.; Zeng, X.; Lu, Y. Preparation of Carbon Dots by Non-Focusing Pulsed Laser Irradiation in Toluene. *Chem. Commun.* **2016**, *52*, 819–822. DOI: 10.1039/C5CC08384B.

[44] Wang, Q.; Zhang, C.; Shen, G.; Liu, H.; Fu, H.; Cui, D. Fluorescent Carbon Dots as an Efficient siRNA Nanocarrier for Its Interference Therapy in Gastric Cancer Cells. *J. Nanobiotechnology.* **2014**, *12*, 58. DOI: 10.1186/s12951-014-0058-0.

[45] Kiran, S.; Misra, R. D. K. Mechanism of Intracellular Detection of Glucose through Nonenzymatic and Boronic Acid Functionalized Carbon Dots. *J. Biomed. Mater. Res. A.* **2015**, *103*, 2888–2897. DOI: 10.1002/jbm.a.35421.

[46] Bourlinos, A. B.; Trivizas, G.; Karakassides, M. A.; Baikousi, M.; Kouloumpis, A.; Gournis, D.; Bakandritsos, A.; Hola, K.; Kozak, O.; Zboril, R.; et al. Green and Simple Route toward Boron Doped Carbon Dots with Significantly Enhanced Non-Linear Optical Properties. *Carbon* **2015**, *83*, 173–179. DOI: 10.1016/j.carbon.2014.11.032.

[47] Zeng, Q.; Shao, D.; He, X.; Ren, Z.; Ji, W.; Shan, C.; Qu, S.; Li, J.; Chen, L.; Li, Q. Carbon Dots as a Trackable Drug Delivery Carrier for Localized Cancer Therapy in Vivo. *J. Mater. Chem. B.* **2016**, *4*, 5119–5126. DOI: 10.1039/C6TB01259K.

[48] Peng, H.; Travas-Sejdic, J. Simple Aqueous Solution Route to Luminescent Carbogenic Dots from Carbohydrates. *Chem. Mater.* **2009**, *21*, 5563–5565. DOI: 10.1021/cm901593y.

[49] Ray, S. C.; Saha, A.; Jana, N. R.; Sarkar, R. Fluorescent Carbon Nanoparticles: Synthesis, Characterization, and Bioimaging Application. *J. Phys. Chem. C.* **2009**, *113*, 18546–18551. DOI: 10.1021/jp905912n.

[50] Wang, J.; Wei, J.; Su, S.; Qiu, J. Novel Fluorescence Resonance Energy Transfer Optical Sensors for Vitamin B12 Detection Using Thermally Reduced Carbon Dots. *New J. Chem.* **2015**, *39*, 501–507. DOI: 10.1039/C4NJ00538D.

[51] Zheng, M.; Ruan, S.; Liu, S.; Sun, T.; Qu, D.; Zhao, H.; Xie, Z.; Gao, H.; Jing, X.; Sun, Z. Self-Targeting Fluorescent Carbon Dots for Diagnosis of Brain Cancer Cells. *ACS Nano.* **2015**, *9*, 11455–11461. DOI: 10.1021/acsnano.5b05575.

[52] Fong, J. F. Y.; Chin, S. F.; Ng, S. M. A Unique "Turn-on" Fluorescence Signalling Strategy for Highly Specific Detection of Ascorbic Acid Using Carbon Dots as Sensing Probe. *Biosens. Bioelectron.* **2016**, *85*, 844–852. DOI: 10.1016/j.bios.2016.05.087.

[53] Zheng, M.; Xie, Z.; Qu, D.; Li, D.; Du, P.; Jing, X.; Sun, Z. On–off–on Fluorescent Carbon Dot Nanosensor for Recognition of Chromium(VI) and Ascorbic Acid Based on the Inner Filter Effect. *ACS Appl. Mater. Interfaces.* **2013**, *5*, 13242–13247. DOI: 10.1021/am4042355.

[54] Martindale, B. C. M.; Hutton, G. A. M.; Caputo, C. A.; Reisner, E. Solar Hydrogen Production Using Carbon Quantum Dots and a Molecular Nickel Catalyst. *J. Am. Chem. Soc.* **2015**, *137*, 6018–6025. DOI: 10.1021/jacs.5b01650.

[55] Wang, F.; Xie, Z.; Zhang, H.; Liu, C-y.; Zhang, Y-g. Highly Luminescent Organosilane-Functionalized Carbon Dots. *Adv. Funct. Mater.* **2011**, *21*, 1027–1031. DOI: 10.1002/adfm.201002279.

[56] Shan, X.; Chai, L.; Ma, J.; Qian, Z.; Chen, J.; Feng, H. B-Doped Carbon Quantum Dots as a Sensitive Fluorescence Probe for Hydrogen Peroxide and Glucose Detection. *Analyst* **2014**, *139*, 2322–2325. DOI: 10.1039/C3AN02222F.

[57] Wang, F.; Wang, S.; Sun, Z.; Zhu, H. Study on Ultrasonic Single-Step Synthesis and Optical Properties of Nitrogen-Doped Carbon Fluorescent Quantum Dots. *Fuller. Nanotubes Carbon Nanostruct.* **2015**, *23*, 769–776. DOI: 10.1080/1536383X.2014.996287.

[58] Li, H.; He, X.; Liu, Y.; Huang, H.; Lian, S.; Lee, S.-T.; Kang, Z. One-Step Ultrasonic Synthesis of Water-Soluble Carbon Nanoparticles with Excellent Photoluminescent Properties. *Carbon* **2011**, *49*, 605–609. DOI: 10.1016/j.carbon.2010.10.004.

[59] Duan, H.; Wang, D.; Li, Y. Green Chemistry for Nanoparticle Synthesis. *Chem. Soc. Rev.* **2015**, *44*, 5778–5792. DOI: 10.1039/C4CS00363B.

[60] Gupta, P.; Mahajan, A. Green Chemistry Approaches as Sustainable Alternatives to Conventional Strategies in the Pharmaceutical Industry. *RSC Adv.* **2015**, *5*, 26686–26705. DOI: 10.1039/C5RA00358J.

[61] Bozetine, H.; Wang, Q.; Barras, A.; Li, M.; Hadjersi, T.; Szunerits, S.; Boukherroub, R. Green Chemistry Approach for the Synthesis of ZnO–Carbon Dots Nanocomposites with Good Photocatalytic Properties under Visible Light. *J. Colloid Interface Sci.* **2016**, *465*, 286–294. DOI: 10.1016/j.jcis.2015.12.001.

[62] Singh, I.; Arora, R.; Dhiman, H.; Pahwa, R. Carbon Quantum Dots: Synthesis, Characterization and Biomedical Applications/Karbon Kuantum Noktalari: Sentez, Karakterizasyon ve Biyomedikal Uygulamalar. *Turk. J. Pharm. Sci.* **2018**, *15*, 219–230. DOI: 10.4274/tjps.63497.

[63] Guo, X.; Zhang, H.; Sun, H.; Tade, M. O.; Wang, S. Green Synthesis of Carbon Quantum Dots for Sensitized Solar Cells. *ChemPhotoChem* **2017**, *1*, 116–119. DOI: 10.1002/cptc.201600038.

[64] Wang, J.; Sahu, S.; Sonkar, S. K.; Tackett Ii, K. N.; Sun, K. W.; Liu, Y.; Maimaiti, H.; Anilkumar, P.; Sun, Y.-P. Versatility with Carbon Dots – from Overcooked BBQ to Brightly Fluorescent Agents and Photocatalysts. *RSC Adv.* **2013**, *3*, 15604–15607. DOI: 10.1039/c3ra42302f.

[65] Hsu, P.-C.; Shih, Z.-Y.; Lee, C.-H.; Chang, H.-T. Synthesis and Analytical Applications of Photoluminescent Carbon Nanodots. *Green Chem.* **2012**, *14*, 917–920. DOI: 10.1039/c2gc16451e.

[66] Jiang, C.; Wu, H.; Song, X.; Ma, X.; Wang, J.; Tan, M. Presence of Photoluminescent Carbon Dots in Nescafe® Original Instant Coffee: Applications to Bioimaging. *Talanta* **2014**, *127*, 68–74. DOI: 10.1016/j.talanta.2014.01.046.

[67] Wang, Z.; Liao, H.; Wu, H.; Wang, B.; Zhao, H.; Tan, M. Fluorescent Carbon Dots from Beer for Breast Cancer Cell Imaging and Drug Delivery. *Anal. Methods* **2015**, *7*, 8911–8917. DOI: 10.1039/C5AY01978H.

[68] Mandani, S.; Dey, D.; Sharma, B.; Sarma, T. K. Natural Occurrence of Fluorescent Carbon Dots in Honey. *Carbon* **2017**, *119*, 569–572. DOI: 10.1016/j.carbon.2017.04.075.

[69] Wei, J.; Liu, B.; Yin, P. Dual Functional Carbonaceous Nanodots Exist in a Cup of Tea. *RSC Adv.* **2014**, *4*, 63414–63419. DOI: 10.1039/C4RA11152D.

[70] Zhou, J.; Sheng, Z.; Han, H.; Zou, M.; Li, C. Facile Synthesis of Fluorescent Carbon Dots Using Watermelon Peel as a Carbon Source. *Mater. Lett.* **2012**, *66*, 222–224. DOI: 10.1016/j.matlet.2011.08.081.

[71] Xue, M.; Zou, M.; Zhao, J.; Zhan, Z.; Zhao, S. Green Preparation of Fluorescent Carbon Dots from Lychee Seeds and Their Application for the Selective Detection of Methylene Blue and Imaging in Living Cells. *J. Mater. Chem. B.* **2015**, *3*, 6783–6789. DOI: 10.1039/C5TB01073J.

[72] Xue, M.; Zhan, Z.; Zou, M.; Zhang, L.; Zhao, S. Green Synthesis of Stable and Biocompatible Fluorescent Carbon Dots from Peanut Shells for Multicolor Living Cell Imaging. *New J. Chem.* **2016**, *40*, 1698–1703. DOI: 10.1039/C5NJ02181B.

[73] Jiang, X.; Shi, Y.; Liu, X.; Wang, M.; Song, P.; Xu, F.; Zhang, X. Synthesis of Nitrogen-Doped Lignin/DES Carbon Quantum Dots as a Fluorescent Probe for the Detection of Fe^{3+} Ions. *Polymers* **2018**, *10*, 1282. DOI: 10.3390/polym10111282.

[74] Devi, S.; Gupta, R. K.; Paul, A. K.; Tyagi, S. Waste Carbon Paper Derivatized Carbon Quantum Dots/(3-Aminopropyl)Triethoxysilane Based Fluorescent Probe for Trinitrotoluene Detection. *Mater. Res. Express.* **2018**, *6*, 025605. DOI: 10.1088/2053-1591/aaf03c.

[75] Deka, M. J.; Dutta, P.; Sarma, S.; Medhi, O. K.; Talukdar, N. C.; Chowdhury, D. Carbon Dots Derived from Water Hyacinth and Their Application as a Sensor for Pretilachlor. *Heliyon* **2019**, *5*, e01985. DOI: 10.1016/j.heliyon.2019.e01985.

[76] Singh, J.; Kaur, S.; Lee, J.; Mehta, A.; Kumar, S.; Kim, K. H.; Basu, S.; Rawat, M. Highly Fluorescent Carbon Dots Derived from Mangifera indica Leaves for Selective Detection of Metal Ions. *Sci. Total Environ.* **2020**, *720*, 137604. DOI: 10.1016/j.scitotenv.2020.137604.

[77] Shu, X.; Chang, Y.; Wen, H.; Yao, X.; Wang, Y. Colorimetric Determination of Ascorbic Acid Based on Carbon Quantum Dots as Peroxidase Mimetic Enzyme. *RSC Adv.* **2020**, *10*, 14953–14957. DOI: 10.1039/D0RA02105A.

[78] Kazaryan, S. A.; Nevolin, V. N.; Starodubtsev, N. F. Synthesis and Study of New Luminescent Carbon Particles with High Emission Quantum Yield. *Inorg. Mater. Appl. Res.* **2019**, *10*, 271–284. DOI: 10.1134/S2075113319020217.

[79] Bhunia, S. K.; Pradhan, N.; Jana, N. R. Vitamin B1 Derived Blue and Green Fluorescent Carbon Nanoparticles for Cell-Imaging Application. *ACS Appl. Mater. Interfaces* **2014**, *6*, 7672–7679. DOI: 10.1021/am500964d.

[80] Anthony, A. M.; Murugan, R.; Subramanian, R.; Selvarangan, G. K.; Pandurangan, P.; Dhanasekaran, A.; Sohrab, A. Ultra-Radiant Photoluminescence of Glutathione Rigidified Reduced Carbon Quantum Dots (r-CQDs) Derived from Ice-Biryani for in Vitro and in Vivo Bioimaging Applications. *Colloids Surf. A.* **2020**, *586*, 124266. DOI: 10.1016/j.colsurfa.2019.124266.

[81] Meena, R.; Singh, R.; Marappan, G.; Kushwaha, G.; Gupta, N.; Meena, R.; Gupta, J. P.; Agarwal, R. R.; Fahmi, N.; Kushwaha, O. S. Fluorescent Carbon Dots Driven from Ayurvedic Medicinal Plants for Cancer Cell Imaging and Phototherapy. *Heliyon* **2019**, *5*, e02483. DOI: 10.1016/j.heliyon.2019.e02483.

[82] Wang, M.; Liu, Y.; Ren, G.; Wang, W.; Wu, S.; Shen, J. Bioinspired Carbon Quantum Dots for Sensitive Fluorescent Detection of Vitamin B12 in Cell System. *Anal. Chim. Acta.* **2018**, *1032*, 154–162. DOI: 10.1016/j.aca.2018.05.057.

[83] Teng, X.; Ma, C.; Ge, C.; Yan, M.; Yang, J.; Zhang, Y.; Morais, P. C.; Bi, H. Green Synthesis of Nitrogen-Doped Carbon Dots from Konjac Flour with "off–on" Fluorescence by Fe^{3+} and l-Lysine for Bioimaging. *J. Mater. Chem. B.* **2014**, *2*, 4631–4639. DOI: 10.1039/c4tb00368c.

[84] Kumari, A.; Kumar, A.; Sahu, S. K.; Kumar, S. Synthesis of Green Fluorescent Carbon Quantum Dots Using Waste Polyolefins Residue for Cu^{2+} Ion Sensing and Live Cell Imaging. *Sens. Actuators B Chem.* **2018**, *254*, 197–205. DOI: 10.1016/j.snb.2017.07.075.

[85] Sha, R.; Jones, S. S.; Vishnu, N.; Soundiraraju, B.; Badhulika, S. A Novel Biomass Derived Carbon Quantum Dots for Highly Sensitive and Selective Detection of Hydrazine. *Electroanalysis* **2018**, *30*, 2228–2232. DOI: 10.1002/elan.201800255.

[86] Murugan, N.; Prakash, M.; Jayakumar, M.; Sundaramurthy, A.; Sundramoorthy, A. K. Green Synthesis of Fluorescent Carbon Quantum Dots from Eleusine Coracana and Their Application as a Fluorescence 'Turn-Off' Sensor Probe for Selective Detection of Cu^{2+}. *Appl. Surf. Sci.* **2019**, *476*, 468–480. DOI: 10.1016/j.apsusc.2019.01.090.

[87] Liu, L.; Mi, Z.; Guo, Z.; Wang, J.; Feng, F. A Label-Free Fluorescent Sensor Based on Carbon Quantum Dots with Enhanced Sensitive for the Determination of Myricetin in Real Samples. *Microchem. J.* **2020**, *157*, 104956. DOI: 10.1016/j.microc.2020.104956.

[88] Wang, Q.; Liu, X.; Zhang, L.; Lv, Y. Microwave-Assisted Synthesis of Carbon Nanodots through an Eggshell Membrane and Their Fluorescent Application. *Analyst* **2012**, *137*, 5392–5397. DOI: 10.1039/c2an36059d.

[89] Ko, N. R.; Nafiujjaman, M.; Cherukula, K.; Lee, S. J.; Hong, S. J.; Lim, H. N.; Park, C. H.; Park, I. K.; Lee, Y. K.; Kwon, I. K. Microwave-Assisted Synthesis of Biocompatible Silk Fibroin-Based Carbon Quantum Dots. *Part. Part. Syst. Char.* **2018**, 35, 1700300.

[90] Lu, S.; Liu, L.; Wang, H.; Zhao, W.; Li, Z.; Qu, Z.; Li, J.; Sun, T.; Wang, T.; Sui, G. Synthesis of Dual Functional Gallic-Acid-Based Carbon Dots for Bioimaging and Antitumor Therapy. *Biomater. Sci.* **2019**, *7*, 3258–3265. DOI: 10.1039/C9BM00570F.

[91] Ramanan, V.; Thiyagarajan, S. K.; Raji, K.; Suresh, R.; Sekar, R.; Ramamurthy, P. Outright Green Synthesis of Fluorescent Carbon Dots from Eutrophic Algal Blooms for in Vitro Imaging. *ACS Sustain. Chem. Eng.* **2016**, *4*, 4724–4731. DOI: 10.1021/acssuschemeng.6b00935.

[92] Feng, Y.; Zhong, D.; Miao, H.; Yang, X. Carbon Dots Derived from Rose Flowers for Tetracycline Sensing. *Talanta* **2015**, *140*, 128–133. DOI: 10.1016/j.talanta.2015.03.038.

[93] Yao, Y.-Y.; Gedda, G.; Girma, W. M.; Yen, C.-L.; Ling, Y.-C.; Chang, J.-Y. Magnetofluorescent Carbon Dots Derived from Crab Shell for Targeted Dual-Modality Bioimaging and Drug Delivery. *ACS Appl. Mater. Interfaces.* **2017**, *9*, 13887–13899. DOI: 10.1021/acsami.7b01599.

[94] Liu, R.; Zhang, J.; Gao, M.; Li, Z.; Chen, J.; Wu, D.; Liu, P. A Facile Microwave-Hydrothermal Approach towards Highly Photoluminescent Carbon Dots from Goose Feathers. *RSC Adv.* **2015**, *5*, 4428–4433. DOI: 10.1039/C4RA12077A.

[95] Feng, J.; Wang, W.-J.; Hai, X.; Yu, Y.-L.; Wang, J.-H. Green Preparation of Nitrogen-Doped Carbon Dots Derived from Silkworm Chrysalis for Cell Imaging. *J. Mater. Chem. B.* **2016**, *4*, 387–393. DOI: 10.1039/C5TB01999K.

[96] Qin, X.; Lu, W.; Asiri, A. M.; Al-Youbi, A. O.; Sun, X. Microwave-Assisted Rapid Green Synthesis of Photoluminescent Carbon Nanodots from Flour and Their Applications for Sensitive and Selective Detection of Mercury(II) Ions. *Sens. Actuators B.* **2013**, *184*, 156–162. DOI: 10.1016/j.snb.2013.04.079.

[97] Yang, C.; Ogaki, R.; Hansen, L.; Kjems, J.; Teo, B. M. Theranostic Carbon Dots Derived from Garlic with Efficient Anti-Oxidative Effects towards Macrophages. *RSC Adv.* **2015**, *5*, 97836–97840. DOI: 10.1039/C5RA16874K.

[98] Bankoti, K.; Rameshbabu, A. P.; Datta, S.; Das, B.; Mitra, A.; Dhara, S. Onion Derived Carbon Nanodots for Live Cell Imaging and Accelerated Skin Wound Healing. *J. Mater. Chem. B.* **2017**, *5*, 6579–6592. DOI: 10.1039/C7TB00869D.

[99] Ramezani, Z.; Qorbanpour, M.; Rahbar, N. Green Synthesis of Carbon Quantum Dots Using Quince Fruit (*Cydonia oblonga*) Powder as Carbon Precursor: Application in Cell Imaging and As^{3+} Determination. *Colloids Surf. A.* **2018**, *549*, 58–66. DOI: 10.1016/j.colsurfa.2018.04.006.

[100] Wei, Y.; Zhang, D.; Fang, Y.; Wang, H.; Liu, Y.; Xu, Z.; Wang, S.; Guo, Y. Detection of Ascorbic Acid Using Green Synthesized Carbon Quantum Dots. *J. Sens.* **2019**, *2019*, 1–10. DOI: 10.1155/2019/9869682.

[101] Eskalen, H.; Uruş, S.; Cömertpay, S.; Kurt, A. H.; Özgan, Ş. Microwave-Assisted Ultra-Fast Synthesis of Carbon Quantum Dots from Linter: Fluorescence Cancer Imaging and Human Cell Growth Inhibition Properties. *Ind. Crops Prod.* **2020**, *147*, 112209. DOI: 10.1016/j.indcrop.2020.112209.

[102] Yang, W.; Zhang, H.; Lai, J.; Peng, X.; Hu, Y.; Gu, W.; Ye, L. Carbon Dots with Red-Shifted Photoluminescence by Fluorine Doping for Optical Bio-Imaging. *Carbon* **2018**, *128*, 78–85. DOI: 10.1016/j.carbon.2017.11.069.

[103] Yang, P.; Zhu, Z.; Chen, M.; Zhou, X.; Chen, W. Microwave-Assisted Synthesis of Polyamine-Functionalized Carbon Dots from Xylan and Their Use for the Detection of Tannic Acid. *Spectrochim. Acta A* **2019**, *213*, 301–308. DOI: 10.1016/j.saa.2019.01.043.

[104] Tan, M.; Zhang, L.; Tang, R.; Song, X.; Li, Y.; Wu, H.; Wang, Y.; Lv, G.; Liu, W.; Ma, X. Enhanced Photoluminescence and Characterization of Multicolor Carbon Dots Using Plant Soot as a Carbon Source. *Talanta* **2013**, *115*, 950–956. DOI: 10.1016/j.talanta.2013.06.061.

[105] Mewada, A.; Pandey, S.; Shinde, S.; Mishra, N.; Oza, G.; Thakur, M.; Sharon, M.; Sharon, M. Green Synthesis of Biocompatible Carbon Dots Using Aqueous Extract of Trapa Bispinosa Peel. *Mater. Sci. Eng. C Mater. Biol. Appl.* **2013**, *33*, 2914–2917. DOI: 10.1016/j.msec.2013.03.018.

[106] Hu, Y.; Yang, J.; Tian, J.; Jia, L.; Yu, J.-S. Waste Frying Oil as a Precursor for One-Step Synthesis of Sulfur-Doped Carbon Dots with pH-Sensitive Photoluminescence. *Carbon* **2014**, *77*, 775–782. DOI: 10.1016/j.carbon.2014.05.081.

[107] D'Angelis do ES Barbosa, C.; Corrêa, J. R.; Medeiros, G. A.; Barreto, G.; Magalhães, K. G.; de Oliveira, A. L.; Spencer, J.; Rodrigues, M. O.; Neto, B. A. D. Carbon Dots (C-Dots) from Cow Manure with Impressive Subcellular Selectivity Tuned by Simple Chemical Modification. *Chem. Eur. J.* **2015**, *21*, 5055–5060. DOI: 10.1002/chem.201406330.

[108] Sun, D.; Ban, R.; Zhang, P.-H.; Wu, G.-H.; Zhang, J.-R.; Zhu, J.-J. Hair Fiber as a Precursor for Synthesizing of Sulfur- and Nitrogen-co-Doped Carbon Dots with Tunable Luminescence Properties. *Carbon* **2013**, *64*, 424–434. DOI: 10.1016/j.carbon.2013.07.095.

[109] Soni, H.; Pamidimukkala, P. S. Green Synthesis of N, S co-Doped Carbon Quantum Dots from Triflic Acid Treated Palm Shell Waste and Their Application in Nitrophenol Sensing. *Mater. Res. Bull.* **2018**, *108*, 250–254. DOI: 10.1016/j.materresbull.2018.08.033.

[110] Luo, B.; Yang, H.; Zhou, B.; Ahmed, S. M.; Zhang, Y.; Liu, H.; Liu, X.; He, Y.; Xia, S. Facile Synthesis of Luffa Sponge Activated Carbon Fiber Based Carbon Quantum Dots with Green Fluorescence and Their Application in Cr(VI) Determination. *ACS Omega* **2020**, *5*, 5540–5547. DOI: 10.1021/acsomega.0c00195.

[111] Barvin, R. K. B.; Prakash, P.; Ganesh, V.; Jeyaprabha, B. Highly Selective and Sensitive Sensing of Toxic Mercury Ions Utilizing Carbon Quantum Dot-Modified Glassy Carbon Electrode. *Int. J. Environ. Res.* **2019**, *13*, 1015–1023. DOI: 10.1007/s41742-019-00236-2.

[112] Saxena, M.; Sarkar, S. Fluorescence Imaging of Human Erythrocytes by Carbon Nanoparticles Isolated from Food Stuff and Their Fluorescence Enhancement by Blood Plasma. *Mat. Express* **2013**, *3*, 201–209. DOI: 10.1166/mex.2013.1126.

[113] Dong, Y.; Chen, C.; Zheng, X.; Gao, L.; Cui, Z.; Yang, H.; Guo, C.; Chi, Y.; Li, C. M. One-Step and High Yield Simultaneous Preparation of Single- and Multi-Layer Graphene Quantum Dots from CX-72 Carbon Black. *J. Mater. Chem.* **2012**, *22*, 8764–8766. DOI: 10.1039/c2jm30658a.

[114] Guo, Y.; Zhang, L.; Cao, F.; Leng, Y. Thermal Treatment of Hair for the Synthesis of Sustainable Carbon Quantum Dots and the Applications for Sensing Hg^{2+}. *Sci. Rep.* **2016**, *6*, 35795. DOI: 10.1038/srep35795.

[115] Liu, S.-S.; Wang, C.-F.; Li, C.-X.; Wang, J.; Mao, L.-H.; Chen, S. Hair-Derived Carbon Dots toward Versatile Multidimensional Fluorescent Materials. *J. Mater. Chem. C.* **2014**, *2*, 6477–6483. DOI: 10.1039/C4TC00636D.

[116] De, B.; Karak, N. A Green and Facile Approach for the Synthesis of Water Soluble Fluorescent Carbon Dots from Banana Juice. *RSC Adv.* **2013**, *3*, 8286–8290. DOI: 10.1039/c3ra00088e.

[117] Lan, J.; Liu, C.; Gao, M.; Huang, C. An Efficient Solid-State Synthesis of Fluorescent Surface Carboxylated Carbon Dots Derived from C60 as a Label-Free Probe for Iron Ions in Living Cells. *Talanta* **2015**, *144*, 93–97. DOI: 10.1016/j.talanta.2015.05.071.

[118] Li, W.; Yue, Z.; Wang, C.; Zhang, W.; Liu, G. An Absolutely Green Approach to Fabricate Carbon Nanodots from Soya Bean Grounds. *RSC Adv.* **2013**, *3*, 20662–20665. DOI: 10.1039/c3ra43330g.

[119] Chen, Z.; Wang, J.; Miao, H.; Wang, L.; Wu, S.; Yang, X. Fluorescent Carbon Dots Derived from Lactose for Assaying Folic Acid. *Sci. China Chem.* **2016**, *59*, 487–492. DOI: 10.1007/s11426-015-5536-1.

[120] Liu, L.; Yi, G.; Li, K.; Ma, J.; Xu, J.; Zhang, W.; Sun, Y.; Zhang, H. Synthesis of Carbon Quantum Dots from Lac Dye

for Silicon Dioxide Imaging and Highly Sensitive Ethanol Detecting. *Dyes Pigm.* **2019**, *171*, 107681. DOI: 10.1016/j.dyepig.2019.107681.

[121] Essner, J. B.; Laber, C. H.; Ravula, S.; Polo-Parada, L.; Baker, G. A. Pee-Dots: Biocompatible Fluorescent Carbon Dots Derived from the Upcycling of Urine. *Green Chem.* **2016**, *18*, 243–250. DOI: 10.1039/C5GC02032H.

[122] Das, P.; Ganguly, S.; Maity, P. P.; Bose, M.; Mondal, S.; Dhara, S.; Das, A. K.; Banerjee, S.; Das, N. C. Waste Chimney Oil to Nanolights: A Low Cost Chemosensor for Tracer Metal Detection in Practical Field and Its Polymer Composite for Multidimensional Activity. *J. Photochem. Photobiol. B.* **2018**, *180*, 56–67. DOI: 10.1016/j.jphotobiol.2018.01.019.

[123] Lu, M.; Zhou, L. One-Step Sonochemical Synthesis of Versatile Nitrogen-Doped Carbon Quantum Dots for Sensitive Detection of Fe^{2+} Ions and Temperature in Vitro. *Mater. Sci. Eng. C Mater. Biol. Appl.* **2019**, *101*, 352–359. DOI: 10.1016/j.msec.2019.03.109.

[124] Ren, X.; Zhang, F.; Guo, B.; Gao, N.; Zhang, X. Synthesis of N-Doped Micropore Carbon Quantum Dots with High Quantum Yield and Dual-Wavelength Photoluminescence Emission from Biomass for Cellular Imaging. *Nanomaterials* **2019**, *9*, 495. DOI: 10.3390/nano9040495.

[125] Wang, J.; Wang, C.-F.; Chen, S. Amphiphilic Egg-Derived Carbon Dots: Rapid Plasma Fabrication, Pyrolysis Process, and Multicolor Printing Patterns. *Angew. Chem. Int. Ed. Engl.* **2012**, *51*, 9297–9301. DOI: 10.1002/anie.201204381.

[126] Pramanik, A.; Biswas, S.; Kumbhakar, P. Solvatochromism in Highly Luminescent Environmental Friendly Carbon Quantum Dots for Sensing Applications: Conversion of Bio-Waste into Bio-Asset. *Spectrochim. Acta A* **2018**, *191*, 498–512. DOI: 10.1016/j.saa.2017.10.054.

[127] Yadav, P. K.; Singh, V. K.; Chandra, S.; Bano, D.; Kumar, V.; Talat, M.; Hasan, S. H. Green Synthesis of Fluorescent Carbon Quantum Dots from Azadirachta Indica Leaves and Their Peroxidase-Mimetic Activity for the Detection of H2O2 and Ascorbic Acid in Common Fresh Fruits. *ACS Biomater. Sci. Eng.* **2019**, *5*, 623–632. DOI: 10.1021/acsbiomaterials.8b01528.

[128] Vasimalai, N.; Vilas-Boas, V.; Gallo, J.; Cerqueira, M. F.; Menéndez-Miranda, M.; Costa-Fernández, J. M.; Diéguez, L.; Espiña, B.; Fernández-Argüelles, M. T. Green Synthesis of Fluorescent Carbon Dots from Spices for in Vitro Imaging and Tumour Cell Growth Inhibition. *Beilstein J. Nanotechnol.* **2018**, *9*, 530–544. DOI: 10.3762/bjnano.9.51.

[129] Dai, J.; Wang, Y. J. Nitrogen-Doped Carbon Quantum Dots with *Pinellia ternata* as Carbon Source for High Sensitive Determination of Chromium(VI). *Appl. Ecol. Env. Res.* **2019**, *17*, 12139–12153. DOI: 10.15666/aeer/1705_1213912153.

[130] Bano, D.; Kumar, V.; Singh, V. K.; Hasan, S. H. Green Synthesis of Fluorescent Carbon Quantum Dots for the Detection of Mercury(II) and Glutathione. *New J. Chem.* **2018**, *42*, 5814–5821. DOI: 10.1039/C8NJ00432C.

[131] Wu, D.; Huang, X.; Deng, X.; Wang, K.; Liu, Q. Preparation of Photoluminescent Carbon Nanodots by Traditional Chinese Medicine and Application as a Probe for Hg^{2+}. *Anal. Methods* **2013**, *5*, 3023–3027. DOI: 10.1039/c3ay40337h.

[132] Xu, Y.; Fan, Y.; Zhang, L.; Wang, Q.; Fu, H.; She, Y. A Novel Enhanced Fluorescence Method Based on Multifunctional Carbon Dots for Specific Detection of Hg^{2+} in Complex Samples. *Spectrochim. Acta A.* **2019**, *220*, 117109. DOI: 10.1016/j.saa.2019.05.014.

[133] Irmania, N.; Dehvari, K.; Gedda, G.; Tseng, P. J.; Chang, J. Y. Manganese-Doped Green Tea-Derived Carbon Quantum Dots as a Targeted Dual Imaging and Photodynamic Therapy Platform. *J. Biomed. Mater. Res.* **2020**, *108*, 1616–1625. DOI: 10.1002/jbm.b.34508.

[134] Zhao, X.; Liao, S.; Wang, L.; Liu, Q.; Chen, X. Facile Green and One-Pot Synthesis of Purple Perilla Derived Carbon Quantum Dot as a Fluorescent Sensor for Silver Ion. *Talanta* **2019**, *201*, 1–8. DOI: 10.1016/j.talanta.2019.03.095.

[135] Xiao-Yan, W.; Xue-Yan, H.; Tian-Qi, W.; Xu-Cheng, F. Crown Daisy Leaf Waste–Derived Carbon Dots: A Simple and Green Fluorescent Probe for Copper Ion. *Surf. Interface Anal.* **2020**, *52*, 148–155.

[136] Liu, S.; Tian, J.; Wang, L.; Zhang, Y.; Qin, X.; Luo, Y.; Asiri, A. M.; Al-Youbi, A. O.; Sun, X. Hydrothermal Treatment of Grass: A Low-Cost, Green Route to Nitrogen-Doped, Carbon-Rich, Photoluminescent Polymer Nanodots as an Effective Fluorescent Sensing Platform for Label-Free Detection of Cu(II) Ions. *Adv. Mater. Weinheim.* **2012**, *24*, 2037–2041. DOI: 10.1002/adma.201200164.

[137] Kim, K.; Kim, J. Synthesis of Carbon Quantum Dots from Jujubes for Detection of Iron(III) Ions. *J. Nanosci. Nanotechnol.* **2018**, *18*, 1320–1322. DOI: 10.1166/jnn.2018.14901.

[138] Shukla, D.; Pandey, F. P.; Kumari, P.; Basu, N.; Tiwari, M. K.; Lahiri, J.; Kharwar, R. N.; Parmar, A. S. Label-Free Fluorometric Detection of Adulterant Malachite Green Using Carbon Dots Derived from the Medicinal Plant Source Ocimum Tenuiflorum. *ChemistrySelect* **2019**, *4*, 4839–4847. DOI: 10.1002/slct.201900530.

[139] Wang, C.; Shi, H.; Yang, M.; Yan, Y.; Liu, E.; Ji, Z.; Fan, J. Facile Synthesis of Novel Carbon Quantum Dots from Biomass Waste for Highly Sensitive Detection of Iron Ions. *Mater. Res. Bull.* **2020**, *124*, 110730. DOI: 10.1016/j.materresbull.2019.110730.

[140] Sha, Y.; Lou, J.; Bai, S.; Wu, D.; Liu, B.; Ling, Y. Facile Preparation of Nitrogen-Doped Porous Carbon from Waste Tobacco by a Simple Pre-Treatment Process and Their Application in Electrochemical Capacitor and CO2 Capture. *Mater. Res. Bull.* **2015**, *64*, 327–332. DOI: 10.1016/j.materresbull.2015.01.015.

[141] Pourreza, N.; Ghomi, M. Green Synthesized Carbon Quantum Dots from Prosopis Juliflora Leaves as a Dual off-on Fluorescence Probe for Sensing Mercury(II) and Chemet Drug. *Mater. Sci. Eng. C Mater. Biol. Appl.* **2019**, *98*, 887–896. DOI: 10.1016/j.msec.2018.12.141.

[142] Zhang, Z.; Hu, B.; Zhuang, Q.; Wang, Y.; Luo, X.; Xie, Y.; Zhou, D. Green Synthesis of Fluorescent Nitrogen–Sulfur Co-Doped Carbon Dots from Scallion Leaves for Hemin Sensing. *Anal. Lett.* **2020**, *53*, 1704–1718. 10.1080/00032719.2020.1716782. DOI: 10.1080/00032719.2020.1716782.

[143] Yang, L.; Sun, X.; Li, D.; Qu, C.; Liu, H.; Wei, M.; Liu, X.; Yang, J. Facile Synthesis of Fluorescent Nitrogen-Doped Carbon Quantum Dots Using Scindapsus as a Carbon Source. *Phys. Status Solidi A.* **2019**, *216*, 1800404. DOI: 10.1002/pssa.201800404.

[144] Gao, S.; Chen, Y.; Fan, H.; Wei, X.; Hu, C.; Wang, L.; Qu, L. A Green One-Arrow-Two-Hawks Strategy for Nitrogen-Doped Carbon Dots as Fluorescent Ink and Oxygen Reduction Electrocatalysts. *J. Mater. Chem. A.* **2014**, *2*, 6320–6325. DOI: 10.1039/c3ta15443b.

[145] Yu, J.; Song, N.; Zhang, Y.-K.; Zhong, S.-X.; Wang, A.-J.; Chen, J. Green Preparation of Carbon Dots by Jinhua Bergamot for Sensitive and Selective Fluorescent Detection of Hg^{2+} and Fe^{3+}. *Sens. Actuators B.* **2015**, *214*, 29–35. DOI: 10.1016/j.snb.2015.03.006.

[146] Dias, C.; Vasimalai, N. P.; Sária, M.; Pinheiro, I.; Vilas-Boas, V.; Peixoto, J.; Espiña, B. Biocompatibility and Bioimaging Potential of Fruit-Based Carbon Dots. *Nanomaterials* **2019**, *9*, 199. DOI: 10.3390/nano9020199.

[147] Tadesse, A.; Hagos, M.; Ramadevi, D.; Basavaiah, K.; Belachew, N. Fluorescent-Nitrogen-Doped Carbon Quantum Dots Derived from Citrus Lemon Juice: Green Synthesis, Mercury(II) Ion Sensing, and Live Cell Imaging. *ACS Omega* **2020**, *5*, 3889–3898. DOI: 10.1021/acsomega.9b03175.

[148] Shi, C.; Qi, H.; Ma, R.; Sun, Z.; Xiao, L.; Wei, G.; Huang, Z.; Liu, S.; Li, J.; Dong, M.; et al. N,S-Self-Doped Carbon Quantum Dots from Fungus Fibers for Sensing Tetracyclines and for Bioimaging Cancer Cells. *Mater. Sci. Eng. C Mater.*

Biol. Appl. **2019**, *105*, 110132. DOI: 10.1016/j.msec.2019.110132.

[149] Chen, Z.; Zhao, Z.; Wang, Z.; Zhang, Y.; Sun, X.; Hou, L.; Yuan, C. Foxtail Millet-Derived Highly Fluorescent Multi-Heteroatom Doped Carbon Quantum Dots towards Fluorescent Inks and Smart Nanosensors for Selective Ion Detection. *New J. Chem.* **2018**, *42*, 7326–7331. DOI: 10.1039/C8NJ01072B.

[150] Wang, N.; Wang, Y.; Guo, T.; Yang, T.; Chen, M.; Wang, J. Green Preparation of Carbon Dots with Papaya as Carbon Source for Effective Fluorescent Sensing of Iron(III) and *Escherichia coli*. *Biosens. Bioelectron.* **2016**, *85*, 68–75. DOI: 10.1016/j.bios.2016.04.089.

[151] Zhao, S.; Lan, M.; Zhu, X.; Xue, H.; Ng, T.-W.; Meng, X.; Lee, C.-S.; Wang, P.; Zhang, W. Green Synthesis of Bifunctional Fluorescent Carbon Dots from Garlic for Cellular Imaging and Free Radical Scavenging. *ACS Appl. Mater. Interfaces.* **2015**, *7*, 17054–17060. DOI: 10.1021/acsami.5b03228.

[152] Alam, A.-M.; Park, B.-Y.; Ghouri, Z. K.; Park, M.; Kim, H.-Y. Synthesis of Carbon Quantum Dots from Cabbage with down- and up-Conversion Photoluminescence Properties: Excellent Imaging Agent for Biomedical Applications. *Green Chem.* **2015**, *17*, 3791–3797. DOI: 10.1039/C5GC00686D.

[153] Rajendran, K.; Rajendiran, N. Bluish Green Emitting Carbon Quantum Dots Synthesized from Jackfruit (*Artocarpus heterophyllus*) and Its Sensing Applications of Hg(II) and Cr(VI) Ions. *Mater. Res. Express.* **2018**, *5*, 024008. DOI: 10.1088/2053-1591/aaae4b.

[154] Rajendran, K.; Rajendran, G.; Kasthuri, J.; Kathiravan, K.; Rajendiran, N. Sweet Corn (Zea mays L. var. rugosa) Derived Fluorescent Carbon Quantum Dots for Selective Detection of Hydrogen Sulfide and Bioimaging Applications. *ChemistrySelect* **2019**, *4*, 13668–13676. DOI: 10.1002/slct.201903385.

[155] Arkan, E.; Barati, A.; Rahmanpanah, M.; Hosseinzadeh, L.; Moradi, S.; Hajialyani, M. Green Synthesis of Carbon Dots Derived from Walnut Oil and an Investigation of Their Cytotoxic and Apoptogenic Activities toward Cancer Cells. *Adv. Pharm. Bull.* **2018**, *8*, 149–155. DOI: 10.15171/apb.2018.018.

[156] Radhakrishnan, K.; Panneerselvam, P.; Marieeswaran, M. A Green Synthetic Route for the Surface-Passivation of Carbon Dots as an Effective Multifunctional Fluorescent Sensor for the Recognition and Detection of Toxic Metal Ions from Aqueous Solution. *Anal. Methods* **2019**, *11*, 490–506. DOI: 10.1039/C8AY02451K.

[157] Atchudan, R.; Edison, T. N. J. I.; Perumal, S.; Clament Sagaya Selvam, N.; Lee, Y. R. Green Synthesized Multiple Fluorescent Nitrogen-Doped Carbon Quantum Dots as an Efficient Label-Free Optical Nanoprobe for in Vivo Live-Cell Imaging. *J. Photochem. Photobiol. A.* **2019**, *372*, 99–107. DOI: 10.1016/j.jphotochem.2018.12.011.

[158] Radhakrishnan, K.; Panneerselvam, P. Green Synthesis of Surface-Passivated Carbon Dots from the Prickly Pear Cactus as a Fluorescent Probe for the Dual Detection of Arsenic(III) and Hypochlorite Ions from Drinking Water. *RSC Adv.* **2018**, *8*, 30455–30467. DOI: 10.1039/C8RA05861J.

[159] Li, C.-L.; Ou, C.-M.; Huang, C.-C.; Wu, W.-C.; Chen, Y.-P.; Lin, T.-E.; Ho, L.-C.; Wang, C.-W.; Shih, C.-C.; Zhou, H.-C.; et al. Carbon Dots Prepared from Ginger Exhibiting Efficient Inhibition of Human Hepatocellular Carcinoma Cells. *J. Mater. Chem. B.* **2014**, *2*, 4564–4571. DOI: 10.1039/c4tb00216d.

[160] Du, F.; Zhang, M.; Li, X.; Li, J.; Jiang, X.; Li, Z.; Hua, Y.; Shao, G.; Jin, J.; Shao, Q.; et al. Economical and Green Synthesis of Bagasse-Derived Fluorescent Carbon Dots for Biomedical Applications. *Nanotechnology* **2014**, *25*, 315702. DOI: 10.1088/0957-4484/25/31/315702.

[161] Shukla, D.; Das, M.; Kasade, D.; Pandey, M.; Dubey, A. K.; Yadav, S. K.; Parmar, A. S. Sandalwood-Derived Carbon Quantum Dots as Bioimaging Tools to Investigate the Toxicological Effects of Malachite Green in Model Organisms. *Chemosphere* **2020**, *248*, 125998. DOI: 10.1016/j.chemosphere.2020.125998.

[162] Mehta, V. N.; Jha, S.; Kailasa, S. K. One-Pot Green Synthesis of Carbon Dots by Using *Saccharum officinarum* Juice for Fluorescent Imaging of Bacteria (*Escherichia coli*) and Yeast (*Saccharomyces cerevisiae*) Cells. *Mater. Sci. Eng. C Mater. Biol. Appl.* **2014**, *38*, 20–27. DOI: 10.1016/j.msec.2014.01.038.

[163] Singh, V.; Rawat, K. S.; Mishra, S.; Baghel, T.; Fatima, S.; John, A. A.; Kalleti, N.; Singh, D.; Nazir, A.; Rath, S. K.; Goel, A. Biocompatible Fluorescent Carbon Quantum Dots Prepared from Beetroot Extract for in Vivo Live Imaging in C. elegans and BALB/c Mice. *J. Mater. Chem. B.* **2018**, *6*, 3366–3371. DOI: 10.1039/C8TB00503F.

[164] Arumugam, N.; Kim, J. Synthesis of Carbon Quantum Dots from Broccoli and Their Ability to Detect Silver Ions. *Mater. Lett.* **2018**, *219*, 37–40. DOI: 10.1016/j.matlet.2018.02.043.

[165] Lai, Z.; Guo, X.; Cheng, Z.; Ruan, G.; Du, F. Green Synthesis of Fluorescent Carbon Dots from Cherry Tomatoes for Highly Effective Detection of Trifluralin Herbicide in Soil Samples. *ChemistrySelect* **2020**, *5*, 1956–1960. DOI: 10.1002/slct.201904517.

[166] Zhang, L.; Wang, Y.; Liu, W.; Ni, Y.; Hou, Q. Corncob Residues as Carbon Quantum Dots Sources and Their Application in Detection of Metal Ions. *Ind. Crops Prod.* **2019**, *133*, 18–25. DOI: 10.1016/j.indcrop.2019.03.019.

[167] Yu, D.; Wang, L.; Zhou, H.; Zhang, X.; Wang, L.; Qiao, N. Fluorimetric Detection of *Candida albicans* Using Cornstalk N-Carbon Quantum Dots Modified with Amphotericin B. *Bioconjug. Chem.* **2019**, *30*, 966–973. DOI: 10.1021/acs.bioconjchem.9b00131.

[168] Xu, Y.; Li, D.; Liu, M.; Niu, F.; Liu, J.; Wang, E. Enhanced-Quantum Yield Sulfur/Nitrogen Co-Doped Fluorescent Carbon Nanodots Produced from Biomass *Enteromorpha prolifera*: Synthesis, Posttreatment, Applications and Mechanism Study. *Sci. Rep.* **2017**, *7*, 4499. DOI: 10.1038/s41598-017-04754-x.

[169] Zhu, C.; Zhai, J.; Dong, S. Bifunctional Fluorescent Carbon Nanodots: Green Synthesis via Soy Milk and Application as Metal-Free Electrocatalysts for Oxygen Reduction. *Chem. Commun. (Camb)* **2012**, *48*, 9367–9369. DOI: 10.1039/c2cc33844k.

[170] Qin, X.; Lu, W.; Asiri, A. M.; Al-Youbi, A. O.; Sun, X. Green, Low-Cost Synthesis of Photoluminescent Carbon Dots by Hydrothermal Treatment of Willow Bark and Their Application as an Effective Photocatalyst for Fabricating Au Nanoparticles–Reduced Graphene Oxide Nanocomposites for Glucose Detection. *Catal. Sci. Technol.* **2013**, *3*, 1027–1035. DOI: 10.1039/c2cy20635h.

[171] Shen, J.; Shang, S.; Chen, X.; Wang, D.; Cai, Y. Facile Synthesis of Fluorescence Carbon Dots from Sweet Potato for Fe^{3+} Sensing and Cell Imaging. *Mater. Sci. Eng. C* **2017**, *76*, 856–864. DOI: 10.1016/j.msec.2017.03.178.

[172] Lu, W.; Qin, X.; Asiri, A. M.; Al-Youbi, A. O.; Sun, X. Green Synthesis of Carbon Nanodots as an Effective Fluorescent Probe for Sensitive and Selective Detection of Mercury(II) Ions. *J. Nanopart. Res.* **2013**, *15*, 1344. DOI: 10.1007/s11051-012-1344-0.

[173] Hoan, B. T.; Thanh, T. T.; Tam, P. D.; Trung, N. N.; Cho, S.; Pham, V.-H. A Green Luminescence of Lemon Derived Carbon Quantum Dots and Their Applications for Sensing of V^{5+} Ions. *Mater. Sci. Eng. B* **2019**, *251*, 114455. DOI: 10.1016/j.mseb.2019.114455.

[174] Ding, H.; Ji, Y.; Wei, J.-S.; Gao, Q.-Y.; Zhou, Z.-Y.; Xiong, H.-M. Facile Synthesis of Red-Emitting Carbon Dots from Pulp-Free Lemon Juice for Bioimaging. *J. Mater. Chem. B.* **2017**, *5*, 5272–5277. DOI: 10.1039/C7TB01130J.

[175] He, M.; Zhang, J.; Wang, H.; Kong, Y.; Xiao, Y.; Xu, W. Material and Optical Properties of Fluorescent Carbon

Quantum Dots Fabricated from Lemon Juice via Hydrothermal Reaction. *Nanoscale Res. Lett.* **2018**, *13*, Art. No. 175. DOI: 10.1186/s11671-018-2581-7.

[176] Chaudhary, N.; Gupta, P. K.; Eremin, S.; Solanki, P. R. One-Step Green Approach to Synthesize Highly Fluorescent Carbon Quantum Dots from Banana Juice for Selective Detection of Copper Ions. *J. Environ. Chem. Eng.* **2020**, *8*, 103720. DOI: 10.1016/j.jece.2020.103720.

[177] Sahu, S.; Behera, B.; Maiti, T. K.; Mohapatra, S. Simple One-Step Synthesis of Highly Luminescent Carbon Dots from Orange Juice: application as Excellent Bio-Imaging Agents. *Chem. Commun. (Camb)* **2012**, *48*, 8835–8837. DOI: 10.1039/c2cc33796g.

[178] Fatahi, Z.; Esfandiari, N.; Ehtesabi, H.; Bagheri, Z.; Tavana, H.; Ranjbar, Z.; Latifi, H. Physicochemical and Cytotoxicity Analysis of Green Synthesis Carbon Dots for Cell Imaging. *EXCLI J.* **2019**, *18*, 454–466. DOI: 10.17179/excli2019-1465.

[179] Huang, H.; Xu, Y.; Tang, C.-J.; Chen, J.-R.; Wang, A.-J.; Feng, J.-J. Facile and Green Synthesis of Photoluminescent Carbon Nanoparticles for Cellular Imaging. *New J. Chem.* **2014**, *38*, 784–789. DOI: 10.1039/c3nj01185b.

[180] Mehta, V. N.; Jha, S.; Basu, H.; Singhal, R. K.; Kailasa, S. K. One-Step Hydrothermal Approach to Fabricate Carbon Dots from Apple Juice for Imaging of Mycobacterium and Fungal Cells. *Sens. Actuators B.* **2015**, *213*, 434–443. DOI: 10.1016/j.snb.2015.02.104.

[181] Xu, Y.; Tang, C.-J.; Huang, H.; Sun, C.-Q.; Zhang, Y.-K.; Ye, Q.-F.; Wang, A.-J. Green Synthesis of Fluorescent Carbon Quantum Dots for Detection of Hg^{2+}. *Chin. J. Anal. Chem.* **2014**, *42*, 1252–1258. DOI: 10.1016/S1872-2040(14)60765-9.

[182] Bao, R.; Chen, Z.; Zhao, Z.; Sun, X.; Zhang, J.; Hou, L.; Yuan, C. Green and Facile Synthesis of Nitrogen and Phosphorus Co-Doped Carbon Quantum Dots towards Fluorescent Ink and Sensing Applications. *Nanomaterials* **2018**, *8*, 386. DOI: 10.3390/nano8060386.

[183] Kasibabu, B. S. B.; D'souza, S. L.; Jha, S.; Kailasa, S. K. Imaging of Bacterial and Fungal Cells Using Fluorescent Carbon Dots Prepared from Carica Papaya Juice. *J. Fluoresc.* **2015**, *25*, 803–810. DOI: 10.1007/s10895-015-1595-0.

[184] Lu, M.; Duan, Y.; Song, Y.; Tan, J.; Zhou, L. Green Preparation of Versatile Nitrogen-Doped Carbon Quantum Dots from Watermelon Juice for Cell Imaging, Detection of Fe^{3+} Ions and Cysteine, and Optical Thermometry. *J. Mol. Liq.* **2018**, *269*, 766–774. DOI: 10.1016/j.molliq.2018.08.101.

[185] Huang, H.; Lv, J.-J.; Zhou, D.-L.; Bao, N.; Xu, Y.; Wang, A.-J.; Feng, J.-J. One-Pot Green Synthesis of Nitrogen-Doped Carbon Nanoparticles as Fluorescent Probes for Mercury Ions. *RSC Adv.* **2013**, *3*, 21691–21696. DOI: 10.1039/c3ra43452d.

[186] Prasannan, A.; Imae, T. One-Pot Synthesis of Fluorescent Carbon Dots from Orange Waste Peels. *Ind. Eng. Chem. Res.* **2013**, *52*, 15673–15678. DOI: 10.1021/ie402421s.

[187] Bandi, R.; Gangapuram, B. R.; Dadigala, R.; Eslavath, R.; Singh, S. S.; Guttena, V. Facile and Green Synthesis of Fluorescent Carbon Dots from Onion Waste and Their Potential Applications as Sensor and Multicolour Imaging Agents. *RSC Adv.* **2016**, *6*, 28633–28639. DOI: 10.1039/C6RA01669C.

[188] Mahat, N. A.; Shamsudin, S. A. Transformation of Oil Palm Biomass to Optical Carbon Quantum Dots by Carbonisation-Activation and Low Temperature Hydrothermal Processes. *Diamond Relat. Mater.* **2020**, *102*, 107660. DOI: 10.1016/j.diamond.2019.107660.

[189] Qi, H.; Teng, M.; Liu, M.; Liu, S.; Li, J.; Yu, H.; Teng, C.; Huang, Z.; Liu, H.; Shao, Q.; et al. Biomass-Derived Nitrogen-Doped Carbon Quantum Dots: Highly Selective Fluorescent Probe for Detecting Fe^{3+} Ions and Tetracyclines. *J. Colloid Interface Sci.* **2019**, *539*, 332–341. DOI: 10.1016/j.jcis.2018.12.047.

[190] Lu, W.; Qin, X.; Liu, S.; Chang, G.; Zhang, Y.; Luo, Y.; Asiri, A. M.; Al-Youbi, A. O.; Sun, X. Economical, Green Synthesis of Fluorescent Carbon Nanoparticles and Their Use as Probes for Sensitive and Selective Detection of Mercury(II) Ions. *Anal. Chem.* **2012**, *84*, 5351–5357. DOI: 10.1021/ac3007939.

[191] Du, W.; Xu, X.; Hao, H.; Liu, R.; Zhang, D.; Gao, F.; Lu, Q. Green Synthesis of Fluorescent Carbon Quantum Dots and Carbon Spheres from Pericarp. *Sci. China Chem.* **2015**, *58*, 863–870. DOI: 10.1007/s11426-014-5256-y.

[192] Surendran, P.; Lakshmanan, A.; Vinitha, G.; Ramalingam, G.; Rameshkumar, P. Facile Preparation of High Fluorescent Carbon Quantum Dots from Orange Waste Peels for Nonlinear Optical Applications. *Luminescence* **2020**, *35*, 196–202. DOI: 10.1002/bio.3713.

[193] Xu, J.; Lai, T.; Feng, Z.; Weng, X.; Huang, C. Formation of Fluorescent Carbon Nanodots from Kitchen Wastes and Their Application for Detection of Fe^{3+}. *Luminescence* **2015**, *30*, 420–424. DOI: 10.1002/bio.2754.

[194] Xiao, P.; Ke, Y.; Lu, J.; Huang, Z.; Zhu, X.; Wei, B.; Huang, L. Photoluminescence Immunoassay Based on Grapefruit Peel-Extracted Carbon Quantum Dots Encapsulated into Silica Nanospheres for p53 Protein. *Biochem. Eng. J.* **2018**, *139*, 109–116. DOI: 10.1016/j.bej.2018.08.012.

[195] Tyagi, A.; Tripathi, K. M.; Singh, N.; Choudhary, S.; Gupta, R. K. Green Synthesis of Carbon Quantum Dots from Lemon Peel Waste: Applications in Sensing and Photocatalysis. *RSC Adv.* **2016**, *6*, 72423–72432. DOI: 10.1039/C6RA10488F.

[196] D'Souza, S. L.; Deshmukh, B.; Bhamore, J. R.; Rawat, K. A.; Lenka, N.; Kailasa, S. K. Synthesis of Fluorescent Nitrogen-Doped Carbon Dots from Dried Shrimps for Cell Imaging and Boldine Drug Delivery System. *RSC Adv.* **2016**, *6*, 12169–12179. DOI: 10.1039/C5RA24621K.

[197] Li, W.; Zhang, Z.; Kong, B.; Feng, S.; Wang, J.; Wang, L.; Yang, J.; Zhang, F.; Wu, P.; Zhao, D. Simple and Green Synthesis of Nitrogen-Doped Photoluminescent Carbonaceous Nanospheres for Bioimaging. *Angew. Chem. Int. Ed. Engl.* **2013**, *52*, 8151–8155. DOI: 10.1002/anie.201303927.

[198] Hou, J.; Li, J.; Sun, J.; Ai, S.; Wang, M. Nitrogen-Doped Photoluminescent Carbon Nanospheres: Green, Simple Synthesis via Hair and Application as a Sensor for Hg^{2+} Ions. *RSC Adv.* **2014**, *4*, 37342–37348. DOI: 10.1039/C4RA04209C.

[199] Wen, X.; Shi, L.; Wen, G.; Li, Y.; Dong, C.; Yang, J.; Shuang, S. Green and Facile Synthesis of Nitrogen-Doped Carbon Nanodots for Multicolor Cellular Imaging and Co^{2+} Sensing in Living Cells. *Sens. Actuators B.* **2016**, *235*, 179–187. DOI: 10.1016/j.snb.2016.05.066.

[200] Yang, X.; Zhuo, Y.; Zhu, S.; Luo, Y.; Feng, Y.; Dou, Y. Novel and Green Synthesis of High-Fluorescent Carbon Dots Originated from Honey for Sensing and Imaging. *Biosens. Bioelectron.* **2014**, *60*, 292–298. DOI: 10.1016/j.bios.2014.04.046.

[201] Ruan, S.; Zhu, B.; Zhang, H.; Chen, J.; Shen, S.; Qian, J.; He, Q.; Gao, H. A Simple One-Step Method for Preparation of Fluorescent Carbon Nanospheres and the Potential Application in Cell Organelles Imaging. *J. Colloid Interface Sci.* **2014**, *422*, 25–29. DOI: 10.1016/j.jcis.2014.02.006.

[202] Wu, Z. L.; Zhang, P.; Gao, M. X.; Liu, C. F.; Wang, W.; Leng, F.; Huang, C. Z. One-Pot Hydrothermal Synthesis of Highly Luminescent Nitrogen-Doped Amphoteric Carbon Dots for Bioimaging from Bombyx mori Silk – Natural Proteins. *J. Mater. Chem. B.* **2013**, *1*, 2868–2873. DOI: 10.1039/c3tb20418a.

[203] Zhang, J.; Yuan, Y.; Liang, G.; Yu, S.-H. Scale-Up Synthesis of Fragrant Nitrogen-Doped Carbon Dots from Bee Pollens for Bioimaging and Catalysis. *Adv. Sci.* **2015**, *2*, 1500002. DOI: 10.1002/advs.201500002.

[204] Wang, L.; Zhou, H. S. Green Synthesis of Luminescent Nitrogen-Doped Carbon Dots from Milk and Its Imaging Application. *Anal. Chem.* **2014**, *86*, 8902–8905. DOI: 10.1021/ac502646x.

[205] Tu, Y. J.; Tian, Y. H.; Yang, Y. L. High-Sensitivity and Selectivity Detection of Permanganate Ions Based on Pig

Liver-Based Carbon Quantum Dots. *Appl. Ecol. Env. Res.* **2019**, *17*, 7249–7263. DOI: 10.15666/aeer/1704_72497263.

[206] Wang, D.; Wang, X.; Guo, Y.; Liu, W.; Qin, W. Luminescent Properties of Milk Carbon Dots and Their Sulphur and Nitrogen Doped Analogues. *RSC Adv.* **2014**, *4*, 51658–51665. DOI: 10.1039/C4RA11158C.

[207] Wang, X.; Yang, P.; Feng, Q.; Meng, T.; Wei, J.; Xu, C.; Han, J. Green Preparation of Fluorescent Carbon Quantum Dots from Cyanobacteria for Biological Imaging. *Polymers* **2019**, *173*, 11–19. DOI: 10.3390/polym11040616.

[208] Ye, Z.; Zhang, Y.; Li, G.; Li, B. Fluorescent Determination of Mercury(II) by Green Carbon Quantum Dots Synthesized from Eggshell Membrane. *Anal. Lett.* **2020**, *53*, 2841-2853. DOI: 10.1080/00032719.2020.1759618.

[209] Yuan, C.; Qin, X.; Xu, Y.; Li, X.; Chen, Y.; Shi, R.; Wang, Y. Carbon Quantum Dots Originated from Chicken Blood as Peroxidase Mimics for Colorimetric Detection of Biothiols. *J. Photochem. Photobiol. A.* **2020**, *396*, 112529. DOI: 10.1016/j.jphotochem.2020.112529.

[210] Xu, J.; Wang, C.; Li, H.; Zhao, W. Synthesis of Green-Emitting Carbon Quantum Dots with Double Carbon Sources and Their Application as a Fluorescent Probe for Selective Detection of Cu^{2+} Ions. *RSC Adv.* **2020**, *10*, 2536–2544. DOI: 10.1039/C9RA08654D.

[211] Wang, Y.; Chang, X.; Jing, N.; Zhang, Y. Hydrothermal Synthesis of Carbon Quantum Dots as Fluorescent Probes for the Sensitive and Rapid Detection of Picric Acid. *Anal. Methods* **2018**, *10*, 2775–2784. DOI: 10.1039/C8AY00441B.

[212] Deng, X.; Feng, Y.; Li, H.; Du, Z.; Teng, Q.; Wang, H. N-Doped Carbon Quantum Dots as Fluorescent Probes for Highly Selective and Sensitive Detection of Fe^{3+} Ions. *Particuology* **2018**, *41*, 94–100. DOI: 10.1016/j.partic.2017.12.009.

[213] Woo, J.; Song, Y.; Ahn, J.; Kim, H. Green One-Pot Preparation of Carbon Dots (CD)-Embedded Cellulose Transparent Film for Fe^{3+} Indicator Using Ionic Liquid. *Cellulose* **2020**, *27*, 4609–4621. DOI: 10.1007/s10570-020-03099-5.

[214] Dehghani, A.; Ardekani, S. M.; Hassan, M.; Gomes, V. G. Collagen Derived Carbon Quantum Dots for Cell Imaging in 3D Scaffolds via Two-Photon Spectroscopy. *Carbon* **2018**, *131*, 238–245. DOI: 10.1016/j.carbon.2018.02.006.

[215] Yao, D.; Liang, A.; Jiang, Z. A Fluorometric Clenbuterol Immunoassay Using Sulfur and Nitrogen Doped Carbon Quantum Dots. *Microchim. Acta* **2019**, *186*, DOI: 10.1007/s00604-019-3431-8.

[216] Anmei, S.; Qingmei, Z.; Yuye, C.; Yilin, W. Preparation of Carbon Quantum Dots from Cigarette Filters and Its Application for Fluorescence Detection of Sudan I. *Anal. Chim. Acta.* **2018**, *1023*, 115–120. DOI: 10.1016/j.aca.2018.03.024.

[217] Zhan, J.; Peng, R.; Wei, S.; Chen, J.; Peng, X.; Xiao, B. Ethanol-Precipitation-Assisted Highly Efficient Synthesis of Nitrogen-Doped Carbon Quantum Dots from Chitosan. *ACS Omega* **2019**, *4*, 22574–22580. DOI: 10.1021/acsomega.9b03318.

[218] Zhao, L.; Wang, Y.; Zhao, X.; Deng, Y.; Xia, Y. Facile Synthesis of Nitrogen-Doped Carbon Quantum Dots with Chitosan for Fluorescent Detection of Fe^{3+}. *Polymers* **2019**, 11. DOI: 10.3390/polym11111731.

[219] Zhou, M.; Zhou, Z.; Gong, A.; Zhang, Y.; Li, Q. Synthesis of Highly Photoluminescent Carbon Dots via Citric Acid and Tris for Iron(III) Ions Sensors and Bioimaging. *Talanta* **2015**, *143*, 107–113. DOI: 10.1016/j.talanta.2015.04.015.

[220] Saljoughi, H.; Khakbaz, F.; Mahani, M. Synthesis of Folic Acid Conjugated Photoluminescent Carbon Quantum Dots with Ultrahigh Quantum Yield for Targeted Cancer Cell Fluorescence Imaging. *Photodiagnosis Photodyn. Ther.* **2020**, *30*, 101687. DOI: 10.1016/j.pdpdt.2020.101687.

[221] Miao, X.; Yan, X.; Qu, D.; Li, D.; Tao, F. F.; Sun, Z. Red Emissive Sulfur, Nitrogen Codoped Carbon Dots and Their Application in Ion Detection and Theraonostics. *ACS Appl. Mater. Interfaces.* **2017**, *9*, 18549–18556. DOI: 10.1021/acsami.7b04514.

[222] Li, D.; Han, D.; Qu, S.-N.; Liu, L.; Jing, P.-T.; Zhou, D.; Ji, W.-Y.; Wang, X.-Y.; Zhang, T.-F.; Shen, D.-Z. Supra-(Carbon Nanodots) with a Strong Visible to Near-Infrared Absorption Band and Efficient Photothermal Conversion. *Light Sci. Appl.* **2016**, *5*, e16120–e16120. DOI: 10.1038/lsa.2016.120.

[223] Zhang, Y.; Cui, P.; Zhang, F.; Feng, X.; Wang, Y.; Yang, Y.; Liu, X. Fluorescent Probes for "off–on" Highly Sensitive Detection of Hg^{2+} and L-Cysteine Based on Nitrogen-Doped Carbon Dots. *Talanta* **2016**, *152*, 288–300. DOI: 10.1016/j.talanta.2016.02.018.

[224] Zhang, X.; Ren, Y.; Ji, Z.; Fan, J. Sensitive Detection of Amoxicillin in Aqueous Solution with Novel Fluorescent Probes Containing Boron-Doped Carbon Quantum Dots. *J. Mol. Liq.* **2020**, *311*, 113278. DOI: 10.1016/j.molliq.2020.113278.

[225] Hu, C.; Liu, Y.; Yang, Y.; Cui, J.; Huang, Z.; Wang, Y.; Yang, L.; Wang, H.; Xiao, Y.; Rong, J. One-Step Preparation of Nitrogen-Doped Graphene Quantum Dots from Oxidized Debris of Graphene Oxide. *J. Mater. Chem. B.* **2013**, *1*, 39–42. DOI: 10.1039/C2TB00189F.

[226] Zhou, L.; Geng, J.; Liu, B. Graphene Quantum Dots from Polycyclic Aromatic Hydrocarbon for Bioimaging and Sensing of Fe^{3+} and Hydrogen Peroxide. *Part. Part. Syst. Charact.* **2013**, *30*, 1086–1092. DOI: 10.1002/ppsc.201300170.

[227] Li, C.; Zhang, X.; Zhang, W.; Qin, X.; Zhu, C. Carbon Quantum Dots Derived from Pure Solvent Tetrahydrofuran as a Fluorescent Probe to Detect pH and Silver Ion. *J. Photochem. Photobiol. A.* **2019**, *382*, 111981. DOI: 10.1016/j.jphotochem.2019.111981.

[228] Frigerio, C.; Ribeiro, D. S. M.; Rodrigues, S. S. M.; Abreu, V. L. R. G.; Barbosa, J. A. C.; Prior, J. A. V.; Marques, K. L.; Santos, J. L. M. Application of Quantum Dots as Analytical Tools in Automated Chemical Analysis: A Review. *Anal. Chim. Acta.* **2012**, *735*, 9–22. DOI: 10.1016/j.aca.2012.04.042.

[229] Han, Y.; You, Y.; Lee, Y.-M.; Nam, W. Double Action: Toward Phosphorescence Ratiometric Sensing of Chromium Ion. *Adv. Mater. Weinheim.* **2012**, *24*, 2748–2754. DOI: 10.1002/adma.201104467.

[230] Zhang, R.; Chen, W. Nitrogen-Doped Carbon Quantum Dots: Facile Synthesis and Application as a "Turn-off" Fluorescent Probe for Detection of Hg^{2+} Ions. *Biosens. Bioelectron.* **2014**, *55*, 83–90. DOI: 10.1016/j.bios.2013.11.074.

[231] Lu, H.; Qi, S.; Mack, J.; Li, Z.; Lei, J.; Kobayashi, N.; Shen, Z. Facile Hg^{2+} Detection in Water Using Fluorescent Self-Assembled Monolayers of a Rhodamine-Based Turn-on Chemodosimeter Formed via a "Click" Reaction. *J. Mater. Chem.* **2011**, *21*, 10878–10882. DOI: 10.1039/c1jm11319d.

[232] Liao, J.; Cheng, Z.; Zhou, L. Nitrogen-Doping Enhanced Fluorescent Carbon Dots: Green Synthesis and Their Applications for Bioimaging and Label-Free Detection of Au^{3+} Ions. *ACS Sustainable Chem. Eng.* **2016**, *4*, 3053–3061. DOI: 10.1021/acssuschemeng.6b00018.

[233] Liu, Y.; Zhao, Y.; Zhang, Y. One-Step Green Synthesized Fluorescent Carbon Nanodots from Bamboo Leaves for Copper(II) Ion Detection. *Sens. Actuators B.* **2014**, *196*, 647–652. DOI: 10.1016/j.snb.2014.02.053.

[234] Kumar, A.; Chowdhuri, A. R.; Laha, D.; Mahto, T. K.; Karmakar, P.; Sahu, S. K. Green Synthesis of Carbon Dots from Ocimum Sanctum for Effective Fluorescent Sensing of Pb^{2+} Ions and Live Cell Imaging. *Sens. Actuators B.* **2017**, *242*, 679–686. DOI: 10.1016/j.snb.2016.11.109.

[235] Shi, L.; Zhao, B.; Li, X.; Zhang, G.; Zhang, Y.; Dong, C.; Shuang, S. Eco-Friendly Synthesis of Nitrogen-Doped Carbon Nanodots from Wool for Multicolor Cell Imaging, Patterning,

and Biosensing. *Sens. Actuators B.* **2016**, *235*, 316–324. DOI: 10.1016/j.snb.2016.05.094.

[236] Sachdev, A.; Gopinath, P. Green Synthesis of Multifunctional Carbon Dots from Coriander Leaves and Their Potential Application as Antioxidants, Sensors and Bioimaging Agents. *Analyst* **2015**, *140*, 4260–4269. DOI: 10.1039/C5AN00454C.

[237] Liu, W.; Diao, H.; Chang, H.; Wang, H.; Li, T.; Wei, W. Green Synthesis of Carbon Dots from Rose-Heart Radish and Application for Fe^{3+} Detection and Cell Imaging. *Sens. Actuators B.* **2017**, *241*, 190–198. DOI: 10.1016/j.snb.2016.10.068.

[238] Edison, T. N. J. I.; Atchudan, R.; Shim, J.-J.; Kalimuthu, S.; Ahn, B.-C.; Lee, Y. R. Turn-off Fluorescence Sensor for the Detection of Ferric Ion in Water Using Green Synthesized N-Doped Carbon Dots and Its Bio-Imaging. *J. Photochem. Photobiol. B.* **2016**, *158*, 235–242. DOI: 10.1016/j.jphotobiol.2016.03.010.

[239] Vandarkuzhali, S. A. A.; Jeyalakshmi, V.; Sivaraman, G.; Singaravadivel, S.; Krishnamurthy, K. R.; Viswanathan, B. Highly Fluorescent Carbon Dots from Pseudo-Stem of Banana Plant: Applications as Nanosensor and Bio-Imaging Agents. *Sens. Actuators B.* **2017**, *252*, 894–900. DOI: 10.1016/j.snb.2017.06.088.

[240] Yin, J.; He, X.; Wang, K.; Xu, F.; Shangguan, J.; He, D.; Shi, H. Label-Free and Turn-on Aptamer Strategy for Cancer Cells Detection Based on a DNA-Silver Nanocluster Fluorescence upon Recognition-Induced Hybridization. *Anal. Chem.* **2013**, *85*, 12011–12019. DOI: 10.1021/ac402989u.

[241] Wu, G.; Feng, M.; Zhan, H. Generation of Nitrogen-Doped Photoluminescent Carbonaceous Nanodots via the Hydrothermal Treatment of Fish Scales for the Detection of Hypochlorite. *RSC Adv.* **2015**, *5*, 44636–44641. DOI: 10.1039/C5RA04989J.

[242] Jin, H.; Gui, R.; Wang, Y.; Sun, J. Carrot-Derived Carbon Dots Modified with Polyethyleneimine and Nile Blue for Ratiometric Two-Photon Fluorescence Turn-on Sensing of Sulfide Anion in Biological Fluids. *Talanta* **2017**, *169*, 141–148. DOI: 10.1016/j.talanta.2017.03.083.

[243] Shi, W.; Wang, Q.; Long, Y.; Cheng, Z.; Chen, S.; Zheng, H.; Huang, Y. Carbon Nanodots as Peroxidase Mimetics and Their Applications to Glucose Detection. *Chem. Commun. (Camb)* **2011**, *47*, 6695–6697. DOI: 10.1039/c1cc11943e.

[244] Zhu, A.; Qu, Q.; Shao, X.; Kong, B.; Tian, Y. Carbon-Dot-Based Dual-Emission Nanohybrid Produces a Ratiometric Fluorescent Sensor for in Vivo Imaging of Cellular Copper Ions. *Angew. Chem. Int. Ed. Engl.* **2012**, *51*, 7185–7189. DOI: 10.1002/anie.201109089.

[245] Zhao, H. X.; Liu, L. Q.; Liu, Z. D.; Wang, Y.; Zhao, X. J.; Huang, C. Z. Highly Selective Detection of Phosphate in Very Complicated Matrixes with an off–on Fluorescent Probe of Europium-Adjusted Carbon Dots. *Chem. Commun. (Camb)* **2011**, *47*, 2604–2606. DOI: 10.1039/c0cc04399k.

[246] Wei, W.; Xu, C.; Ren, J.; Xu, B.; Qu, X. Sensing Metal Ions with Ion Selectivity of a Crown Ether and Fluorescence Resonance Energy Transfer between Carbon Dots and Graphene. *Chem. Commun. (Camb)* **2012**, *48*, 1284–1286. DOI: 10.1039/C2CC16481G.

[247] Shi, W.; Li, X.; Ma, H. A Tunable Ratiometric pH Sensor Based on Carbon Nanodots for the Quantitative Measurement of the Intracellular pH of Whole Cells. *Angew. Chem. Int. Ed. Engl.* **2012**, *51*, 6432–6435. DOI: 10.1002/anie.201202533.

[248] Li, H.; Zhang, Y.; Wang, L.; Tian, J.; Sun, X. Nucleic Acid Detection Using Carbon Nanoparticles as a Fluorescent Sensing Platform. *Chem. Commun. (Camb)* **2011**, *47*, 961–963. DOI: 10.1039/C0CC04326E.

[249] Lu, W.; Gong, X.; Yang, Z.; Zhang, Y.; Hu, Q.; Shuang, S.; Dong, C.; Choi, M. M. F. High-Quality Water-Soluble Luminescent Carbon Dots for Multicolor Patterning, Sensors, and Bioimaging. *RSC Adv.* **2015**, *5*, 16972–16979. DOI: 10.1039/C4RA16233A.

[250] Zhu, L.; Yin, Y.; Wang, C.-F.; Chen, S. Plant Leaf-Derived Fluorescent Carbon Dots for Sensing, Patterning and Coding. *J. Mater. Chem. C.* **2013**, *1*, 4925–4932. DOI: 10.1039/c3tc30701h.

[251] Jeong, C. J.; Roy, A. K.; Kim, S. H.; Lee, J.-E.; Jeong, J. H.; In, I.; Park, S. Y. Fluorescent Carbon Nanoparticles Derived from Natural Materials of Mango Fruit for Bio-Imaging Probes. *Nanoscale* **2014**, *6*, 15196–15202. DOI: 10.1039/C4NR04805A.

[252] Wei, Q.; Liu, T.; Pu, H.; Sun, D.-W. Determination of Acrylamide in Food Products Based on the Fluorescence Enhancement Induced by Distance Increase between Functionalized Carbon Quantum Dots. *Talanta* **2020**, *218*, 121152. DOI: 10.1016/j.talanta.2020.121152.

[253] Chandra, S.; Singh, V. K.; Yadav, P. K.; Bano, D.; Kumar, V.; Pandey, V. K.; Talat, M.; Hasan, S. H. Mustard Seeds Derived Fluorescent Carbon Quantum Dots and Their Peroxidase-like Activity for Colorimetric Detection of H_2O_2 and Ascorbic Acid in a Real Sample. *Anal. Chim. Acta* **2019**, *1054*, 145–156. DOI: 10.1016/j.aca.2018.12.024.

[254] Yang, Z. C.; Wang, M.; Yong, A. M.; Wong, S. Y.; Zhang, X. H.; Tan, H.; Chang, A. Y.; Li, X.; Wang, J. Intrinsically Fluorescent Carbon Dots with Tunable Emission Derived from Hydrothermal Treatment of Glucose in the Presence of Monopotassium Phosphate. *Chem. Commun. (Camb)* **2011**, *47*, 11615–11617. DOI: 10.1039/c1cc14860e.

[255] Sha, Y.; Lou, J.; Bai, S.; Wu, D.; Liu, B.; Ling, Y. Hydrothermal Synthesis of Nitrogen-Containing Carbon Nanodots as the High-Efficient Sensor for Copper(II) Ions. *Mater. Res. Bull.* **2013**, *48*, 1728–1731. DOI: 10.1016/j.materresbull.2012.12.010.

[256] Yang, S.-T.; Cao, L.; Luo, P. G.; Lu, F.; Wang, X.; Wang, H.; Meziani, M. J.; Liu, Y.; Qi, G.; Sun, Y.-P. Carbon Dots for Optical Imaging in Vivo. *J. Am. Chem. Soc.* **2009**, *131*, 11308–11309. DOI: 10.1021/ja904843x.

[257] Yang, S.-T.; Wang, X.; Wang, H.; Lu, F.; Luo, P. G.; Cao, L.; Meziani, M. J.; Liu, J.-H.; Liu, Y.; Chen, M.; et al. Carbon Dots as Nontoxic and High-Performance Fluorescence Imaging Agents. *J. Phys. Chem. C* **2009**, *113*, 18110–18114. DOI: 10.1021/jp9085969.

[258] Das, P.; Bose, M.; Ganguly, S.; Mondal, S.; Das, A. K.; Banerjee, S.; Das, N. C. Green Approach to Photoluminescent Carbon Dots for Imaging of Gram-Negative Bacteria *Escherichia coli*. *Nanotechnology* **2017**, *28*, 195501. DOI: 10.1088/1361-6528/aa6714.

[259] Dong, Y.; Pang, H.; Yang, H. B.; Guo, C.; Shao, J.; Chi, Y.; Li, C. M.; Yu, T. Carbon-Based Dots Co-Doped with Nitrogen and Sulfur for High Quantum Yield and Excitation-Independent Emission. *Angew. Chem. Int. Ed. Engl.* **2013**, *52*, 7800–7804. DOI: 10.1002/anie.201301114.

[260] Wang, W.-J.; Xia, J.-M.; Feng, J.; He, M.-Q.; Chen, M.-L.; Wang, J.-H. Green Preparation of Carbon Dots for Intracellular pH Sensing and Multicolor Live Cell Imaging. *J. Mater. Chem. B.* **2016**, *4*, 7130–7137. DOI: 10.1039/C6TB02071B.

[261] Hu, Y.; Zhang, L.; Li, X.; Liu, R.; Lin, L.; Zhao, S. Green Preparation of S and N Co-Doped Carbon Dots from Water Chestnut and Onion as Well as Their Use as an off–on Fluorescent Probe for the Quantification and Imaging of Coenzyme A. *ACS Sustain. Chem. Eng.* **2017**, *5*, 4992–5000. DOI: 10.1021/acssuschemeng.7b00393.

[262] Yang, R.; Guo, X.; Jia, L.; Zhang, Y.; Zhao, Z.; Lonshakov, F. Green Preparation of Carbon Dots with Mangosteen Pulp for the Selective Detection of Fe^{3+} Ions and Cell Imaging. *Appl. Surf. Sci.* **2017**, *423*, 426–432. DOI: 10.1016/j.apsusc.2017.05.252.

[263] Lee, D.-E.; Koo, H.; Sun, I.-C.; Ryu, J. H.; Kim, K.; Kwon, I. C. Multifunctional Nanoparticles for Multimodal Imaging and Theragnosis. *Chem. Soc. Rev.* **2012**, *41*, 2656–2672. DOI: 10.1039/C2CS15261D.